THE UNIVERSITY OF MANITOBA

CONTROL OF POWER SYSTEM HARMONICS WITH FIRING ANGLE MODULATION OF A THYRISTOR CONTROLLED REACTOR

by

Garry Brian Mazur

A thesis

presented to the University of Manitoba

in partial fulfillment of the

requirements for the degree of

Master of Science

in the

Department of Electrical Engineering

 Winnipeg , Manitoba , 1985

ISBN 0-315-33597-1

CONTROL OF POWER SYSTEM HARMONICS WITH FIRING ANGLE MODULATION OF A THYRISTOR CONTROLLED REACTOR

BY

GARRY BRIAN MAZUR

A thesis submitted to the Faculty of Graduate Studies of the University of Manitoba in partial fulfillment of the requirements of the degree of

MASTER OF SCIENCE

I hereby declare that I am the sole author of this thesis.

I authorize the University of Manitoba to lend this thesis to other institutions or individuals for the purpose of scholarly research.

Garry Brian MAZUR

I further authorize the University of Manitoba to reproduce this thesis by photocopying or by other means, in total or in part, at the request of other institutions or individuals for the purpose of scholarly research.

Garry Brian MAZUR

The University of Manitoba requires the signatures of all persons using or photo-copying this thesis. Please sign below , and give address and date.

ABSTRACT

In many power systems special controls are introduced to modulate a system component's terminal characteristics in order to solve system problems and improve system performance. This is especially true in power systems with dc converters since the dc system and its controls have the capability to change real and reactive power loading from minimum to maximum within a few fundamental frequency cycles. This is some orders of magnitude faster than most other power system components such as generator govenors and exciters, and load tapchangers.

Static var compensators of the thyristor controlled reactor (TCR) type and the thyristor switched capacitor (TSC) type are similar to dc converters in terms of control capability and speed of response. It would seem reasonable to consider modulation controls for static var compensators also.

A concept which applies modulation of the firing angle of a thyristor controlled reactor in order to solve a power system problem is proposed and studied. The problem is one where a second harmonic voltage appearing at the high voltage bus of a thyristor controlled reactor results in non-symmetric voltage zero crossings. This results in the generation of non-characteristic even harmonic currents by the TCR. Equidistant firing control systems do not improve the situation . Thus the TCR can aggravate a resonant condition that may exist between the power system and the compensator capacitors. This kind of problem has occurred at the Hydro-Quebec Châteauguay Station.

The solution of the problem at the Châteauguay Station is not specfically addressed in the thesis, but the concepts for a suitable firing angle controller are

developed and verified using digital simulation.

The operation of the thyristor controlled reactor with equidistant firing control and in the presence of a second harmonic voltage is studied. A simple digital model is developed in order to simulate the TCR operation. Analysis of the waveforms suggests that sinusoidal modulation of the firing angle would be beneficial. Fourier analysis and symmetrical component analysis of the TCR waveforms are used to determine the harmonic content.

The TCR is studied when operating with sinusoidal modulation of its firing angle and in the presence of fundamental frequency voltages. It is shown that the magnitude and phase of the lower order harmonics of the TCR currents are dependent on the peak magnitude and phase of the sinusoidal signal. The positive sequence harmonic components of the TCR line currents are shown to be suitable signals for use as input signals for the firing modulation controller.

An algorithm for measuring these sequence components is developed and tested. A modulation controller that uses the positive sequence dc current component or the positive sequence second harmonic component of the line current is designed and tested with the digital model of the TCR. The simulation tests show that firing angle modulation can be used to manipulate the harmonic content of the TCR line currents and hence can be used to control sequence voltages developed across the ac system impedances into which these currents flow.

ACKNOWLEDGEMENTS

Professor R. W. Menzies, the author's thesis supervisor, provided many suggestions and valuable discussions for which the author is greatly appreciative.

The author is grateful to the National Science and Engineering Research Council for financial support from the Post Graduate Scholarship program for the period during which this research was accomplished.

The author wishes to thank Brown Boveri Corporation (BBC) for providing some literature and data about the Châteauguay Station.

The author also wishes to thank Professor A. Gole for his helpful suggestions ,especially with regards to simulation techniques.

CONTENTS

LIST OF FIGURES

Figure.....Page

Figure ..... Page

LIST OF TABLES

Table ..... Page

Table .....Page

LIST OF SYMBOLS AND ABBREVIATIONS

Some of the more frequently occurring symbols and abbreviations are tabulated below. Other symbols which occur less frequently are explained where used. Where possible, IEEE notation is used. However, in some cases the symbols and abbreviations are defined to accommodate the specific meaning used in this thesis.

Symbol	Representation
FC	Fixed Capacitor
G	Gain
Hz	Hertz (cycles/second)
I_b	Base Current (amps)
K_I	PI-Controller Integral Gain
K_P	PI-Controller Proportional Gain
KV	Kilovolts
L	Inductance (Henries)
MVA	Mega-Volt-Amperes
PI-controller	Proportional-integral controller
PLL	Phase-locked Loop
pu.	per unit
R_{TH}	Effective Thyristor Resistance (ohms)

Symbol	Representation
RMS	Root Mean Square
S_B	Base MVA
SVC	Static Var Compensator
t	Time (seconds)
T	Time Constant (seconds)
TCR	Thyristor Controlled Reactor
TSC	Thyristor Switched Capacitor
U_b	Base Voltage (volts)
Z	Impedance (ohms)
Z_{base}	Base Impedance (ohms)
α	Actual Firing Angle
α_o	Nominal Firing Angle
Δ	Incremental Change
Δt	Time-step (seconds)
ϕ	Phase (radians)
ω	Angular Frequency (radians/seconds)
ω_r	PLL Frequency (radians/seconds)
ω_s	System Frequency (radians/seconds)

CHAPTER ONE

INTRODUCTION

1.1. APPLICATION OF STATIC VAR COMPENSATORS IN POWER SYSTEMS

Static var compensators (SVC's) use reactors and capacitors in conjunction with thyristors, resulting in the ability to vary the reactive power output of the compensator in response to changing power system conditions. SVC systems can be divided into two types:

(a) Thyristor controlled reactor and fixed capacitor (TCR + FC) type.

(b) Thyristor controlled reactor and thyristor switched capacitor (TCR + TSC) type.

The thyristor valves of thyristor switched capacitors are always fired at a point such that conduction begins exactly at the natural current zero. Of course, conduction stops at a current zero in a thyristor circuit. As a result there are no harmonics generated by the thyristor switching. On the other hand, thyristors associated with controlled reactors can be fired at any time between 0° and 90° after the peak of the voltage across the thyristor-reactor circuit. This controlled firing generates harmonics of different frequencies.

The primary objective of this thesis is the analysis and control of harmonics generated by static var compensators. The TCR + FC type of compensator is of most interest with regards to harmonic generation and is the type that is considered for this study.

The basic single line configuration of the TCR + FC compensator is shown in

Figure 1.1 . The compensator elements are connected to the system with a step-up transformer. The TCR circuit is connected in a delta configuration. The fixed capacitors can be designed as a filter if necsssary and 12-pulse configurations can be used for cancelation of lower order harmonics.

Although the basic arrangement may be similar in many applications, control circuits differ considerably for each application. Compensation problems involve either :

(a) Load compensation.

(b) Voltage control of a transmission system at a given terminal.

In load compensation the objective is to transform the line currents drawn by an unbalanced and non-unity power factor load into a balanced set of real line currents. Such loads are normally concentrated in one plant and are best handled by a shunt compensator connected at the same terminal as the load.

Compensation of industrial loads such as arc furnaces and rolling mills are characteristic of the load compensation problem. In order to achive symmetrical loading, it is necessary to control each phase independently. The quantities characterizing the load are measured and the line currents are controlled by varying the susceptance of the SVC.

In voltage control, the objective is the regulation and in some cases balancing of the terminal voltages without regard to the actual cause of the variation (and unbalance). Where load balancing is not a requirement, it is not necessary to control each phase independently. A common controller can provide the desired firing angle order to all three phases. Feedback controls that maintain the measured terminal voltage at the desired reference value are a viable solution to the control problem for transmission system support, where the parameters of the ac system are neither accurately known nor measurable.

This thesis does not address the methods used for control of the reactive power of the SVC to satisfy the load compensation and voltage control requirements. Such control strategies and the theory behind the strategies are well documented in the references listed at the end of the thesis. This thesis addresses the concept of modulating the firing order determined by the normal reactive power and voltage controllers in order to reduce or eliminate a harmonic current component that is troublesome to the system. More specifically, firing angle modulation suitable for a thyristor controlled reactor that has a common controller for all three phases is studied. A similar modulation concept could be applied to SVC's with separate controllers for each phase.

1.2. CHARACTERISTIC AND NON-CHARACTERISTIC HARMONICS OF THE THYRISTOR CONTROLLED REACTOR - FIXED CAPACITOR COMPENSATOR

The harmonic components of the currents in the fixed capacitors are determined only by the harmonic components of the compensator bus voltages, whereas the harmonic content of the currents of the thyristor controlled reactor is a function of the firing angle and the harmonic components of the bus voltages.

In a balanced system and when the compensator bus voltages have only a fundamental frequency component, harmonics are generated by the non-sinusoidal current of the TCR that results from delayed firing.

If the back-to-back thyristors associated with each reactor are fired alternately and symmetrically such that the reactor current has equal positive and negative current-time area, all harmonics of even order cancel. Therefore there are no even harmonics among the characteristic harmonics of the TCR.

Thus the characteristic harmonics of the TCR compensator line and reactor currents include harmonics of odd order only. The magnitude of these harmonics varies with firing angle. Triplen harmonics (harmonics of order divisible by three)

exist in the reactor currents at most firing angles. Such harmonics have the same phase in each branch of the TCR. By connecting the TCR in delta , there is a cancellation of these harmonics in the line currents of the TCR. Therefore for the basic six-pulse circuit, harmonic currents of order $6N \pm 1$ for N = 1, 2, 3, ... flow into the system.

The preceding definition of characteristic harmonics assumes that the ac system is balanced and that there are no asymmetries between the phases. The control variables are assumed to be symmetrical in each of the phases as well. Any asymmetry or unbalance that occurs causes as its immediate consequence the generation of harmonics of all orders.

The following asymmetries and unbalances are important in determining the magnitude of non-characteristic (even) harmonics that are present in the TCR currents :

(a) Ac system voltage unbalance.

(b) Reactor and transformer tolerances.

(c) Asymmetries of firing angle between phases and between positive and negative half-cycles. **Reference 3** gives some appreciation of the level of non-characteristic harmonic currents that can arise for relatively small unbalances and asymmetries.

1.3. CONTROL OF HARMONIC GENERATION OF THE THYRISTOR CONTROLLED REACTOR

The compensator configuration can reduce the magnitude of harmonic currents which enter the ac system. The back-to-back thyristor arrangement that is inherent to the TCR provides the symmetry that eliminates even order harmonics. The delta connection that results in the cancellation of triplen harmonics in the line is also inherent to the TCR. The choice of configuration then reduces to use of the 6-pulse

or 12-pulse circuit. With a 12-pulse circuit, characteristic harmonic currents of order $6N \pm 1$ for N = 1, 3, 5, ...are cancelled and do not flow into the system.

Filters to reduce the lower order characteristic harmonic currents are used in many applications. Filter designs are dependent on the harmonic impedance of the ac system, as seen from the compensator bus. Filters can be an expensive component of the SVC. Often a 12-pulse circuit can be more economical than providing 5^{th} and 7^{th} filters.

The presence of non-characteristic harmonic currents can be minimized by specifying stringent tolerances for reactor and transformer impedances. Unbalances in the ac system impedances and voltages are usually minimized by careful design. When severe unbalances are anticipated, this careful design includes the application of compensators for load balancing. Thus, in transmission systems the role of a static var compensator is often one of voltage control only.

Firing asymmetries have a major effect on the generation and hence control of non-characteristic harmonic currents. Under most conditions firing asymmetries can be reduced to a few fractions of a degree and are insignificant. The accuracy of the firing angle can be influenced by the SVC regulators and by the synchronizing system. Imperfections in the control regulators and the synchronizing system, including phase-locked loop (PLL) synchronizing systems, can result in the generation of large harmonic currents.

In Chapter 2 it is shown that harmonic voltages in the source, even though balanced, result in non-equidistant zero crossings. This causes large firing asymmetries even with equidistant PLL firing control. For such cases it is beneficial to introduce firing modulation to minimize asymmetries and harmonic current levels.

1.4. OUTLINE OF THE THESIS

The objective of the thesis is to investigate the possibility of eliminating or controlling a specified problem harmonic of the line current of the thyristor controlled reactor. The 120 Hz and the dc component of the TCR currents often cause system problems. If these harmonic components can be influenced by appropriate modulation, the TCR may in fact provide damping to the ac system at that frequency.

In Chapter 2 the system studied, which is similar to the **Hydro-Quebec** system at **Châteauguay**, is described. A simple model of the system which reproduces the effects on the operation of the SVC of a second harmonic resonance between the compensator capacitors and ac system is formulated. An analysis of the Châteauguay system waveforms is performed using an analytical approach and digital simulation. This analysis suggests that it is feasible to modulate the TCR firing angle to produce current waveforms that will cancel the dc or the 120 Hz components. Thus the SVC may be able to damp any resonant instability that exists.

In Chapter 3 the line and reactor currents of the TCR are analyzed for the case when the TCR is operating with a balanced fundamental frequency source, and with sinusoidal firing angle modulation. Fourier analysis and symmetrical component analysis of the TCR currents are performed using analytical methods and simulation. The influence of the sinusoidal modulation magnitude and relative phase on the harmonic content of the TCR currents is shown.

In Chapter 4 the method of measuring the harmonic current components that are to be used as the control parameters is described. Digital simulation is used to demonstrate the measuring technique. Instantaneous real and imaginary components of the positive sequence dc or second harmonic line current phasors are computed using the digital model's PLL voltages for reference phasors. A modulation controller is then designed and tested with the digital simulation. It is demonstrated that with sinusiodal modulation the TCR produces 120 Hz (or dc) currents of the

appropriate magnitude and phase to cancel currents produced by second harmonic source voltages, therefore cancelling that component in the TCR line current.

The conclusion is that the modulation concept has merit and could be applied to damp a resonant condition in the ac system. Suggestions for further studies are discussed.

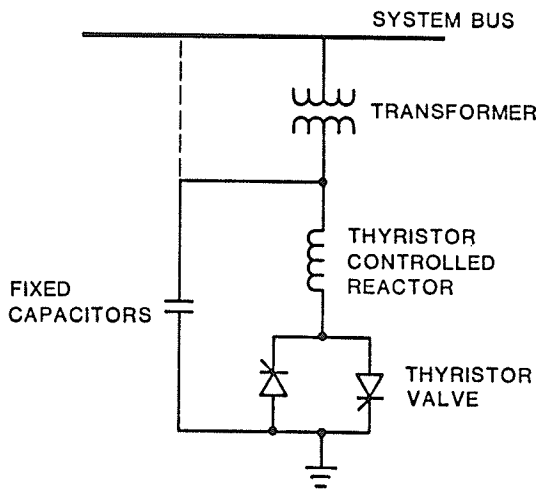

Figure 1.1. Basic Configuration of the SVC
- TCR + FC Type

CHAPTER 2

PERFORMANCE OF THE THYRISTOR CONTROLLED REACTOR WITH SECOND HARMONIC COMPONENT SUPERIMPOSED UPON THE FUNDAMENTAL FREQUENCY SOURCE

2.1. DESCRIPTION OF SYSTEM CONFIGURATION

The idea of modulating the firing angle of a static compensator to stabilize a system resonant condition arises from operational experience at Hydro-Quebec's Châteauguay station. Châteauguay is the Hydro-Quebec 1000 MW back-to-back dc tie. On the 120 KV ac converter bus, two static var compensators of the TCR + TSC type are provided for voltage control and reactive power balance. Both the dc converters and thyristor controlled reactors are connected in a 12-pulse configuration. The station is equipped with 3^{rd}, 5^{th}, 11^{th}, 13^{th}, and high-pass filter banks. Figure 2.1 shows the station single line diagram. The diagram is taken from **Brown Boveri Publication No. CH-N 22.001.85, HVDC Back-to-Back Tie, Poste Châteauguay, Hydro-Quebec / Canada.**

During commissioning of the Châteauguay station, it was observed that a resonance at second harmonic occurs under certain operating conditions. The phenomenon was explained as follows:

A minor system disturbance excites the second harmonic resonance mode, which in turn causes distortion on the 120 KV bus. This distortion is then possibly amplified by the converter controls and the TCR controls, causing saturation

of the converter and the SVC transformers and subsequent tripping of the converter and SVC.

One solution to the problem is to permanently de-tune the power system in order to avoid the resonant condition. At Châteauguay, this means keeping a minimun number of Beauharnois generators connected to the 120 KV converter bus to maintain sufficient short-circuit capacity. To eliminate this kind of operating restriction, one could free Beauharnois units by adding equipment such as synchronous condensers. Alternatively, the SVC's could be moved to a bus that is independent from the converter bus.

Another solution is to add second harmonic damping controls to the converter and static var compensator controls. Damping controls added to the converter pole controls are being tested at the station. It is not known if damping controls are being designed for the static var compensators.

It is the objective of this chapter to analyze the operation of the thyristor controlled reactor under a second harmonic resonant condition and to identify a concept for modulation of the firing angle of the TCR such that the TCR would provide a damping effect on such resonant conditions.

Figure 2.2 is an equivalent of the static var compensator system suitable for analysis of the second harmonic resonant condition. This investigation assumes the SVC is connected directly to the high voltage bus. Thus a more clear evaluation of the dc component of the SVC currents is possible for the initial study. The TSC is treated as a fixed capacitor, since it is not a harmonic current source. The equivalent TCR is connected in a 6-pulse configuration. This is a reasonable simplication because the 12-pulse configuration is expected to have the same performance as the 6-pulse configuration with respect to the second harmonic resonance problem.

At Châteauguay, a small second harmonic source resulting from a minor disturbance within the ac system can excite a large second harmonic voltage at the

compensator bus under a resonant conditon. Waveforms measured at the station are shown in Figure 2.3. The measured line-to-line voltages at the compensator bus have a positive sequence second harmonic component equal to 30 % of the fundamental in magnitude, with a phase lag of -30° with respect to the phase of the fundamental.

The currents and voltages measured at the station can be reproduced by an analytical analysis of the circuit shown in Figure 2.4. The analysis is described in the following sections.

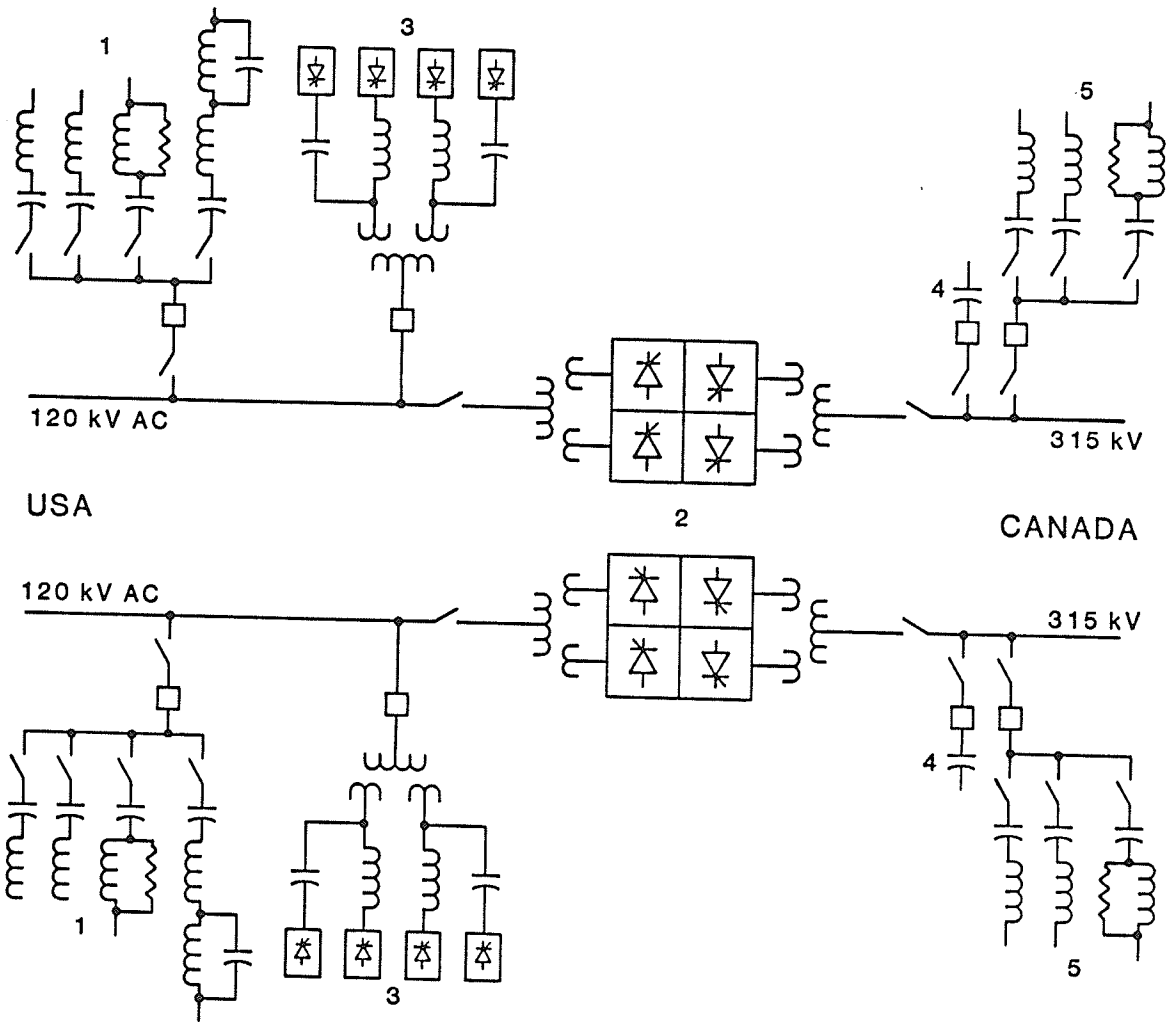

1 - AC filters 120 kV (3 & 5, 11,13, HP)

2 - Back-to-back converters -140.6 kV, 1000 MW

3 - Static compensators

4 - Fixed capacitors

5 - 315 kV AC filters (11, 13, HP)

Figure 2.1. Châteauguay Station Single Line Diagram

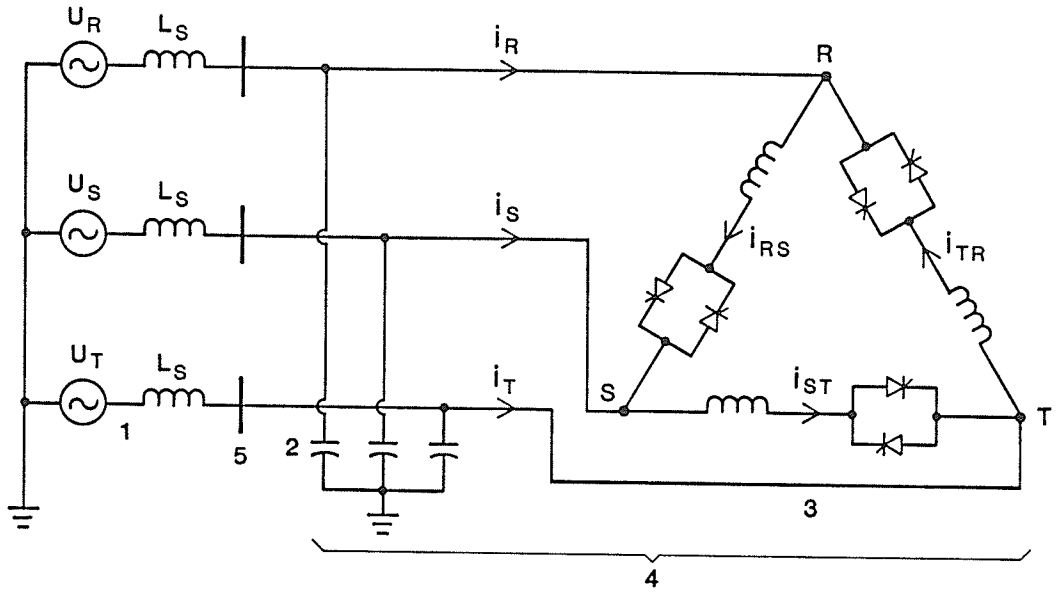

1 - AC system equivalent
2 - Fixed capacitors
3 - Thyristor-controlled reactor (TCR)
4 - SVC
5 - Compensator HV bus

i_R, i_S, i_T : TCR line currents

i_{RS}, i_{ST}, i_{TR} : TCR reactor currents

Figure 2.2. Equivalent Of The SVC System

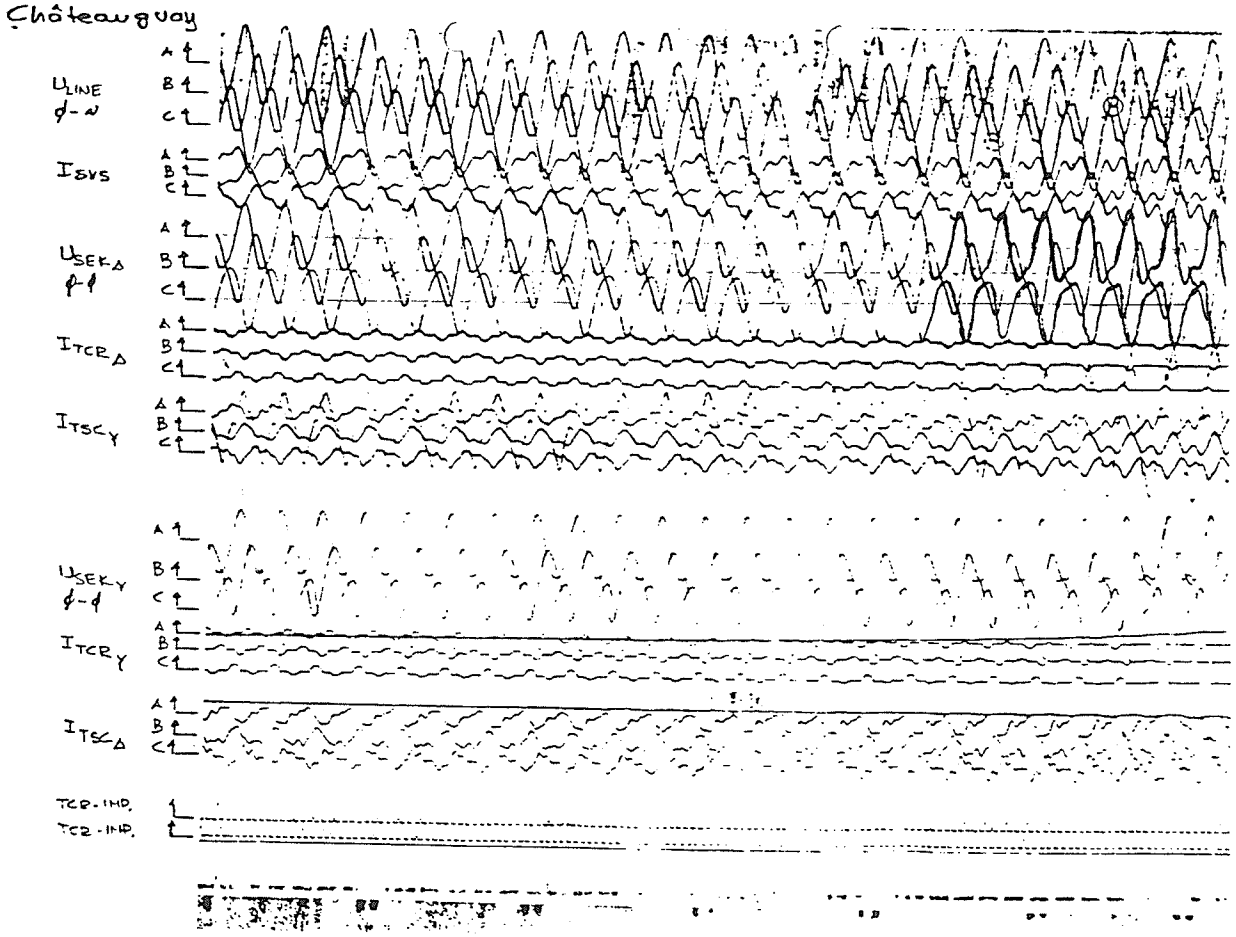

Figure 2.3. Waveforms Measured At Châteauguay Station

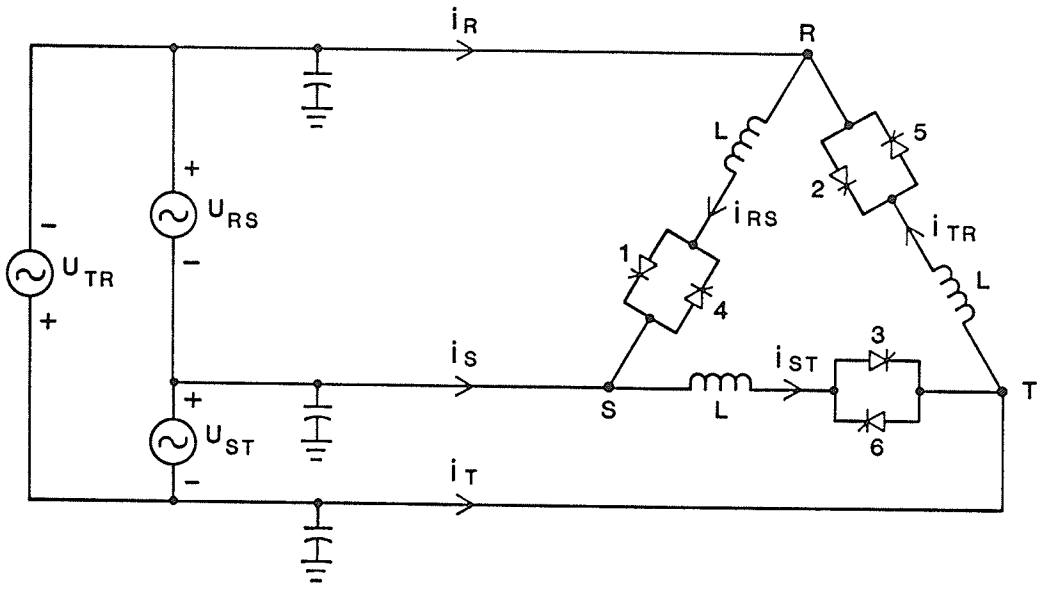

U_{RS}, U_{ST}, U_{TR} : Compensator voltages, including balanced 2nd harmonic equal 30% of fundamental

i_R, i_S, i_T : TCR line currents

i_{RS}, i_{ST}, i_{TR} : TCR reactor currents

Figure 2.4. Simplified Model For Harmonic Analysis Of TCR Currents

2.2. ANALYTICAL ANALYSIS OF TCR CURRENTS

The voltage and current waveforms shown in Figure 2.5 reproduce the phenomenon measured at the Châteauguay station. The waveforms of Figure 2.5 are obtained from a digital simulation of the circuit shown in Figure 2.4 and are very similar to the waveforms in Figure 2.3. Figure 2.6 shows the line currents for the same case.

It should be noted that the digital simulation outputs are usually shown starting from time t= 0. Therefore for some firing angles where a thyristor would be conducting at $t \leq 0$, a start up transient can be seen. An example is the first firing of thyristor 6 in Figure 2.5.(b).

The source voltage waveforms are defined by the equation

$$U_{xy} = \sqrt{2}\, U_1 \cos (\theta_s - \phi_f) + \sqrt{2}\, U_2 \cos (2\, \theta_s - \phi_h) \qquad (2.1)$$

where the parameters for each line-to-line voltage are defined in Table 2.1.

TABLE 2.1. Parameters For Respective Voltages

XY	ϕ_f	ϕ_h
RS	0°	30°
ST	120°	150°
TR	-120°	-90°

U_1 and U_2 denote the RMS values of the respective voltages and $\theta_s = \omega t$. Note that ϕ_f and ϕ_h denote the phase position of the respective voltage components, the zero degree reference being the positive x-axis(cos ωt phasor reference).

The theoretical current waveforms shown in Figure 2.5 are for a firing angle

$\alpha_o = 45°$. The reference for the firing angle is taken at the peak of the fundamental component of the voltage U_{rs}. An equidistant firing system derived from a phase-locked loop (PLL) is assumed. In the next section it is shown that the PLL voltages are in phase with the fundamental component of the corresponding source voltages. Note that the zero crossings of the source voltage waveforms are not equidistant due the presence of the second harmonic component. Consequently equidistant firing of the thyristors results in TCR current waveforms that are not symmetrical with respect to the zero current axis. The TCR currents therefore have even harmonic components.

The current waveforms shown in Figure 2.5 are calculated analytically as follows:

The differential equation describing the circuit shown in Figure 2.4 is

$$U_{xy} = L \frac{d}{dt} (i_{xy}(t)) = \omega L \frac{d}{d\theta_s} (i_{xy}(\theta_s)) \qquad (2.2)$$

where $\theta_s = \omega t$. The equation applies whenever one of the thyristors is conducting.

The solution of this equation is given by the expression

$$i_{xy} = \sqrt{2} \frac{U_1}{\omega L} (\sin(\theta_s - \phi_f) + (-1)^{n+1} \sin \alpha_o + 0.15 U_1 \sin(2\theta_s - \phi_h) - 0.15 U_1 \sin(2\alpha_o - \phi_{h1})) \qquad (2.3)$$

for $\alpha_o + \phi_1 + n\pi \leq \theta_s \leq \alpha_o + \phi_1 + \gamma_{xy} + n\pi$ and for $U_2 = 30\ \%$ of U_1 .

The parameters for each of the TCR currents are defined in Table 2.2.

Table 2.2. Parameters For Respective TCR Currents $\alpha_o = 45°$						
XY	ϕ_f	ϕ_h	ϕ_1	ϕ_{h1}	γ_{xy}^{+}	γ_{xy}^{-}
RS	0°	30°	0°	30°	70°	110°
ST	120°	150°	120°	-90°	90°	90°
TR	-120°	-90°	240°	150°	105°	60°

Note that γ_{xy} is the duration that the thyristor conducts and is called the conduction period. The parameter n in the equation denotes conduction in the positve half-cyle or negative half-cyle of the voltage. When $n=0$, Equation 2.3 describes the current for the positive half-cycle. When $n=1$, Equation 2.3 describes the current for the negative half-cycle. Referencing Figure 2.4, thyristors 1, 3 and 5 are denoted as positive half-cycle thyristors and thyristors 4, 6 and 2 are denoted as negative half-cycle thyristors. The conduction period associated with the positive half-cycle is denoted as γ_{xy}^{+} . The conduction period asssociated with the negative half-cycle is denoted as γ_{xy}^{-} . Phase RS of the delta connected TCR is the reference phase, with $\theta_s = 0°$ at the peak of the fundamental component of the voltage U_{rs}.

The complete analytical solution of Equation 2.3 requires that the conduction period be known. From Equation 2.3, $i_{xy} = 0$ at $\theta_s = \alpha_o + \phi_1 + \gamma_{xy} + n\,\pi$. Thus the conduction angle is defined by the transcendental equation

$$\sqrt{2}\,\frac{U_1}{\omega_L}\sin\left(\alpha_o+\phi_1+n\pi+\gamma_{xy}-\phi_f\right) + 0.15\,U_1\sin\left(2(\alpha_o+\phi_1+n\pi\right.$$

$$\left.+\gamma_{xy}) - \phi_h\right) = 0.15\,U_1\sin\left(2\alpha_o-\phi_{h1}\right) - (-1)^{n+1}\sin\left(\alpha_o\right) \qquad (2.4)$$

Equation 2.4 can be solved for γ_{xy} by a numerical technique. The entries in Table 2.2 for γ_{xy}^{+}, γ_{xy}^{-} and $\alpha_o = 45°$ were calculated using the single variable search algorithm of **Davies, Swann, and Campey** . The digital simulation model described in Section 2.3 is an alternate numerical solution method which gives the same results for γ_{xy} , as can be verified by measuring the conduction periods from Figure 2.5.

The Fourier analysis of the line currents and reactor currents is calculated using the expression

$$f(\theta) = \frac{a_o}{2} + \sum_{n=1}^{n=\infty} (a_n \cos(n\theta) + b_n \sin(n\theta)) \qquad (2.5a)$$

$$f(\theta) = \frac{a_o}{2} + \sum_{n=1}^{n=\infty} c_n \cos(n\theta + \phi_n) \qquad (2.5b)$$

The following relationships apply:

$$c_n = \sqrt{(a_n)^2 + (b_n)^2}$$

$$a_n = c_n \cos(\phi_n) \qquad b_n = -c_n \sin(\phi_n)$$

$$\phi_n = -\arctan\left(\frac{b_n}{a_n}\right)$$

$$a_n = \frac{1}{\pi} \int_0^{2\pi} f(\theta) \cos(n\theta)\, d\theta \qquad n = 1, 2, \ldots \qquad (2.6a)$$

$$b_n = \frac{1}{\pi} \int_0^{2\pi} f(\theta) \sin(n\theta)\, d\theta \qquad n = 1, 2, 3, \ldots \qquad (2.6b)$$

These relationships associate the a_n coefficient with the positive x-axis ($\cos\omega t$ reference phasor) and the $-b_n$ coefficient with the positive y-axis. ϕ_n is positive measured counter-clockwise from the positive x-axis.

The expressions for calculating the coefficients a_n and b_n defined by Equation 2.6 for $f(\theta)$ given by Equation 2.3 are included in Appendix 2.2.1 of

Reference 7, the listing of the Fourier and symmetrical component analysis program **FOURHAR**. The program calculates the Fourier coefficients, given the firing angle, the RMS fundamental frequency voltage U_1 in per unit, and the data shown in Table 2.2. Note that the per unit system is defined in Appendix 1.1. The program assumes that the source voltage has a 30 % second harmonic component. Note that the conduction period must be obtained from a numerical solution of Equation 2.4 for any specified firing angle. The program output is shown in Appendix 2.2.2 of Reference 7 for the case $\alpha_o = 45°$ and a source 120 Hz component of 30 % at a phase of $-30°$ relative to the fundamental.

The Fourier analysis results for the first three terms taken from Appendix 2.2.2 of Reference 7 are summarized below :

$$i_{rs} = -.043 + .202\ cos(\theta_s - 96°) + .078\ cos(2\theta_s - 60°) \quad (2.7a)$$
$$i_{st} = -.048 + .182\ cos(\theta_s + 150°) + .075\ cos(2\theta_s + 120°) \quad (2.7b)$$
$$i_{tr} = .084 + .207\ cos(\theta_s + 24.3°) + .125\ cos(2\theta_s + 33°) \quad (2.7c)$$

$$i_r = (-.073 + .204\ cos(\theta_s - 126°) + .087\ cos(2\theta_s - 116°))\sqrt{3} \quad (2.7d)$$
$$i_s = (-.003 + .186\ cos(\theta_s + 115°) + .088\ cos(2\theta_s + 120°))\sqrt{3} \quad (2.7e)$$
$$i_t = (.076 + .200\ cos(\theta_s - .95°) + .082\ cos(2\theta_s + 1.3°))\sqrt{3} \quad (2.7f)$$

The program **FOURHAR** also computes the symmetrical components relative to R-phase for each harmonic using the transformation

$$\begin{bmatrix} I_o \\ I_1 \\ I_2 \end{bmatrix} = \begin{bmatrix} 1 & 1 & 1 \\ 1 & a & a^2 \\ 1 & a^2 & a \end{bmatrix} \cdot \begin{bmatrix} I_x \\ I_y \\ I_z \end{bmatrix} \quad (2.8)$$

where $a = -0.5 + j\ 0.866$, $a^2 = -0.5 - j\ 0.866$ and I_o , I_1 and I_2 are the zero, positive, and negative sequences respectively.

Sequence data for the $\alpha_o = 45°$ case shown in Appendix 2.2.2 of Reference 7 is summarized in Table 2.3.

Table 2.3. Symmetrical Components of TCR Currents

α_0 = 45°. Source 2nd Harmonic: 30 % @ -30°

Harmonic	Sequence	Reactor Current		Line Current	
-	-	Mag.-PU	Phase-Deg.	Mag. -PU	Phase-Deg.
DC	+ve	0.043	-118.	(√3) 0.043	-148.
	-ve	0.043	118.	(√3) 0.043	148.
	zero	0.002	0.	0.0	....
60 Hz	+ve	0.1966	-94	(√3) 0.1966	-124.
	-ve	0.011	162.	(√3) 0.011	-124.
	zero	0.009	-67.	0.0	....
120 Hz	+ve	0.086	-88.	(√3) 0.086	-118.
	-ve	0.0035	-76.5	(√3) 0.0035	-46.5
	zero	0.0418	32.	0.0	....

Within the reactor circuit large 120 Hz (44 % of fundamental) and dc (22 %) currents flow as a result of the asymmetries resulting from the existence of the 30 % second harmonic component in the source. There is a 5.5 % negative sequence fundamental frequency component in the line and reactor currents, a result of the large difference in conduction angles for the positive and negative half-cycles.

For the configuration under investigation, the second harmonic phase voltage denoted by U_{2r} and the second harmonic line current denoted by I_{2r} are given by Equation 2.9 .

$$U_{2r} = 0.3 \frac{U_1}{\sqrt{3}} \cos(2\theta_s - 60°) \qquad I_{2r} = 0.086 \cos(2\theta_s - 118°) \tag{2.9}$$

The voltage produced by this current flowing into the system is denoted as V_{2r} and is

$$V_{2r} = -Z_s I_{2r} \tag{2.10}$$

where $Z = j\,X_s$ if the system is inductive (resonant at a frequency greater 120 Hz) and $Z = -j\,X_s$ if the ac system is capacitive. Then the system voltage is defined by the equation

$$V_{2r} = 0.086\,X\ (-28°) \qquad \textit{inductive} \qquad (2.11a)$$

$$V_{2r} = 0.086\,X\ (152°) \qquad \textit{capacitive} \qquad (2.11b)$$

Figure 2.7 suggests that the compensator can augment the second harmonic system voltage under the operating condition where the resonant frequency exceeds 120 Hz. It is acknowledged that the effect of transformer phase shifts have been neglected in this analysis. Note that if the phase of the TCR currents could be controlled appropriately, the TCR could be used to damp instead of augment any system resonance even when the resonant frequency exceeds 120 Hz.

The Fourier analysis of the TCR currents operating with constant firing angle and in the presence of second harmonic source voltages shows that significant levels of non-characteristic even harmonics exist (particularly dc and 120 Hz components). From the waveforms shown in Figure 2.5 , it is clear that modulation of the firing angle is desirable to restore symmetry with respect to the zero current axis. One possible scenario for a modulation signal is to fire thyristor 1 at $\alpha_1 < \alpha_o$, $(\alpha_1 = \alpha_o - \Delta)$ and to fire thyristor 4 at $\alpha_4 > \alpha_o$, $(\alpha_4 = \alpha_o + \Delta)$. Similarly for thyristors 3 and 6, $\alpha_3 = \alpha_o - \Delta$ and $\alpha_6 = \alpha_o + \Delta$. For thyristors 2 and 5 larger deviation from α_o is needed, such as $\alpha_2 = \alpha_o - 2\Delta$ and $\alpha_5 = \alpha_o + 2\Delta$.

Such a firing arrangement suggests that sinusoidal modulation of the firing angle should be considered.Sinusoidal modulation where $\alpha = \alpha_o + \hat{\Delta}\cos(\omega t + \delta)$ is investigated in this study.

The concept of using sinusoidal modulation to cancel the dc or 120 Hz current components in the TCR line currents is to be tested using digital simulation of the

TCR operating under resonant conditions. The digital model used for the simulation is described in the next section of this chapter.

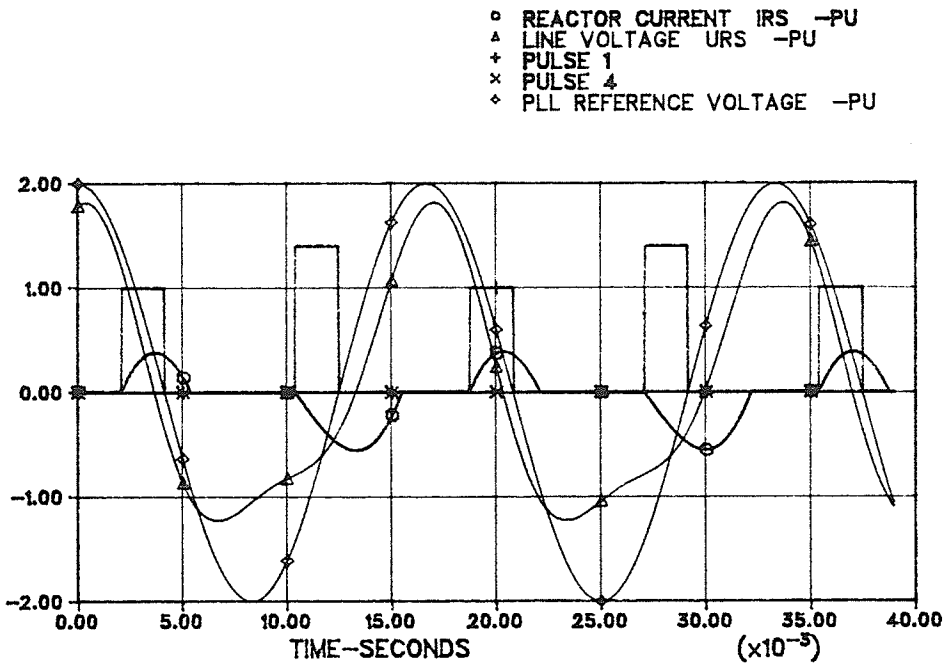

Figure 2.5.(a) TCR Model Current, Voltage, And Firing Pulse Waveforms $\alpha_o = 45°$
Source 2^{nd} Harmonic Voltage 30 % @ -30°

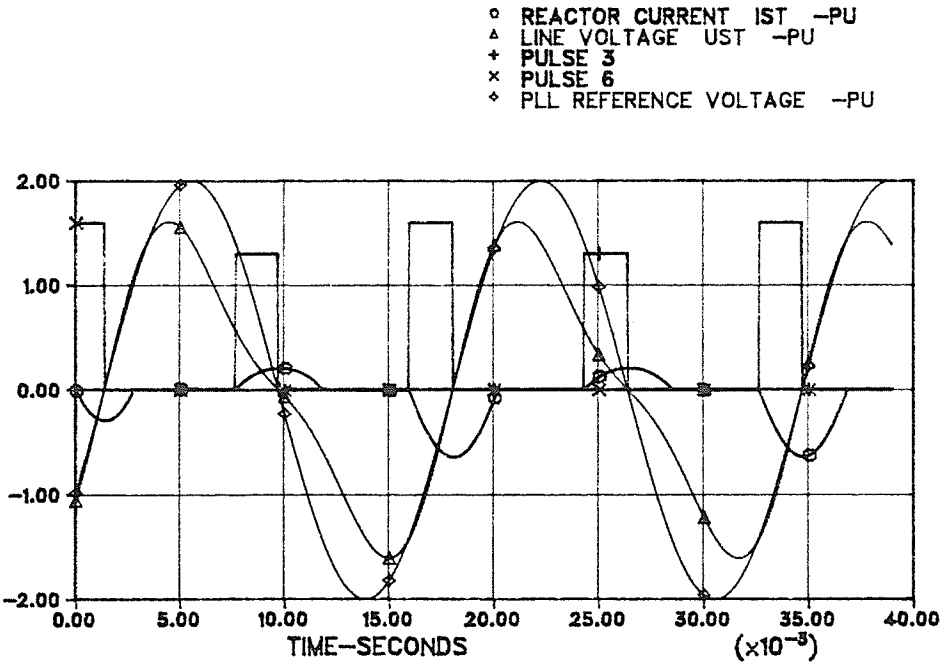

Figure 2.5.(b) TCR Model Current, Voltage, And Firing Pulse Waveforms $\alpha_o = 45°$
Source 2^{nd} Harmonic Voltage 30 % @ -30°

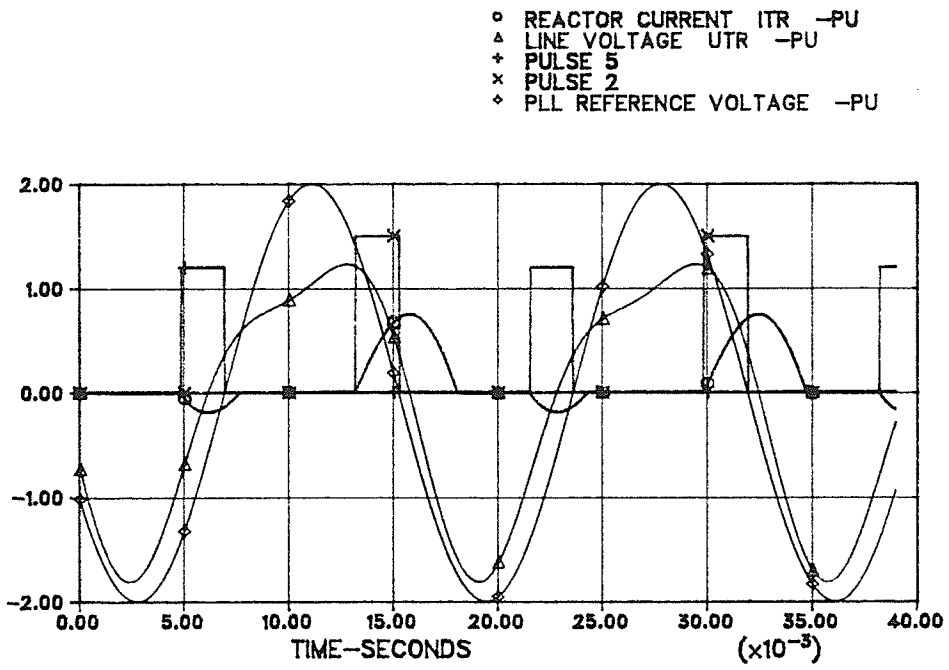

Figure 2.5.(c) TCR Model Current, Voltage, And Firing Pulse Waveforms $\alpha_o = 45°$
Source 2^{nd} Harmonic Voltage 30 % @ -30°

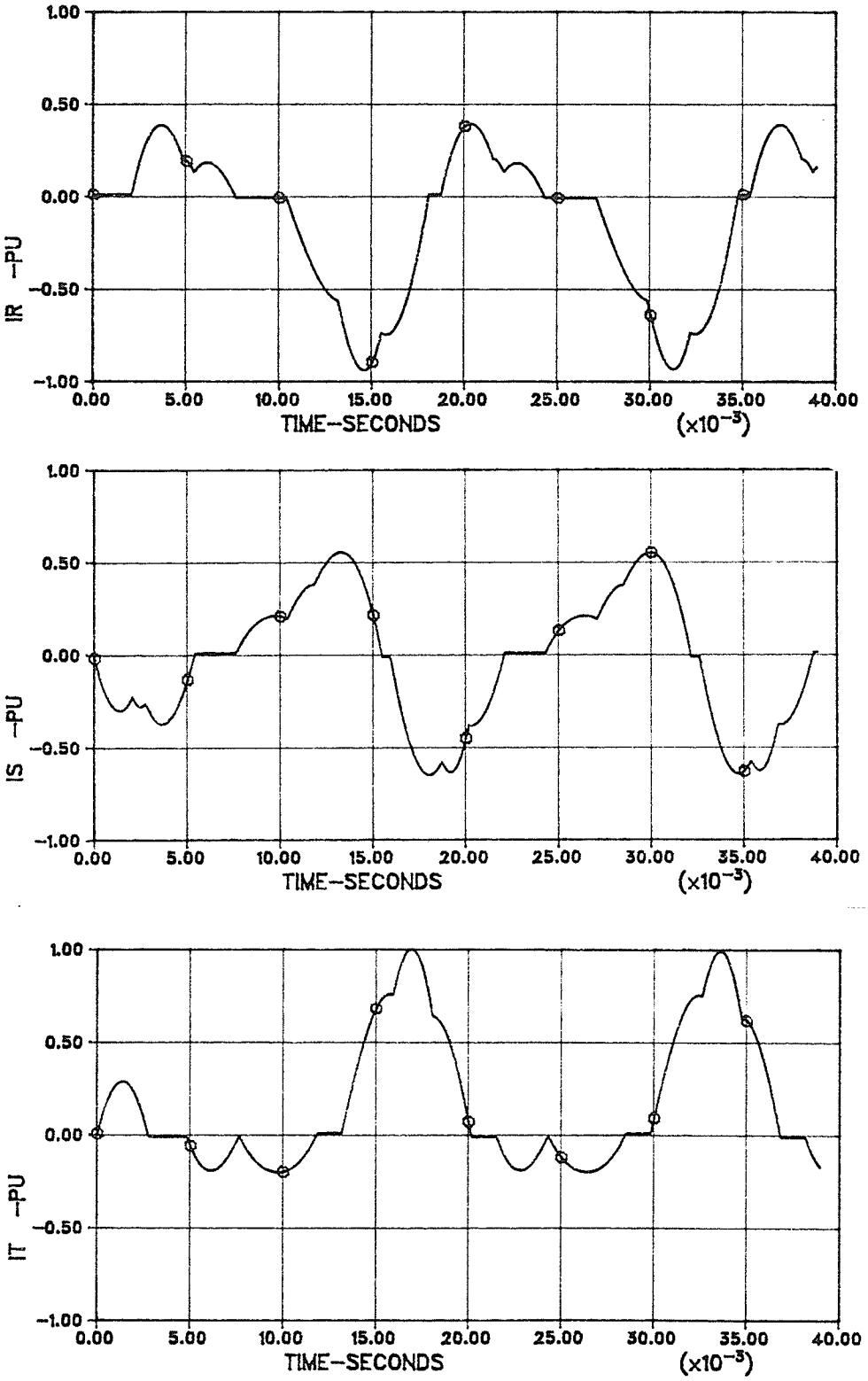

Figure 2.6. TCR Model Line Current Waveforms α_o = 45°
Source 2^{nd} Harmonic Voltage 30 % @ -30°

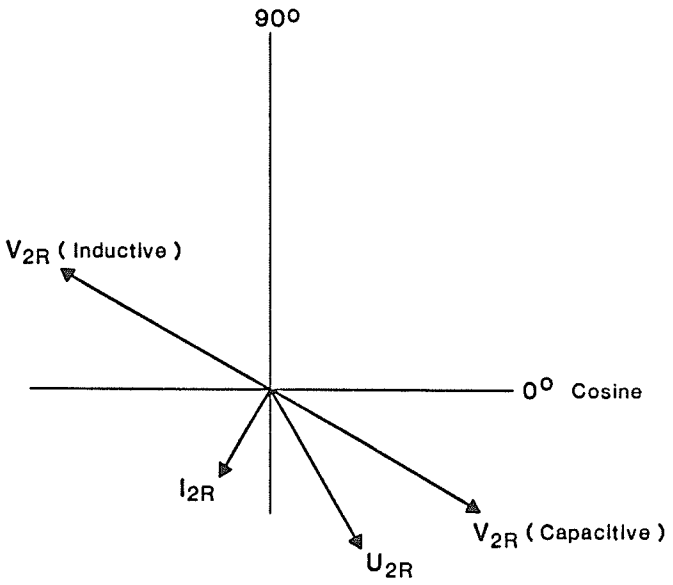

U_{2R} : AC system voltage

V_{2R} : Voltage developed across AC system impedance due to I_{2R}

I_{2R} : SVC line current at 2nd harmonic

Figure 2.7. Phasor Diagram Of Second Harmonic Voltages Associated With The TCR

2.3. DIGITAL MODEL OF THE TCR-FC COMPENSATOR

The circuit of Figure 2.4 represents the case when the thyristor controlled reactor is operating under a second harmonic resonant condition. This is the circuit that is simulated for the purpose of checking the performance of the TCR with sinusoidal modulation of the firing angle.

An important part of the simulation is the representation of the phase-locked loop firing control system. It is an important factor in the performance of the TCR in the presence of second harmonic voltages. The PLL is also used as the reference signal for the measurement of the positive sequence dc and second harmonic current phasors which are used as control parameters for the modulation controller.

The simulation of the circuit shown in Figure 2.4 is accomplished with four Fortran subroutines (**SOURCE, THYR6, STAEQ6, FIRPULS15**) and the main program. The main program controls the system simulation using the above subroutines, handles the data output and performs other housekeeping tasks. Control functions such as the phase-locked loop and modulation controls are simulated using the following control system modelling subroutines :

(a) **REALP2** - real pole.

(b) **INTGL2** - integration by trapezoidal rule.

(c) **TIMD5** - timer with hysteresis, delay on pick-up and release.

(d) **AVGFIL5** - digital averaging filter.

The listings of the subroutines are included as Appendix 2.1.1 to Appendix 2.1.8 of Reference 7.

Subroutine **SOURCE** simulates the line-to-line voltages that appear at the TCR terminals. Source voltages are represented as infinite sources having a specified fundamental frequency magnitude and phase. The source can have a second harmonic component with a specified magnitude and phase as well.

The fixed capacitors are not represented since in the circuit that is modelled the infinite sources are connected directly across the capacitors. Thus the capacitor currents are completely defined.

A state equation formulation of the thyristor controlled reactor is used. The state variables are the TCR reactor currents. The circuit shown can be analyzed as three independent single phase circuits. The back-to-back thyristors are represented as parallel resistors. The effective thyristor resistance at any instant in time is denoted as R_{TH} . The differential equation for the circuit is

$$\frac{d}{dt} i_{xy}(t) = \frac{1}{L} U_{xy}(t) - \frac{R_{TH}}{L} i_{xy}(t) \tag{2.12}$$

Applying the trapezoidal rule of integration gives the solution algorithm as

$$i_{xy}(\omega t_{k+1}) = \frac{\Delta t/2L}{(1 + R_{TH} \frac{\Delta t}{2L})} \left\{ U_{xy}(\omega t_{k+1}) + U_{xy}(\omega t_k) \right\}$$

$$+ \left\{ (1 - R_{TH} \frac{\Delta t}{2L}) \ / \ (1 + R_{TH} \frac{\Delta t}{2L}) \right\} i(\omega t_k) \tag{2.13}$$

where t_{k+1} denotes the current time step and t_k denotes the previous time step. The symbol xy represents rs , st or tr for each of the respective phases.

When the currents and voltages are defined as per unit quantities Equation 2.13 has the form

$$i_{xy}(\omega t_{k+1}) = Z_{base} \frac{\Delta t/2L}{(1 + R_{TH} \frac{\Delta t}{2L})} \left\{ U_{xy}(\omega t_{k+1}) + U_{xy}(\omega t_k) \right\}$$

$$+ \left\{ (1 - R_{TH} \frac{\Delta t}{2L}) \ / \ (1 + R_{TH} \frac{\Delta t}{2L}) \right\} i(\omega t_k) \tag{2.14}$$

where the variables have units as follows :

(a) Z_{base} , R_{TH} - ohms .

(b) L - henries.

(c) Δt - time step in seconds.

(d) $\frac{\Delta t}{2L}$ - mhos.

The subroutine **STAEQ6** outputs the three TCR reactor currents and the line currents using Equation 2.14 , given the present time step's thyristor resistance values and source voltages, and the currents and source voltages of the previous time step.

Each thyristor is represented as a resistor. The resistor assumes the value R_{on} or R_{off} in accordance with the on/off status of the thyristor. The status of the thyristor is determined by the logic shown in Figure 2.8. Subroutine **THYR6** computes the thyristor status at each time step. The values of R_{off} and R_{on} are required in ohms. $R_{off} = 60\ k\Omega$ is used which gives an off-state current of 0.002 pu.(per unit), a typical value for a thyristor circuit. $R_{on} = 0.01\ k\Omega$ is used, giving an on-state thyristor voltage of 0.0008 pu., two times larger than typical. When the ratio of R_{on} / R_{off} gets too large, numerical instability is observed. These values give good results without any numerical stability problems. The on state losses are not of concern in this study in any case. Note that $Z_{base} = 129.96\ k\Omega$ is used in the per unit calculations.

The phase-locked loop firing control system of the TCR is modelled by subroutine **FIRPULS15** . A block diagram of the PLL system is shown in Figure 2.9.

The phase error for the PLL is calculated by measuring the positive and negative zero crossings of the three source voltages U_{rs}, U_{st} and U_{tr}. When a zero crossing is detected, linear interpolation between time steps is used to reduce the sensitivity of the measurement to time step size and to improve accuracy. The phase error is defined as $(\theta_r - \theta_s)$ where the zero crossing of the PLL voltages are known to be as shown in Table 2.4 . The PLL error is the average of the six individual error

measurements where the averaging is carried out each time step. Note that θ_r and θ_s denote the PLL and the system phase position respectively.

Table 2.4. Phase-Locked Loop Reference Voltage Zero Crossings

PLL Voltage	+ve Crossing	-ve Crossing
V_{rs}	0°	180°
V_{st}	120°	300°
V_{tr}	240°	60°

In Figure 2.5 the source voltage shown has a second harmonic component equal to 30 % of the fundamental. The PLL voltages are also shown. The errors measurable from the figure are shown in Table 2.5.

Table 2.5. Phase-Locked Loop Phase Error
Source Voltage 2nd Harmonic: 30 % @ -30°.

RS +	-17.4°	ST +	0°	TR +	17.4°
RS -	10.8°	ST -	0°	TR -	-10.8°

Clearly the average error sums to zero when the PLL is in phase with the ac system source voltages, as is the case in Figure 2.5. In fact the PLL voltages are in phase with the fundamental component of the ac system voltages. Figure 2.10 shows this significant point explicitly.

By using the average error signal, the PLL is made insensitive to the variation of each individual error that results from the 120 Hz balanced three voltage component. Consequently no filtering of the signal ER is used for the majority of the

study (a second harmonic component superimposed on the fundamental is considered in this study). With reference to Figure 2.9, filtering is provided using the real pole transfer function shown by specifying a non-zero value for T_L. In order to look after ripple arising from unbalances and various combinations of higher order harmonics, filtering of ER would normally be used with T_L having a setting of 8.33 milliseconds (one half cycle at 60 Hz).

The response of the PLL system to frequency and phase changes was adjusted to give reasonable performance for the case with $T_L = 0.0$ and also for the case with $T_L = 8.3\ ms$. Near optimal settings found for the PLL system are shown in Table 2.6. The variables in the table can identified from Figure 2.10 .

Table 2.6. Phase-Locked Loop Settings

Parameter	Without Error Filter	With Error Filter
G [-]	1.00	1.00
T_L [sec]	0.0	0.0083
K_P [rad/deg-sec]	10.0	7.0
K_I [rad/deg-sec^2]	0.4 250.0	0.4 115.0
REF1 [deg]	15.0	15.0
REF2 [deg]	5.0	5.0
T_1 [sec]	0.04	0.04
T_2 [sec]	0.06	0.06

Note that the purpose of changing K_I is to accomodate a frequency change. For transient phase changes , a large integral gain is not desirable since after the correction the integral part $\Delta\omega$ must be zero again. Hence the proportional term should do the correction. On the other hand, for frequency changes the integral term must output a new steady-state value for $\Delta\omega$ to supplement the base reference radian frequency of 377 radians/second. This gain switching eliminates the need for a frequency measurement input to the PLL.

The responses of the PLL system to step changes in phase and frequency are shown in Figures 2.11 through 2.14. In all the figures, the PLL is locked to the system prior to the disturbance.

Figure 2.11 shows the response to a 10° phase step $(T_L = 0.0)$. The PLL corrects the phase error within 75 milliseconds. Note that the error signal prior to and subsequent to the disturbance has no ripple on it due to the second harmonic source voltage. Figure 2.12 shows the PLL response to a 2 Hz step frequency change. The phase error exceeds 15° which causes the integral gain to be increased temporarily. The PLL compensates within 160 milliseconds.

Figures 2.13 and 2.14 show similar responses for $T_L = 8.3\ ms$. In order to keep the PLL system stable it is necessary to reduce the gain K_P . The PLL is correspondingly slower to correct for phase error. (The gains for the PLL with filtering have not been optimized as well as for the $T_L = 0.0$ case.)

The phase position error of the PLL in steady-state does not exceed 0.011° during any given simulation , as shown by Figure 2.15. To be in phase lock at the start of a simulation , it is necessary to initialize the phase measuring system error registers with the appropriate steady-error values (Table 2.5 data for source 120 Hz voltage at phase of -30°). Otherwise, at the startup of the simulation case there will be a transient phase error until the PLL is able to respond.

In steady-state operation the PLL system issues firing pulses that are equidistant, within the tolerance of the time step. Table 2.7 shows the measured jitter in the firing pulses for a time step of 50 μs . The PLL is operating at 60 Hz.

Table 2.7. Jitter Of Firing Pulses

$\Delta t = 50\mu s$

Pulse No.	Time of Pulse (ms)	Time Between Adjacent Pulse (ms)	Time Between Same Pulse (ms)
6	1.65	**	**
**	**	2.75	**
1	4.40	**	**
**	**	2.80	**
2	7.20	**	**
**	**	2.80	**
3	10.0	**	**
**	**	2.75	**
4	12.75	**	**
**	**	2.80	**
5	15.55	**	**
**	**	2.75	**
6	18.30	**	16.65
**	**	2.75	**
1	21.10	**	16.70
**	**	2.75	**
2	23.85	**	16.65
**	**	2.80	**
3	26.65	**	16.65
**	**	2.75	**
4	29.40	**	16.65
**	**	2.80	**
5	32.20	**	16.65

The firing pulses are output relative to the PLL phase position θ_r which is calculated with modulus 2 π . The firing pulses are generated when the logic shown in Table 2.8 is satisfied.

Table 2.8. Logic For Pulse Generation	
Pulse	Range Of θ_r
1	$\alpha+90° \leq \theta_r \leq 180°$
2	$\alpha+150° \leq \theta_r \leq 240°$
3	$\alpha+210° \leq \theta_r \leq 300°$
4	$\alpha+270° \leq \theta_r \leq 360°$
5	$\alpha+330° \leq \theta_r \leq 360°$ *or* $\alpha \leq \theta_r \leq 60°$
6	$\alpha+30° \leq \theta_r \leq 120°$

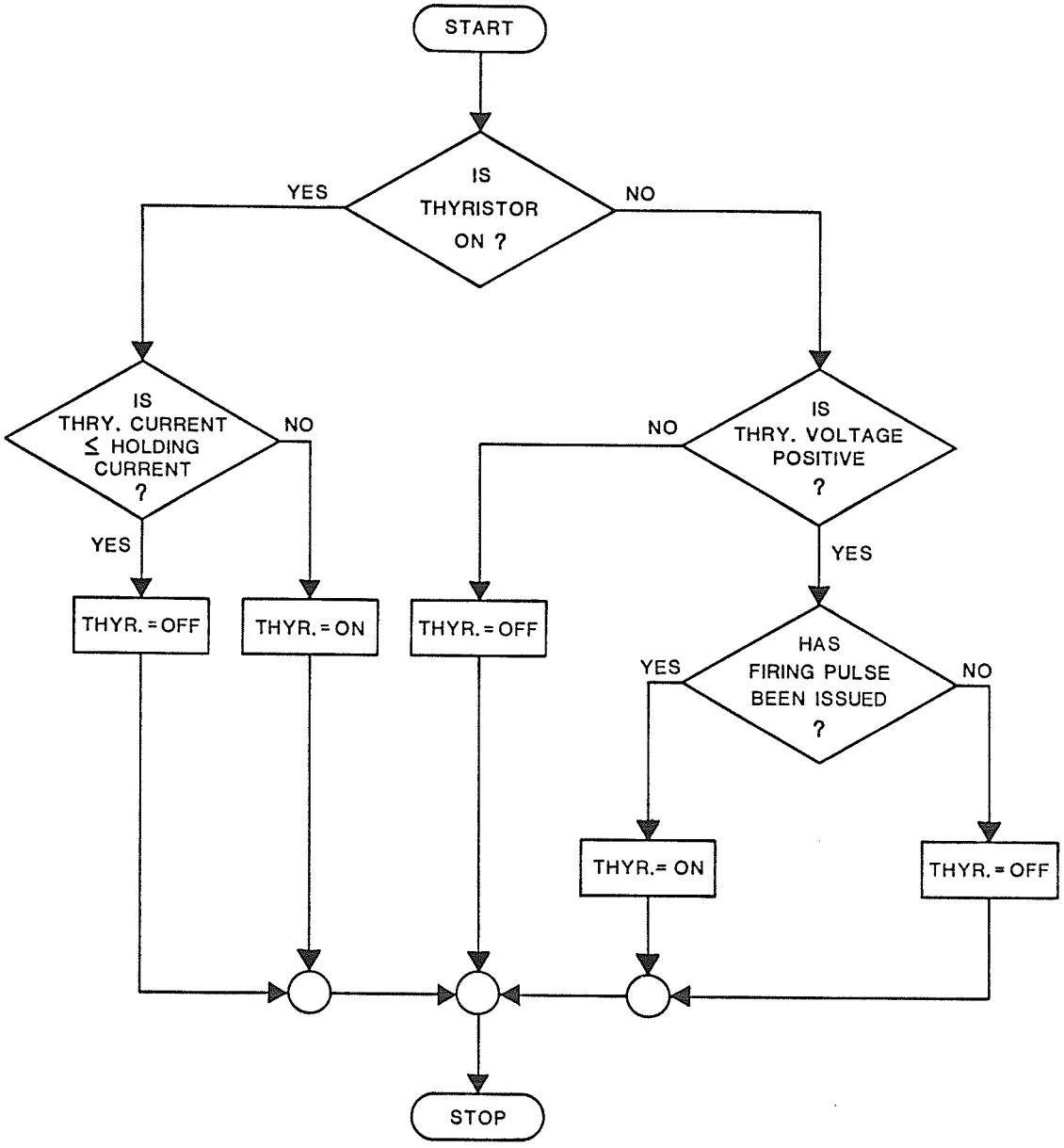

Figure 2.8. Logic For Thyristor Model

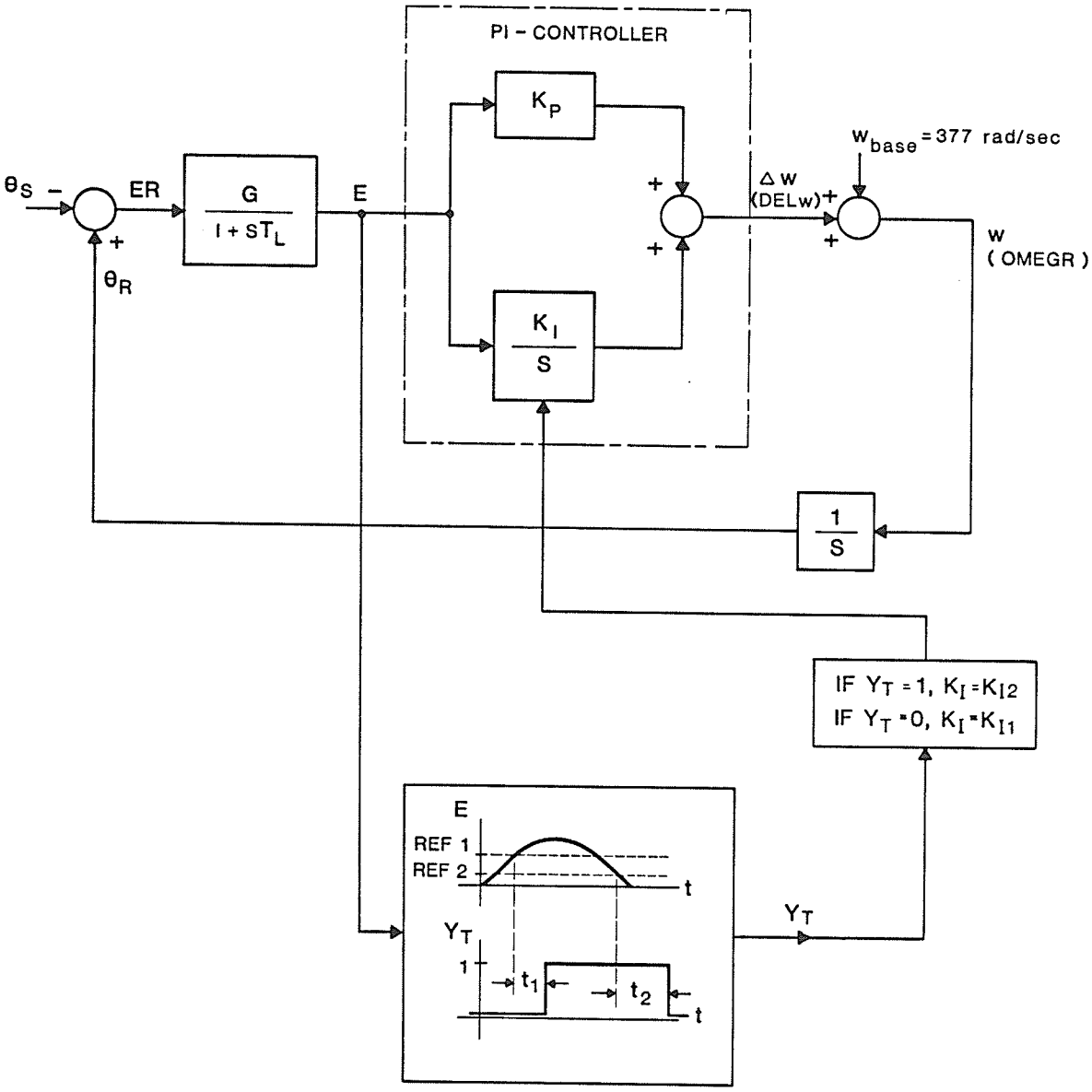

Figure 2.9. Phase-locked Loop Block Diagram

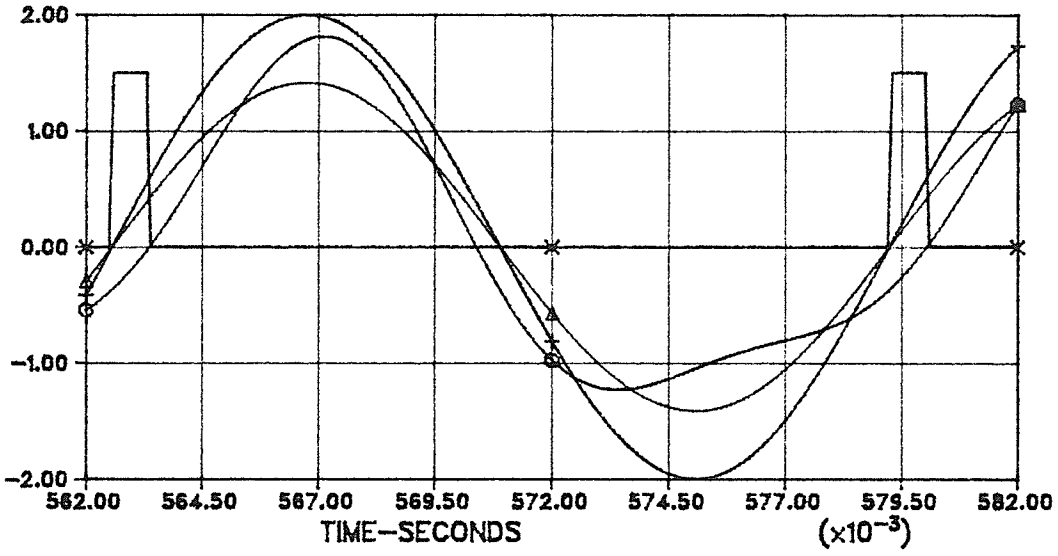

Figure 2.10. PLL Reference Voltage And System Voltage - PLL In Phase Lock

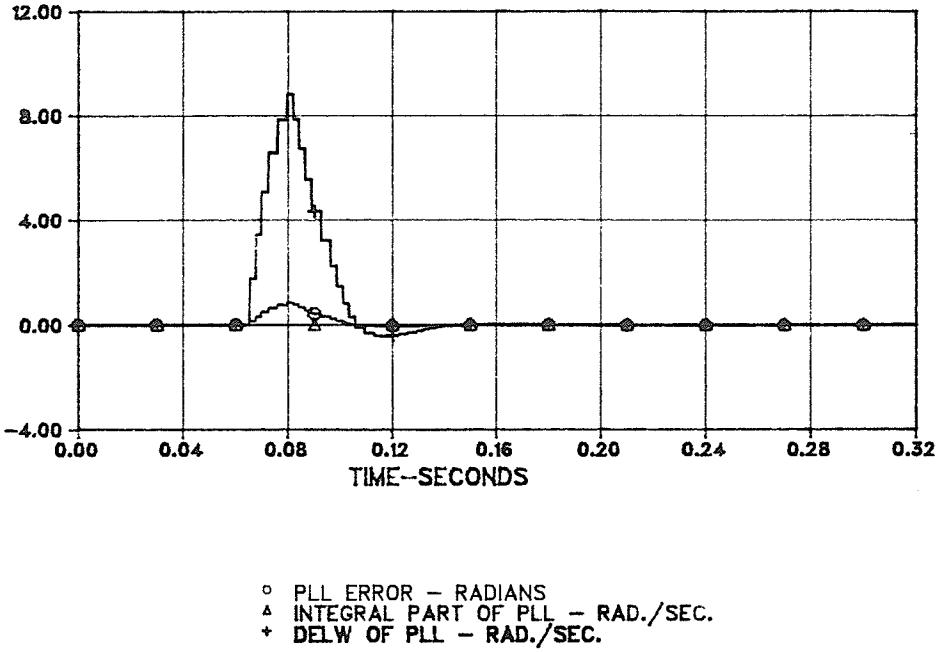

Figure 2.11. PLL Response For Phase Step Of 10°
No Filtering Of Phase Error

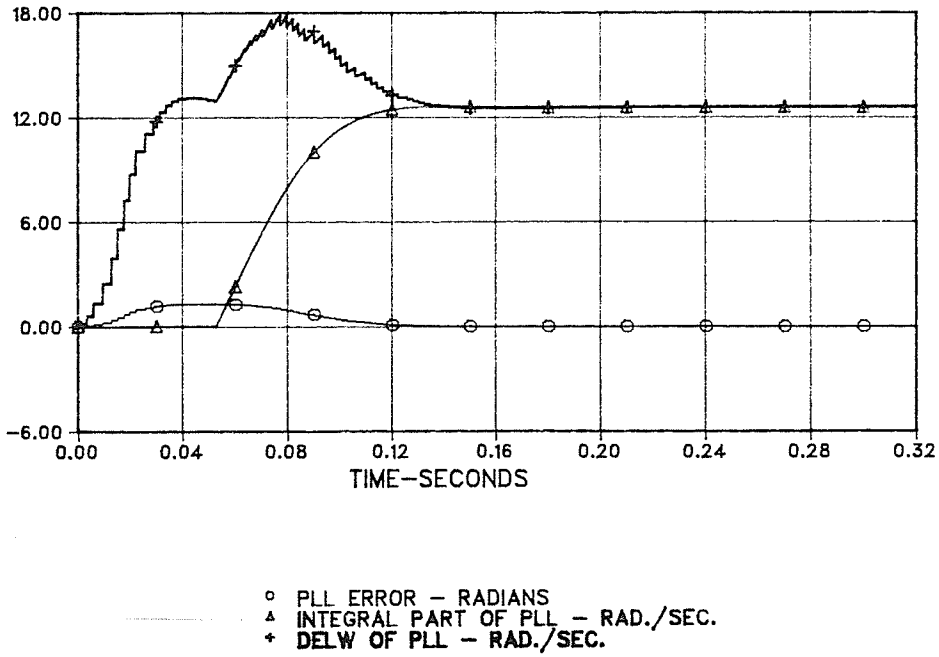

Figure 2.12. PLL Response For Frequency Step Of 2 Hz
No Filtering Of Phase Error

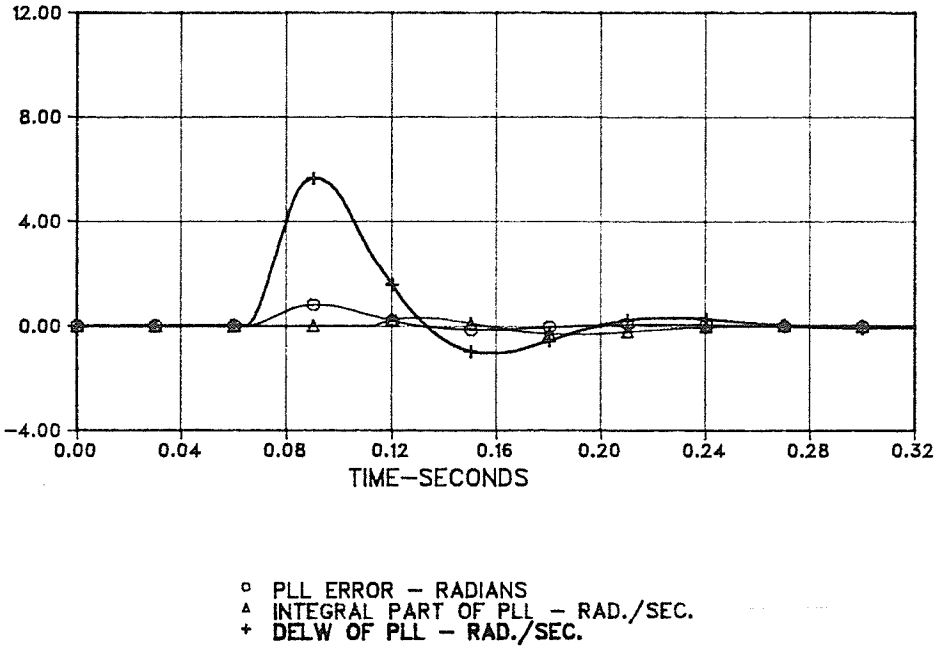

Figure 2.13. PLL Response For Phase Step Of 10°
8.3 ms Filtering Of Phase Error

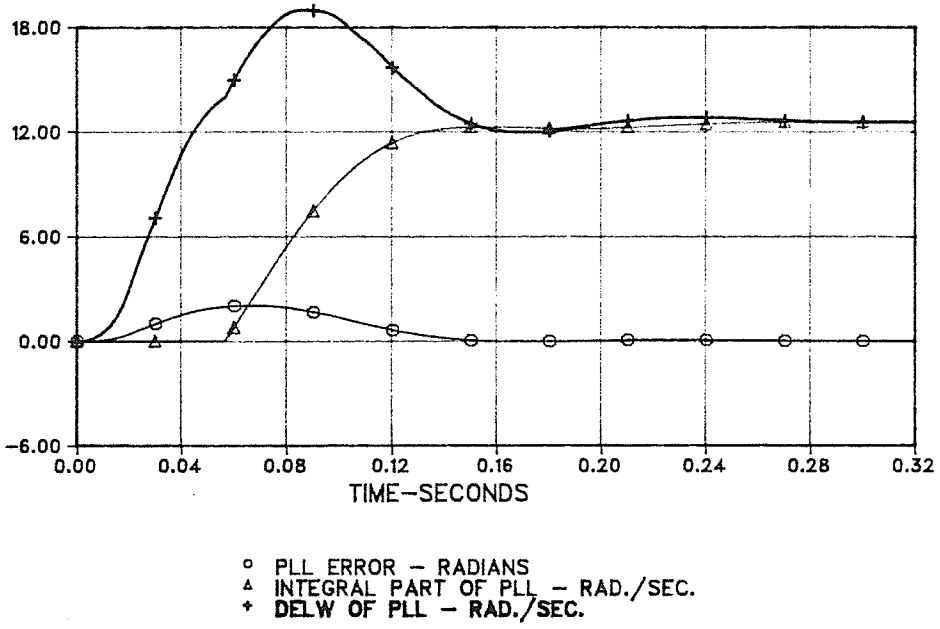

Figure 2.14. PLL Response For Frequency Step Of 2 Hz
8.3 ms Filtering Of Phase Error

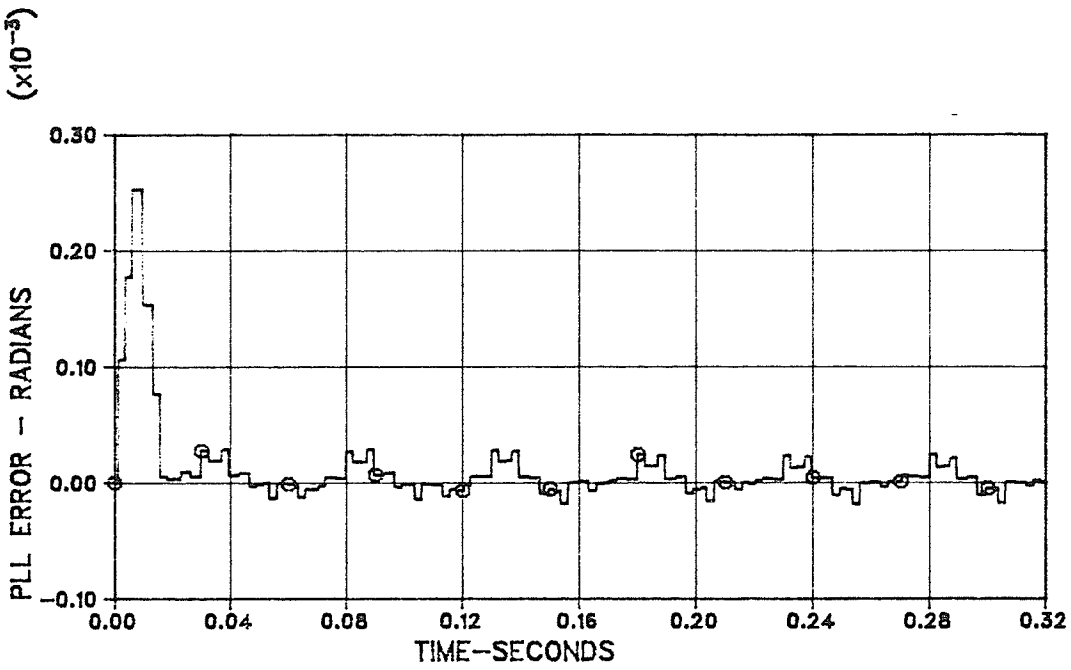

Figure 2.15. Steady-state Error Of PLL
Source 2^{nd} Harmonic Voltage 30 % @ - 30°

2.4. NUMERICAL FOURIER ANALYSIS OF TCR MODEL CURRENTS

A numerical Fourier analysis program is included to permit a direct analysis of the TCR waveforms generated by the digital model. The basis for the Fourier analysis is again defined by Equations 2.5 and 2.6. The integration required for the calculation of the coefficients a_n and b_n is done using the trapezoidal rule

$$\int_{t_k}^{t_{k+1}} f(t)\,dt = \frac{\Delta t}{2}\left\{ f(t_k) + f(t_{k+1}) \right\} \tag{2.15}$$

where Δt is the sampling period, t_k is the previous sample and t_{k+1} is the curent sample. The algorithm for computation of both the coefficients reduces to

$$a_n(\ b_n) = \frac{1}{N}\left[g_o + g_N + 2 \sum_{n=1}^{n=N-1} g_n \right] \tag{2.16}$$

where N is the number of sub-intervals per cycle. The function g represents the product $f \cdot \cos\omega_r t$ or $f \cdot \sin\omega_r t$ as appropriate. The arguments of the sine and cosine use the PLL position $\theta_r = \omega_r t$ for computing the Fourier coefficients. The program also includes a symmetrical component analysis of the waveforms.

The Fortran code for the numerical Fourier series program is included as Appendix 2.3.1. of Reference 7. The details of the expressions used for calculating the Fourier series terms and the symmetrical components can be seen in the appendix. The per unit system used in the program is consistent with that used in the previous sections of this chapter.

The numerical analysis of the TCR model waveforms for the case when the TCR is operating with $\alpha_o = 45°$ and with a second harmonic source voltage of 30 % magnitude at a phase of -30° is included as Appendix 2.3.2. of Reference 7. The Fourier analysis results taken from this appendix for the first three terms of the series are summarized below :

$$i_{rs} = -.0411 + .2083\cos(\theta_r - 94.7°) + .0792\cos(2\theta_r - 62.5°) \quad (2.17a)$$

$$i_{st} = -.0503 + .1888\cos(\theta_r + 151.°) + .0783\cos(2\theta_r + 120.3°) \quad (2.17b)$$

$$i_{tr} = +.0866 + .2123\cos(\theta_r + 25.2°) + .1286\cos(2\theta_r + 32.7°) \quad (2.17c)$$

$$i_r = (-.0737 + .2102\cos(\theta_r - 125.1°) + .0907\cos(2\theta_r - 117.2°))\sqrt{3} \quad (2.17d)$$

$$i_s = (-.0053 + .1927\cos(\theta_r + 116.3°) + .0909\cos(2\theta_r + 117.2°))\sqrt{3} \quad (2.17e)$$

$$i_t = (+.0791 + .2062\cos(\theta_r - 0.2°) + .0853\cos(2\theta_r + 0.7°))\sqrt{3} \quad (2.17f)$$

The results obtained from the numerical analysis of the model waveforms agree very well with the results exhibited in Equation 2.7 (which are included as Appendix 2.2.2. of Reference 7).

CHAPTER 3

THE TCR WITH FIRING ANGLE MODULATION - A CONTROLLED HARMONIC GENERATOR

3.1. ANALYTICAL ANALYSIS OF THE TCR WITH SINUSOIDAL FIRING ANGLE MODULATION

The objective in using sinusoidal modulation of the TCR firing angle is to generate TCR currents having a second harmonic (or dc) component with the appropriate magnitude and phase in order to cancel the same harmonic component produced as a result of the second harmonic source voltage. It is instructive to consider first the effect of modulation of the TCR firing angle on the harmonic content of the line currents, when operating with a balanced fundamental frequency ac system source voltage .

Sinusoidal modulation of the firing angle is defined by the equation:

$$\alpha = \alpha_o + \hat{\Delta} \cos(\theta_r + \delta) \quad = \alpha_o + \Delta \tag{3.1}$$

where

(a) α is the actual firing angle .

(b) α_o is the nominal firing angle from the main SVC controls.

(c) $\hat{\Delta}$ is the peak of the modulation.

(d) δ is the phase of the modulation.

(e) Δ is the modulation sinusoid.

(f) and $\theta_r = \omega t$, the PLL phase position.

Since firing of the thyristors is normally occurring at 60° intervals, with firing in each TCR phase occurring at 180° intervals, sinusoidal modulation can also be described by the equation

$$\Delta_{xy} = \hat{\Delta} \cos[\ (k-1)120° + \delta\ ] \tag{3.2}$$

where θ_s is arbitrarily set to zero degrees and is defined in Table 3.1.

Table 3.1. Firing Angle Definition For Sinusoidal Modulation

XY	k	Δ_{xy}	*Firing Angle* α_i
RS	1	$\hat{\Delta} \cos \delta$	$\alpha_1 = \alpha_o + \Delta_{rs}$ $\alpha_4 = \alpha_o - \Delta_{rs}$
ST	2	$\hat{\Delta} \cos(\delta + 120°)$	$\alpha_3 = \alpha_o + \Delta_{st}$ $\alpha_6 = \alpha_o - \Delta_{st}$
TR	3	$\hat{\Delta} \cos(\delta + 240°)$	$\alpha_5 = \alpha_o + \Delta_{tr}$ $\alpha_2 = \alpha_o - \Delta_{tr}$

Using this convention, and phase RS as the reference, Figure 3.1 shows the reference frame for the three phases. The thyristor numbering and current reference directions are as shown in Figure 2.4.

The analytical expression for the TCR currents for the circuit shown in Figure 2.4 when considering modulation as defined by Equations 3.1 and 3.2 is as follows:

In the positive half-cycle

$$i_{xy} = \sqrt{2} U_1 \left[\sin(\theta_s + \phi_f) - \sin(\alpha_o + \Delta) \right] \tag{3.3}$$

where $\alpha_o + \Delta + \phi_1 \leq \theta_s \leq \pi - (\alpha_o + \Delta) + \phi_1$.

In the negative half-cycle

$$i_{xy} = \sqrt{2}U_1\left[\sin(\theta_s + \phi_f) + \sin(\alpha_o - \Delta)\right] \tag{3.4}$$

where $\pi + (\alpha_o - \Delta) + \phi_1 \leq \theta_s \leq 2\pi - (\alpha_o - \Delta) + \phi_1$.

Equations 3.3 and 3.4 define i_{xy} in per unit. Consequently the impedance multiplying factor $1 / \omega L$ drops out of the equations. U_1 is the RMS voltage specified in per unit. Table 3.2 defines ϕ_1 and ϕ_f for the respective phases.

Table 3.2. Parameters for TCR currents

XY	ϕ_f	ϕ_1
RS	0°	0°
ST	-120°	120°
TR	120°	240°

Fourier analysis and symmetrical component transformations are used to analyze the line and TCR currents defined by Equations 3.3 and 3.4 respectively. Again the Fourier series and its coefficients are defined by Equations 2.5 and 2.6. The detailed equations used in the calculation of the Fourier series coefficients are shown in the listing of the program **FOURMOD** in Appendix 3.3.1. of Reference 7. The program outputs the magnitude and phase of the terms of the Fourier series $\frac{a_o}{2} + \sum_{n=1}^{n=7} c_n \cos(\omega t + \phi_n)$. The TCR reactor currents are given in per unit relative to the TCR reactor current base. The TCR line currents are given in per unit relative to the line current base. The symmetrical component analysis is carried out

in accordance with the transformation defined by Equation 2.8.

The characteristic harmonics of the thyristor controlled reactor are defined in Chapter 1. The definition assumes a balanced fundamental frequency source. A harmonic analysis of the TCR reactor currents described by Equations 3.3 and 3.4 (and the line currents computed from these reactor currents) should give only the characteristic harmonics for the case when the modulation magnitude is zero. Figure 3.2 shows the results of such a Fourier analysis, using the program **FOURMOD**.

The analysis for the *no modulation* case shows that there are no even harmonics (including the dc component). Of the odd harmonics, only the 3^{rd}, 5^{th}, and 7^{th} are plotted. The figure shows the magnitude of the TCR reactor current harmonic components for the entire range of firing angle. The magnitude is given in per unit, where 1.00 pu. is defined to be equal to the magnitude of the fundamental component of the TCR reactor current at $\alpha = 0°$. The harmonic components of the line currents in per unit are also given by Figure 3.2, where 1.00 pu. is the magnitude of the fundamental component of the line current at $\alpha = 0°$. Of course, the 3^{rd} harmonic component curve applies only to reactor currents, the third harmonic not being characteristic of the line currents.

Thus, for the TCR with equidistant firing at firing angle α_o and in the presence of a balanced fundamental frequency source, Figure 3.2 describes the harmonic current components. With sinusoidal modulation, the firing of thyristors is no longer equidistant. The analysis of TCR currents using **FOURMOD** is shown in Appendix 3.3.2 of Reference 7 for the case with $\alpha_o = 45°$, $\hat{\Delta} = 30°$ and $\delta = 0°$.

The first three terms of the Fourier series are summarized in Equation 3.5 .

$$i_{rs} = -.1977 + .3409\ cos\,(\theta_s - 90.0°) + .1875\ \cos(2\theta_s + 0.0°) \qquad (3.5a)$$

$$i_{st} = .0942 + .2243\ cos\,(\theta_s + 150.0°) + .1113\ \cos(2\theta_s - 60.0°) \qquad (3.5b)$$

$$i_{tr} = .0942 + .2243\ cos\,(\theta_s + 30.0°) + .1113\ \cos(2\theta_s + 60.0°) \qquad (3.5c)$$

$$i_r = (-.1685 + .2846\ cos\,(\theta_s - 113.2°) + .0943\ \cos(2\theta_s - 36.2°)\ )\sqrt{3} \qquad (3.5d)$$

$$i_s = (.1685 + .2846\ cos\,(\theta_s + 113.2°) + .0943\ \cos(2\theta_s - 143.6°)\ )\sqrt{3} \qquad (3.5e)$$

$$i_t = (.0000 + .2243\ cos\,(\theta_s + 00.0°) + .1113\ \cos(2\theta_s + 90.0°)\ )\sqrt{3} \qquad (3.5f)$$

The firing asymmetry results in generation of non-characteristic even harmonics, which include the dc component. The large difference between the positive half-cycle and negative half-cycle conduction period results in unbalances between the phases of the fundamental component and the harmonics. There is a 15.5% unbalance in the fundamental component for this 30° peak modulation level.

Figure 3.3 shows that the phase of the second harmonic positive sequence component of the line current rotates in the direction of increasing phase δ of the modulation signal. The magnitude remains constant at 0.099 pu. for a peak modulation $\hat{\Delta} = 30°$. Note that relative to the magnitude of the 60 Hz signal at $\alpha = 45°$, a peak modulation of 30° results in 37.6% second harmonic component.

Figure 3.4 shows that the phase of the dc positive sequence component rotates in a direction opposite to that of increasing phase of the modulation signal. A peak modulation $\hat{\Delta} = 30°$ results in a dc component magnitude of 0.0973 pu., or 37% with respect to the 60 Hz component at $\alpha = 45°$.

Tables 3.3 shows the behaviour of the line current positive and negative sequence phasors for several other harmonics. In terms of phase angle, the dc, third harmonic, and sixth harmonic sequence phasors rotate in the direction of decreasing phase when the phase δ of the firing angle modulation increases. The fourth harmonic negative sequence phasor behaves in a similar manner as the second harmonic positive sequence phasor, the latter shown in Figure 3.1 . The fifth harmonic positive sequence component's phase decreases whereas the seventh harmonic negative

Table 3.3. Phase of Symmetrical Components

Of Line Current Harmonics Versus

Firing Angle Modulation Phase

$\hat{\Delta} = 30°$ $\alpha_o = 45°$

Mod. Phase (Deg.)	DC (Deg.)	2^{nd} (Deg.)	3^{rd} (Deg.)		4^{th} (Deg.)		5^{th} (Deg.)		6^{th} (Deg.)		7^{th} (Deg.)	
δ	-ve	-ve	+ve	-ve	+ve	-ve	+ve	-ve	+ve	-ve	+ve	-ve
0	210	210	240	300	330	30	60	120	150	210	60	120
30	240	--	300	240	--	0	0	120	120	240	60	180
60	270	30	0	180	150	330	300	120	90	270	60	240
90	300	--	60	120	--	300	240	120	60	300	60	300
120	330	210	120	60	330	270	180	120	30	330	60	0
150	0	--	180	0	--	240	120	120	0	0	60	60
180	30	30	240	300	150	210	60	120	330	30	60	120
210	60	--	300	240	--	180	0	120	300	60	60	180
240	90	210	0	180	330	150	300	120	270	90	60	240
270	120	--	60	120	--	120	240	120	240	120	60	300
300	150	30	120	60	150	90	180	120	210	150	60	0
330	180	--	180	0	--	60	120	120	180	180	60	60

sequence component's phase increases with increasing phase δ. Note, the symbol -- denotes that the magnitude associated the phase entry has a zero value.

The magnitudes of the sequence components depend on the peak modulation $\hat{\Delta}$ and the firing angle α_o, with the phase of the modulation having no influence on the magnitude of the sequence phasors. On the other hand when the modulation phase δ is held constant , a change in firing angle α_o results only in a change in current phasor magnitude, as long as firing angle limits are not encountered.

Figures 3.5 through 3.7 show the effect of changing the firing angle modulation magnitude $\hat{\Delta}$ on the positive sequence dc, 120 Hz and 60 Hz phasors. The modulation phase is held constant at $\delta=0°$. The reference for the per unit values is the 60

Hz component magnitude at $\alpha_o = 0°$ (1.00 pu). Clearly, at $\hat{\Delta} = 0°$, only characteristic harmonics exist. For all firing angles, the magnitudes of the dc and 120 Hz line current positive sequences phasors increase with increasing modulation magnitude as expected. The phase of these current components is independent of the modulation magnitude. The modulation of firing angle does change the 60 Hz component of line current to some extent, as can be seen in Figure 3.7. Any change represents the interaction that would exist between the modulation controller and the normal controls determining the nominal firing angle.

The above analysis suggests that by controlling the magnitude and phase of the firing angle modulation signal appropriately, it is possible to control the harmonic content of the thyristor controlled reactor. That is, at least for one specified non-characteristic harmonic at a time the TCR can be used to output a desired magnitude and phase.

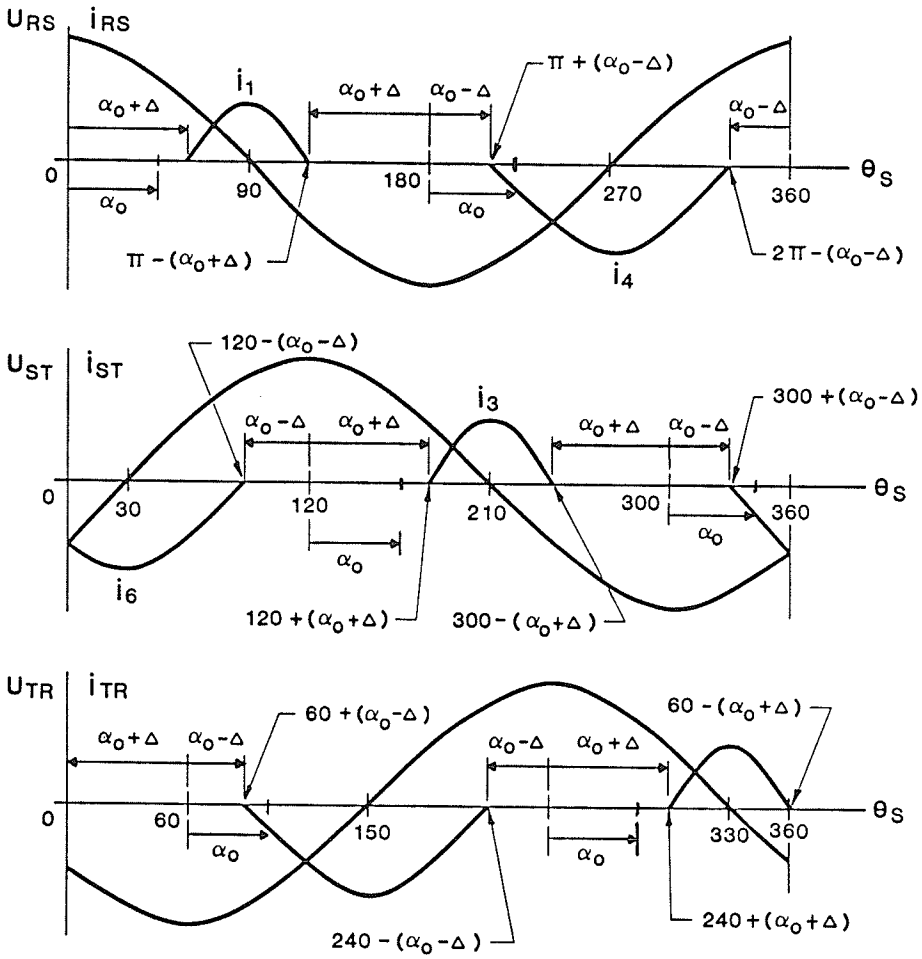

Figure 3.1. Phase Reference Frame For Sinusoidal Modulation - Balanced Fundamental Source

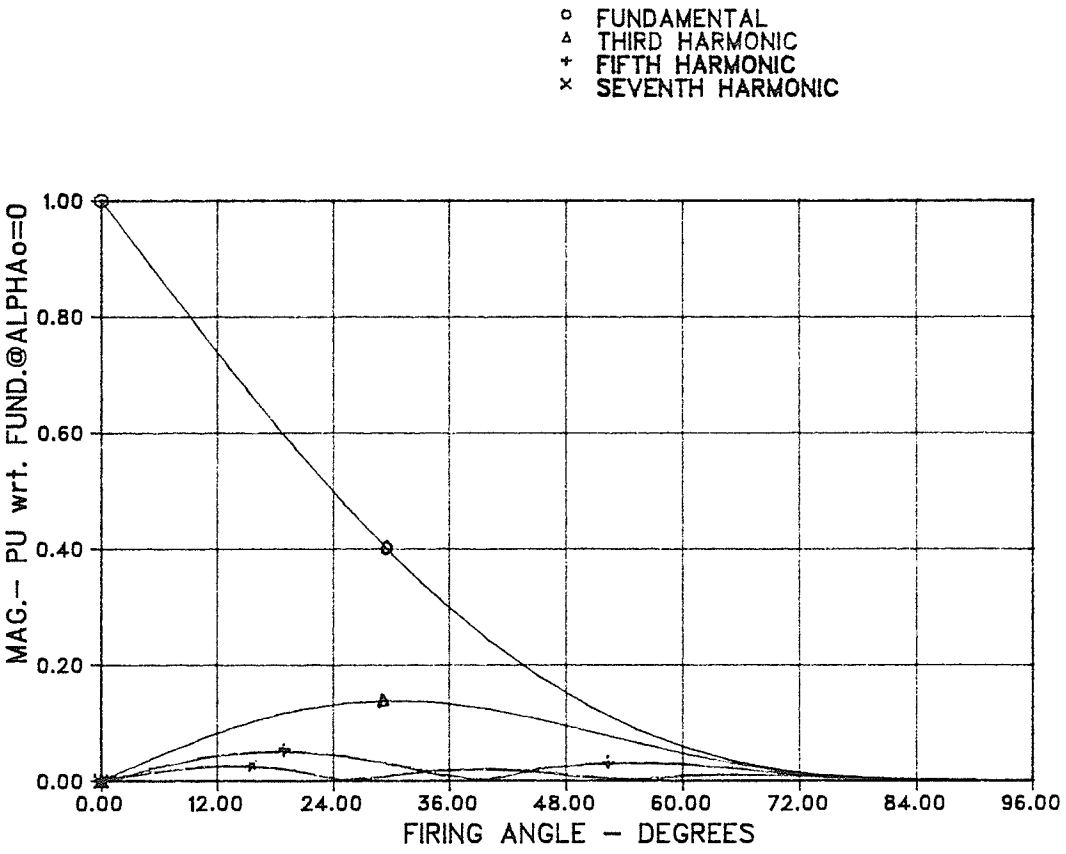

Figure 3.2. TCR Characteristic Harmonics Versus Firing Angle - No Modulation

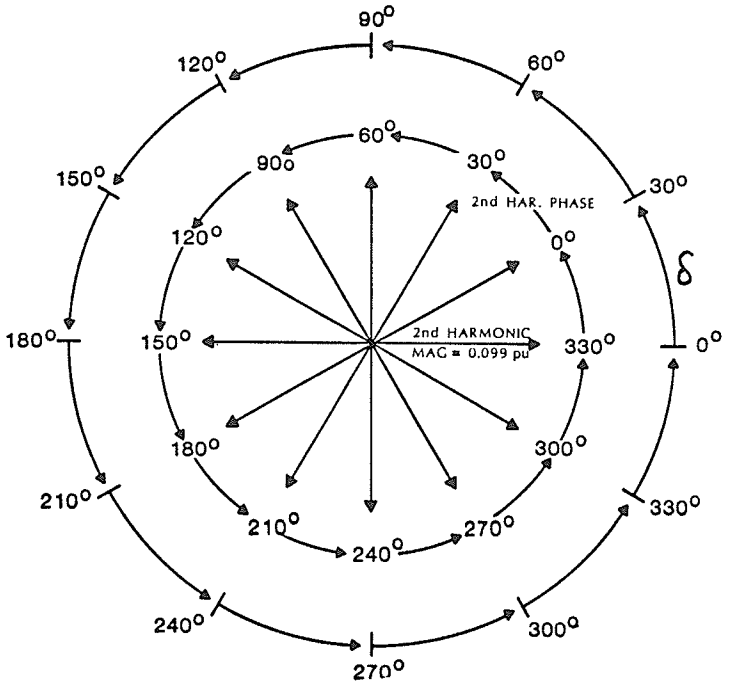

Figure 3.3. Phase Of Positive Sequence Second Harmonic Line Current Versus Phase δ Of Modulation $\alpha_o = 45°$ $\hat{\Delta} = 30°$

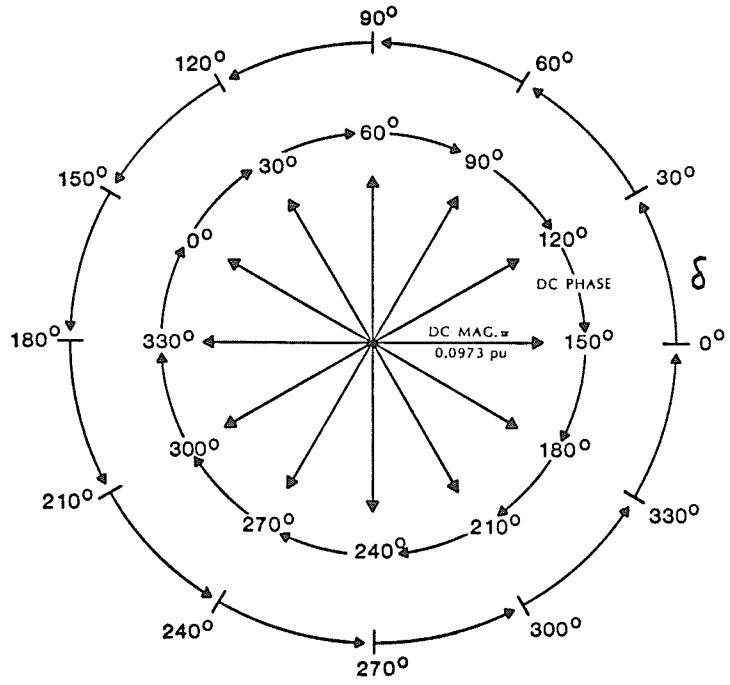

Figure 3.4. Phase Of Positive Sequence DC Line Current Versus Phase δ Of Modulation $\alpha_o = 45°$ $\hat{\Delta} = 30°$

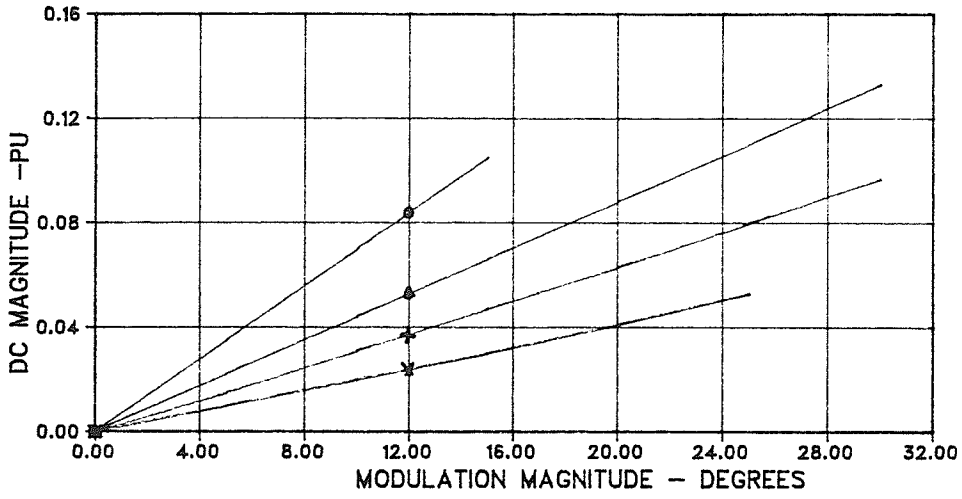

Figure 3.5. Magnitude Of Positive Sequence DC Line Current Versus Modulation Peak Magnitude $\hat{\Delta}$. $\delta = 0°$

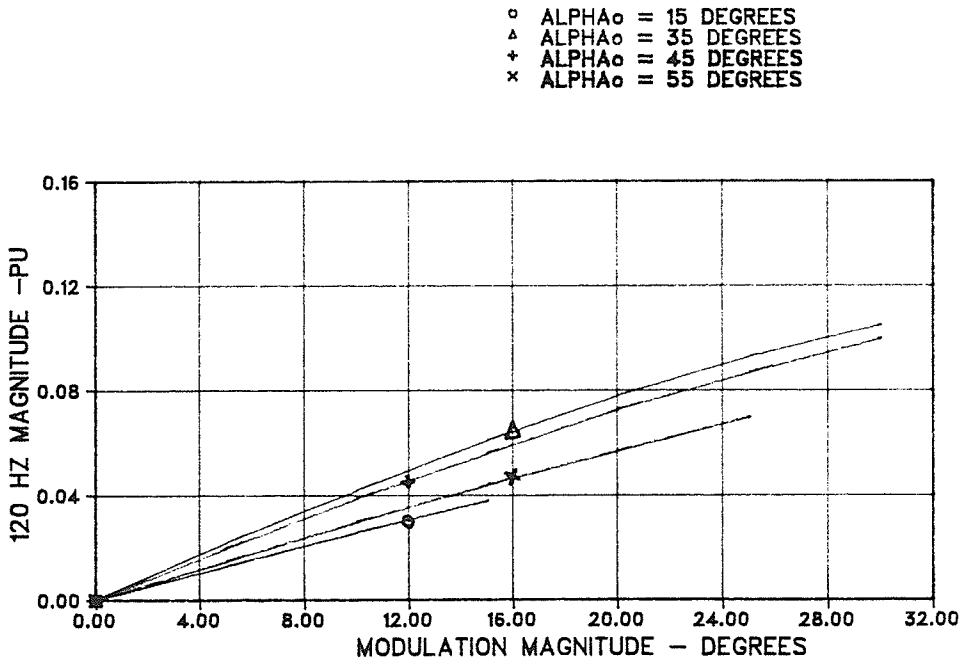

Figure 3.6. Magnitude Of Positive Sequence 2^{nd} Harmonic Line Current Versus Modulation Peak Magnitude $\hat{\Delta}$. $\delta = 0°$

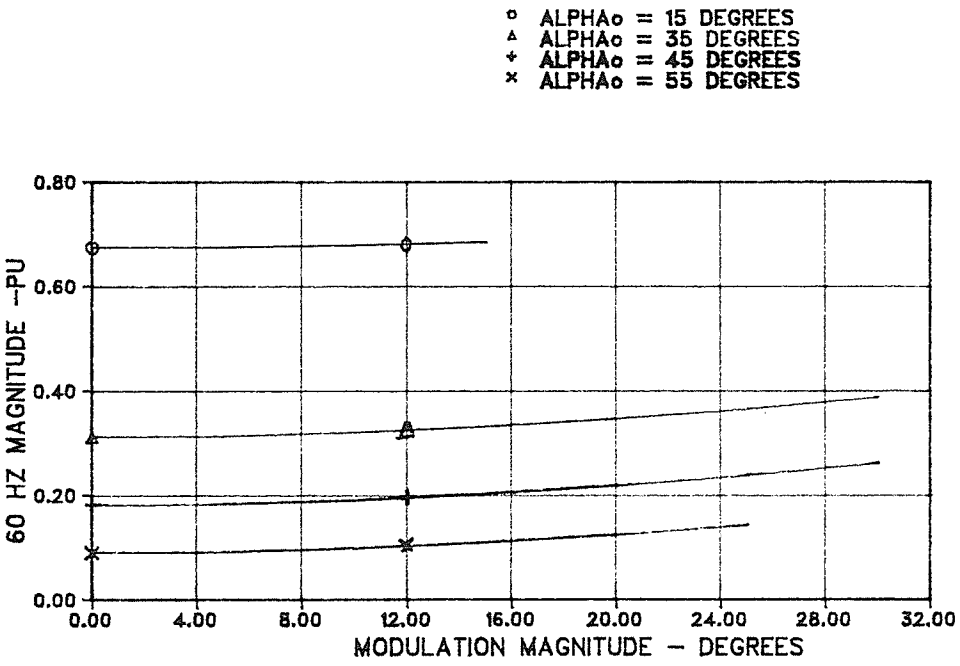

Figure 3.7. Magnitude Of Positive Sequence 60 Hz Line Current Versus Modulation Peak Magnitude $\hat{\Delta}$. $\delta = 0°$

3.2. SIMULATION OF THE TCR WITH FIRING ANGLE MODULATION

The digital model of the thyristor controlled reactor is used to evaluate the performance of controller using firing angle modulation to eliminate specified harmonic components in the TCR line current. In this section, it is shown that the digital model with sinusoidal modulation of firing angle gives the same results as the analytical analysis in Section 3.1.

The modulation controller, which is described in Chapter 4, outputs a phasor quantity, expressed in terms of its real component CRL and imaginary component CIMG. A sinusoidal time-varying signal at fundamental frequency defined by

$$\Delta = \hat{\Delta} \cos(\omega_r + \delta) \tag{3.6}$$

can be derived from this phasor information using the relationships

$$\hat{\Delta} = \sqrt{CRL^2 + CIMG^2} \qquad \delta = \arctan \frac{CIMG}{CRL} \tag{3.7}$$

Then the equations given in Table 3.1 can be used directly to compute the modulation required for each thyristor.

Alternatively, the sinusoid defined by Equation 3.6 can be constructed by using two phase-locked loop signals, one in quadrature with the other. This is shown by the equation

$$\hat{\Delta} \cos(\omega_r t + \delta) = CRL\ (\cos\omega_r t) + CIMG\ (-\sin\omega_r t) \tag{3.8}$$

where $CRL = \hat{\Delta} \cos\delta$ and $CIMG = \hat{\Delta} \sin\delta$. Sampling the resultant firing angle modulation signal at 60° intervals defines for each fundamental frequency cycle the six modulation quantities $\Delta\alpha_i$, $i = 1, 6$ that are required. By assigning samples 180° apart to positive and negative half-cycle thyristors, the modulation defined by the equations given in Table 3.1 can be realized.

The TCR model computes the appropriate modulation signal using the CRL and CIMG phasor components. These two quantities can be derived from the closed-loop controller output or can be manually set. Manual control of the modulation is used in this section to show that the model gives essentially the same results as are derived analytically in Section 3.1.

The case with $\alpha_o = 45°$, $\hat{\Delta} = 30°$ and $\delta = 0°$ was simulated. An analysis of the digital model current waveforms using the program FOURNUM gives for the first three terms of the Fourier series.

$$i_{rs} = -.1988 + .3412\ cos\,(\theta_s - 88.9°) + .1771\ cos(2\theta_s - 0.9°) \quad (3.9a)$$

$$i_{st} = .0969 + .2328\ cos\,(\theta_s + 150.0°) + .1131\ cos(2\theta_s - 62.0°) \quad (3.9b)$$

$$i_{tr} = .0950 + .2306\ cos\,(\theta_s + 29.9°) + .1120\ cos(2\theta_s + 57.3°) \quad (3.9c)$$

$$i_r = (-.1697 + .2873\ cos\,(\theta_s - 113.6°) + .0875\ cos(2\theta_s - 39.6°)\ )\sqrt{3} \quad (3.9d)$$

$$i_s = (.1707 + .2889\ cos\,(\theta_s + 113.9°) + .0909\ cos(2\theta_s - 141.9°)\ )\sqrt{3} \quad (3.9e)$$

$$i_t = (.0011 + .2319\ cos\,(\theta_s + 0.2°) + .1122\ cos(2\theta_s + 87.9°)\ )\sqrt{3} \quad (3.9f)$$

This result compares closely with Equation 3.5. The complete output for the case is given in Appendix 3.3.3. of Reference 7 and is directly comparable to the analytical results of Appendix 3.3.2. of Reference 7.

Figure 3.8 shows the TCR current and voltage waveforms and the firing pulses. The sinusoidal distribution of the firing pulses can be noted. The firing angles measured from the figure and modulation data for each phase are shown in Table 3.4. The firing pulse asymmetry results in significant differences between the positive half-cycle and negative half-cycle conduction periods.

Table 3.4. Firing Angle Modulation Data $\hat{\Delta} = 30°$ $\delta = 0°$ $\alpha_o = 45°$			
Phase	$\Delta\alpha$	**Actual Firing Angle**	
RS	**30°**	$\alpha_1 = 75°$	$\alpha_4 = 15°$
ST	**-15°**	$\alpha_3 = 30°$	$\alpha_6 = 60°$
TR	**-15°**	$\alpha_5 = 30°$	$\alpha_2 = 60°$

The simulations for cases with fixed modulation magnitude and varying phase, and fixed phase with varying modulation magnitude, give the same results as the analytical analysis. Thus the simulation results for all those cases are not repeated here.

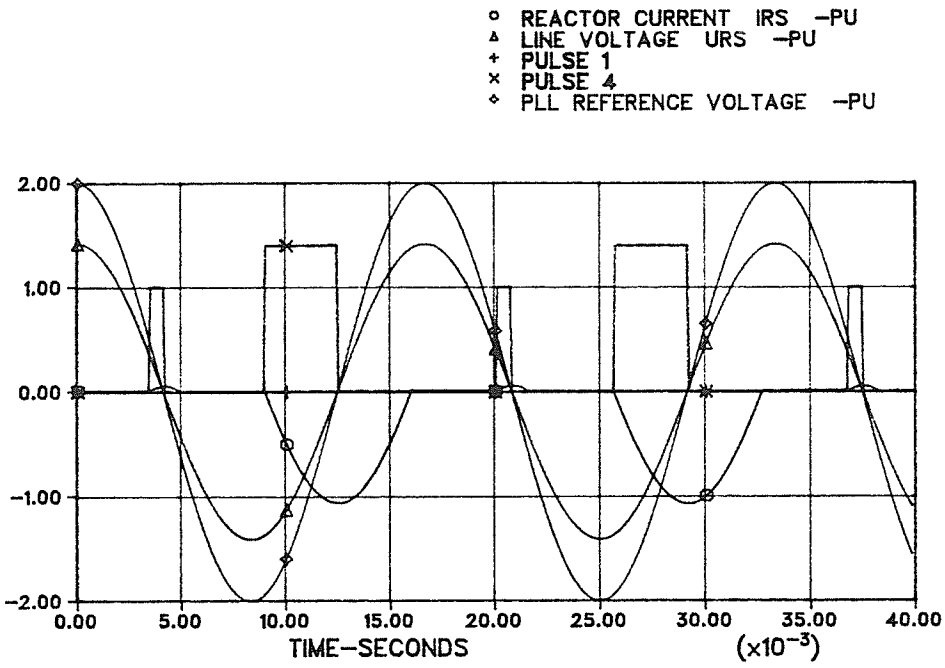

Figure 3.8.(a) TCR Current, Voltage, And Firing Pulse Waveforms
α_o = 45° 60 Hz Source
Sinusoidal Modulation. $\hat{\Delta}$ = 30° δ = 0°

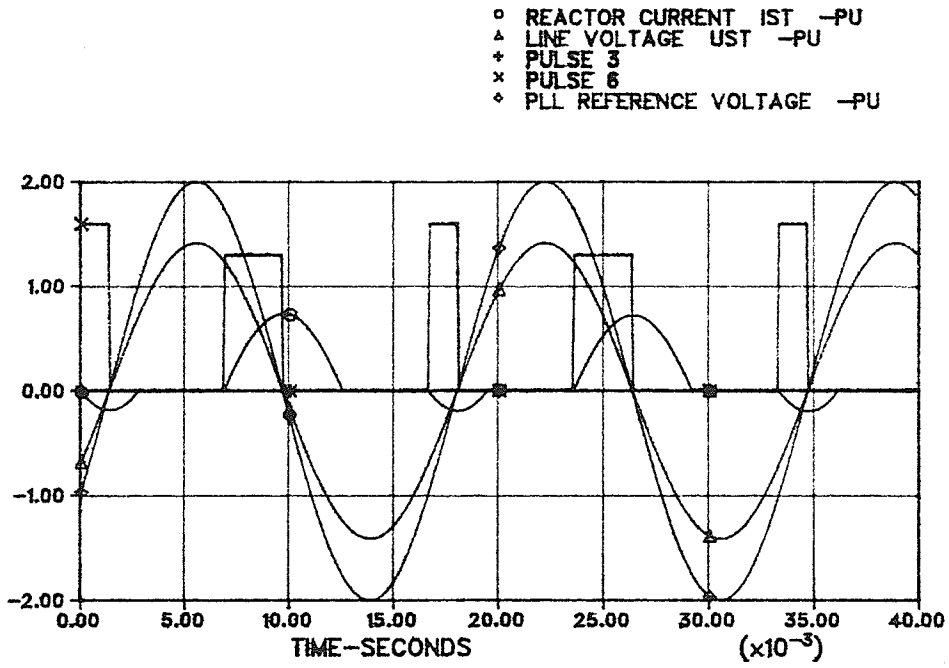

Figure 3.8.(b) TCR Current, Voltage, And Firing Pulse Waveforms
α_o = 45° 60 Hz Source
Sinusoidal Modulation. $\hat{\Delta}$ = 30° δ = 0°

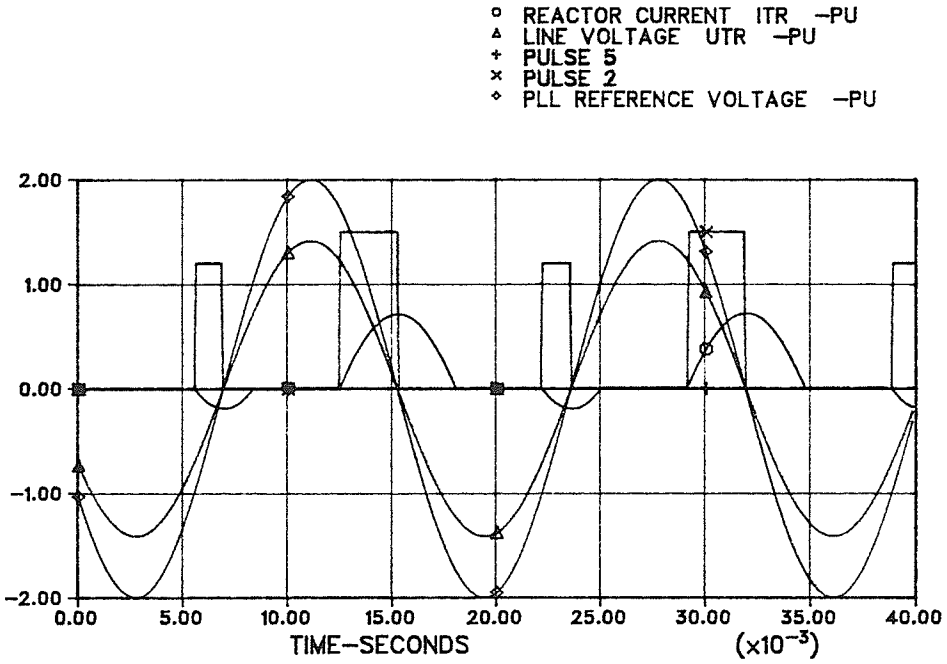

Figure 3.8.(c) TCR Current, Voltage, And Firing Pulse Waveforms
α_o = 45° 60 Hz Source
Sinusoidal Modulation, $\hat{\Delta}$ = 30° δ = 0°

CHAPTER 4

DESCRIPTION AND PERFORMANCE OF FIRING ANGLE MODULATION CONTROLLER

4.1 CONTROL PARAMETER MEASUREMENT

From Table 3.2, it appears that the sequence components of the line currents would be suitable control parameters for the firing angle modulation controller. The positive sequence should be used for the second harmonic. The negative sequence should be used for the fourth harmonic. Either sequence component could be used if it is desirable to use the dc component as the control parameter. In subsequent sections, only the second harmonic component or the dc component is considered as a control parameter.

For control purposes, a relatively fast measurement of the sequence components is required. The paper listed as Reference 4 describes some techniques of coordinate transformation suitable for control systems used for compensation and balancing of three phase loads. The techniques described in the paper use the transformation from (r,s,t) - coordinates to (α,β) - coordinates and the symmetrical component transformation.

The $(r,s,t) - to - (\alpha,\beta)$ transformation is a scalar transformation and as such applies to instantaneous values of current and voltage, as well as to phasor values. The symmetrical component transformation is a vector transformation. In order to apply the symmetrical component transformation to instantaneous signals, the (α,β) - components must be translated to their vector (phasor) equivalents. To

accomplish this, the instantaneous value of the quadrature component of the signal must be determined. The paper describes techniques for such *vector identification* .

Another method that can be used to accomplish vector identification is to make use of the phase-locked loop signals. The PLL is locked to the fundamental positive sequence system voltage and therefore may be used as the phasor reference. The PLL also follows fundamental frequency excursions. A controller thus can use the PLL reference to produce other reference phasors at harmonic frequencies. This measuring technique is further described in the following sections.

The (α,β) - transformation that is used is defined by:

$$\begin{bmatrix} i_\alpha(t) \\ i_\beta(t) \end{bmatrix} = \begin{bmatrix} \frac{2}{3} & \frac{-1}{3} & \frac{-1}{3} \\ 0 & \frac{1}{\sqrt{3}} & \frac{-1}{\sqrt{3}} \end{bmatrix} \cdot \begin{bmatrix} i_r(t) \\ i_s(t) \\ i_t(t) \end{bmatrix} \tag{4.1}$$

The ground phase component is neglected since no zero sequence can flow in TCR line connections.

The symmetrical component transformation that is used is defined by:

$$\begin{bmatrix} \tilde{i}_1 \\ \tilde{i}_2 \end{bmatrix} = \frac{1}{2} \begin{bmatrix} 1 & j \\ 1 & -j \end{bmatrix} \cdot \begin{bmatrix} \tilde{i}_\alpha \\ \tilde{i}_\beta \end{bmatrix} \tag{4.2}$$

The symbol $\tilde{i}$ denotes a phasor or vector. The symbol $\tilde{i}_1$ denotes the positive sequence phasor and $\tilde{i}_2$ denotes the negative sequence phasor. The symbols $\tilde{i}_\alpha$ and $\tilde{i}_\beta$ denote the phasor values of the time- varying signals i_α and i_β respectively.

Clearly to compute instantaneous values for the symmetrical components of the time-varying signals i_r, i_s and i_t a transformation symbolically defined by

$$\begin{bmatrix} \tilde{i}_\alpha \\ \tilde{i}_\beta \end{bmatrix} = \begin{bmatrix} T_{11} & T_{12} \\ T_{21} & T_{22} \end{bmatrix} \cdot \begin{bmatrix} i_\alpha(t) \\ i_\beta(t) \end{bmatrix} \tag{4.3}$$

is required.

The basis for finding the appropriate transformation T follows from the requirement to extract from a signal the phasor components of a specified frequency as a dc value. Consider a signal $f(t)$ described by its Fourier series as

$$f(t) = \frac{c_o}{2} + \sum_{n=1}^{n=\infty} c_n \cos(n\omega t + \phi_n) \tag{4.4}$$

If the signal is multiplied by the sinusoid $\cos(\omega_r t + \theta_r)$ where $\omega_r = n\omega$ for $n = k$ then

$$f(t) \cdot \cos(\omega_r t + \theta_r) = \frac{c_k}{2} \cos(\phi_k) \cos(\theta_r) \tag{4.5}$$

$$+ \frac{c_k}{2} \sin(\phi_k) \sin(\theta_r) + \sum_{n=1, n\neq k}^{n=\infty} d_n \cos(n\omega_r t + \gamma_n)$$

The first two terms, the dc value of the signal, result from the term of the series that has the frequency equal to ω_r. d_n and γ_n denote the magnitude and phase respectively of the terms resulting from the product of sinusoids. Similarly,

$$f(t) \cdot \sin(\omega_r t + \theta_r) = \frac{c_k}{2} \cos(\phi_k) \sin(\theta_r) \tag{4.6}$$

$$- \frac{c_k}{2} \sin(\phi_k) \cos(\theta_r) + \sum_{n=1, n\neq k}^{n=\infty} g_n \sin(n\omega_r t + \xi_n)$$

Recall that the component c_k can be expressed as

$$c_k = \hat{c}_k \cos(k\omega t + \phi_k) \tag{4.7}$$

$$= \hat{c}_k \cos(\phi_k) \cos(k\omega t) + \hat{c}_k \sin(\phi_k) (-\sin(k\omega t))$$

$$= \mathrm{Re}[\tilde{c}_k] \cos(k\omega t) + \mathrm{Im}[\tilde{c}_k] (-\sin(k\omega t))$$

where $\cos(\omega t)$ is the phasor reference (then $-sin(\omega t)$ corresponds to the $+j-axis$).

Therefore

$$2 f(t) \cdot \cos(\omega_r t + \theta_r) \tag{4.8a}$$

$$= \mathrm{Re}[\tilde{c}_k] \cos(\theta_r) + \mathrm{Im}[\tilde{c}_k] \sin(\theta_r) + (sinusoids)$$

$$2 f(t) \cdot \sin(\omega_r t + \theta_r) \tag{4.8b}$$

$$= \mathrm{Re}[\tilde{c}_k] \sin(\theta_r) - \mathrm{Im}[\tilde{c}_k] \cos(\theta_r) + (sinusoids)$$

$\mathrm{Re}[\tilde{c}_k]$ denotes the real part and $\mathrm{Im}[\tilde{c}_k]$ denotes the imaginary part of the phasor $\tilde{c}_k$.

In general, the sinusoidal terms must be filtered, and thus are neglected in the next steps. Note that ω_r and θ_r are synchronized to the phase-locked loop. Θ_r is an arbitrary but constant phase position of the PLL with respect to the reference coordinate system.

Solving for the components of the phasor c_k using Equation 4.8, gives

$$\begin{bmatrix} \frac{1}{2} \mathrm{Re}[\tilde{c}_k] \\ \frac{1}{2} \mathrm{Im}[\tilde{c}_k] \end{bmatrix} = \begin{bmatrix} f(t) \cos \omega_r t \\ -f(t) \sin \omega_r t \end{bmatrix} \tag{4.9}$$

From Equation 4.9, and considering the (α,β) -system of currents which are defined by

$$\tfrac{1}{2}\,\tilde{i}_{\alpha} = i_{\alpha}(t)\cos(\omega_r t) + j\;\tilde{i}_{\alpha}(t)\,(-\sin(\omega_r t)) \tag{4.10}$$

$$\tfrac{1}{2}\,\tilde{i}_{\beta} = i_{\beta}(t)\cos(\omega_r t) + j\;\tilde{i}_{\beta}(t)\,(-\sin(\omega_r t))$$

Clearly $T_{11} = T_{22} = (\cos(\omega_r t) - j\,\sin(\omega_r t)\;)$ and $T_{12} = T_{21} = 0$.

Substituting Equation 4.10 into Equation 4.2 gives the result

$$\begin{bmatrix} \tilde{i}_1 \\ \tilde{i}_2 \end{bmatrix} = \begin{bmatrix} i_{\alpha}(t)\,C + i_{\beta}(t)\,S & j(i_{\beta}(t)\,C - i_{\alpha}(t)\,S) \\ i_{\alpha}(t)\,C - i_{\beta}(t)\,S & j(-i_{\beta}(t)\,C - i_{\alpha}(t)\,S) \end{bmatrix}. \tag{4.11}$$

where $C = \cos(\omega_r t)$ and $S = \sin(\omega_r t)$.

Using Equation 4.11, the positive sequence phasor real and imaginary components for the k^{th} are given by the equation

$$\begin{bmatrix} \mathrm{Re}[\tilde{i}_1] \\ \mathrm{Im}[\tilde{i}_1] \end{bmatrix} = \begin{bmatrix} \cos(\omega_r t) & \sin(\omega_r t) \\ -\sin(\omega_r t) & \cos(\omega_r t) \end{bmatrix} \cdot \begin{bmatrix} i_{\alpha}(t) \\ i_{\beta}(t) \end{bmatrix}. \tag{4.12}$$

The negative sequence phasor real and imaginary components are given by the equation

$$\begin{bmatrix} \mathrm{Re}[\tilde{i}_2] \\ \mathrm{Im}[\tilde{i}_2] \end{bmatrix} = \begin{bmatrix} \cos(\omega_r t) & -\sin(\omega_r t) \\ -\sin(\omega_r t) & -\cos(\omega_r t) \end{bmatrix} \cdot \begin{bmatrix} i_{\alpha}(t) \\ i_{\beta}(t) \end{bmatrix}. \tag{4.13}$$

Figure 4.1 shows how Equation 4.12 is implemented for measuring the positive sequence real and imaginary phasor components of the TCR line currents. The (α,β) - system is calculated using Equation 4.1. The positive sequence harmonic component of the signal that is measured is determined by parameter K. If $K = 0$, the dc component is measured. If $K = 1$, the 60 Hz component is measured, and so on.

The phase position of the reference sinusoid is determined by θ_r, which is

adjusted to correct the phase position of the PLL to coincide with the desired coordinate system.

Subroutine **PSEQ** in the digital model calculates the positive sequence real and imaginary parts of the phasor for the dc, the 60 Hz, and the 120 Hz components exactly as shown in Figure 4.1. $\Theta_r = -90°$ is required to correct the phase of the measuring system to give the same results as the numerical Fourier analysis program **FOURNUM**. The listing for subroutine **PSEQ** is included in Appendix 2.1.6. of Reference 7.

Filtering to eliminate the sinusoidal terms shown in Equation 4.5 and 4.6 is accomplished using an averaging filter. The signal is sampled 24 times per cycle and stored in a shift-register containing 24 registers. Each new sample is stored in register 1, the previous samples shifted up one register. The output is derived by summing the contents of the 24 registers and averaging the result (1/24) after each sample pulse. Thus, the output will give the dc component of any sinusoid whose period is a multiple of the fundamental period, including the fundamental. **AVGFIL25** is the subroutine that does the filtering. Its listing is shown in Appendix 2.1.8. of Reference 7.

Figures 4.2, 4.3 and 4.4 show the output of subroutine **PSEQ** and **AVGFIL25** for the dc, fundamental and the second harmonic components respectively of the TCR line currents. The measurements are from the simulation of the case $\alpha_o = 45°$. The TCR source has a second harmonic voltage of 30 % magnitude at a phase of -30°. The figures show the response from the startup of the simulation. Note that it takes one cycle for the filter to initialize. The filter is very effective in eliminating large oscillations. As an example, for the second harmonic component the 60 Hz signal represents a large sinusoidal noise signal with zero dc average which must be filtered .

Table 4.1 shows a comparison of the output of the measurement technique described above and the output of the Fourier analysis program **FOURNUM** which provides an analysis of the digital simulation current waveforms. Note that the **FOURNUM** program outputs RMS values in per unit and the measuring system outputs peak values in per unit. The scale factor between the two results is $\sqrt{6}$. The sequence measuring system provides signals with an accuracy adequate for use as a control parameter for the modulation controller. The measuring system delay is at most a cycle (60 Hz).

Table 4.1. Comparsion Of Numerical Fourier Analysis With Model Sequence Measuring System

$\alpha_o = 45°$. *Source* 2^{nd} *Harmonic* : 30% @ $-30°$.

********	**Fourier Analysis**		**Model**	
+ve Seq.	**Mag-pu**	**Phase-deg.**	**Mag-pu**	**Phase-deg.**
DC	**.0436**	**-147.7**	**(.0450) $\sqrt{6}$**	**-147.3**
60 Hz	**.2036**	**-122.8**	**(.2060) $\sqrt{6}$**	**-122.8**
120 Hz	**.0874**	**-118.4**	**(.0886) $\sqrt{6}$**	**-119.2**

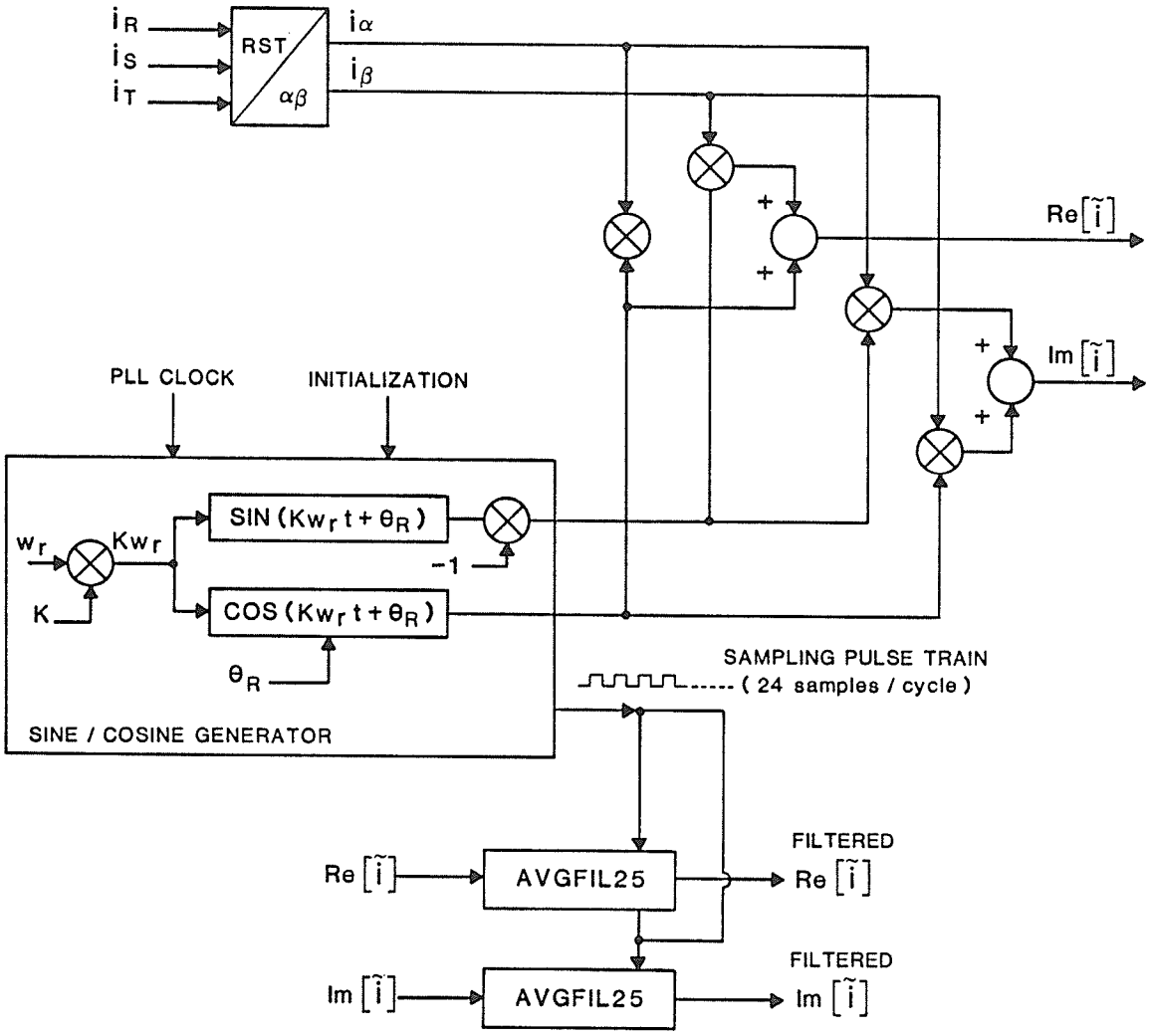

Figure 4.1. Measurement Of Positive Sequence Phasor Components Of TCR Line Currents

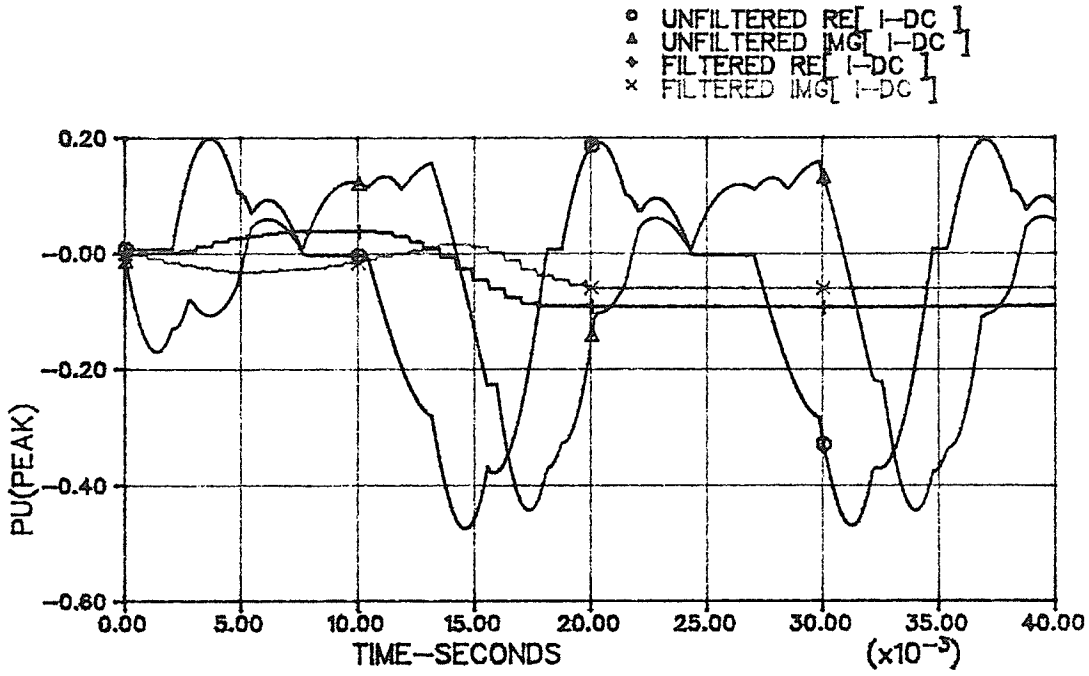

Figure 4.2. Measured Positive Sequence DC Line Current Component. $\alpha_o = 45°$
No Modulation

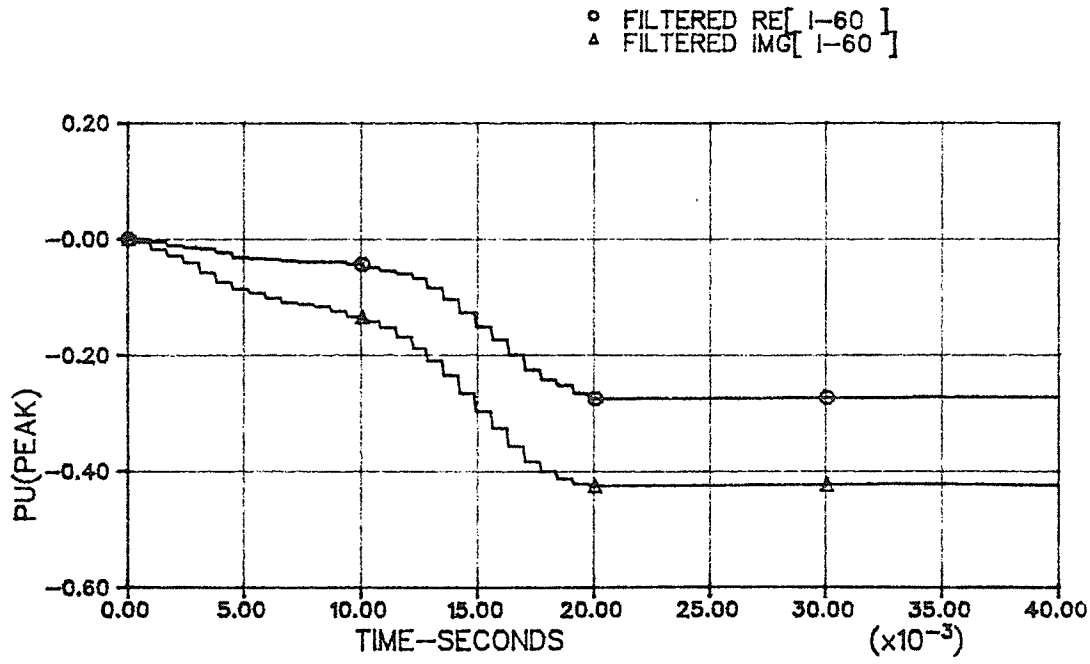

Figure 4.3. Measured Positive Sequence 60 Hz Line Current Component. $\alpha_o = 45°$
No Modulation

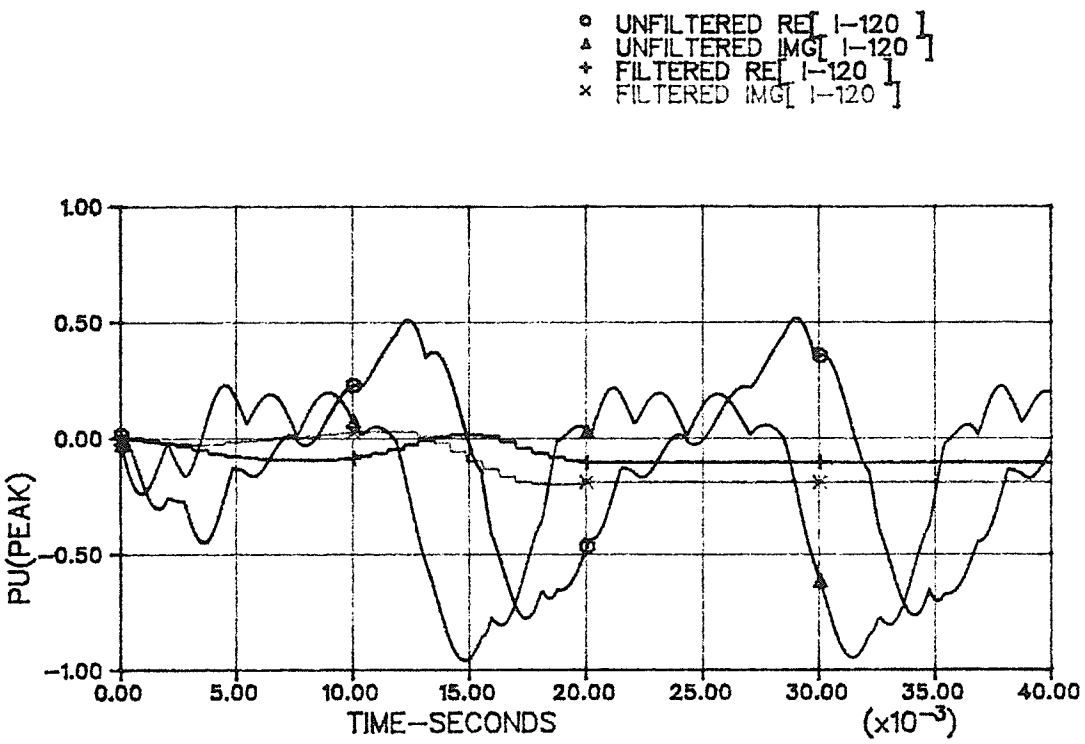

Figure 4.4. Measured Positive Sequence 120 Hz Line Current Component. $\alpha_o = 45°$ No Modulation

4.2 DESCRIPTION OF THE MODULATION CONTROLLER

The modulation controller block diagram is shown in Figure 4.5. The modulation controller consists of one real-pole type filter and one proportional integral type of controller for each component of the measured phasor, and controls to generate the modulation signal $\Delta\alpha$. The output of each controller is taken through a two-pole switch to allow for a capability to define the firing angle modulation manually.

The controller outputs **CRL** and **CIMG** represent the real and imaginary parts respectively of the modulation signal phasor. The sinusoidal modulation signal can be reconstructed as shown in the figure using phase-locked loop signals. Reconstruction of the appropriate modulation signal is described in more detail in Section 3.2

The remaining elements in the closed-loop control system are shown in the dotted boxes. The thyristor controlled reactor model consists of the state equation formulation of the TCR (subroutine **STAEQ6**), the thyristor representation (subroutine **THYR6**) and the firing pulse control system, including the phase-locked loop (subroutine **FIRPULS15**). These models are described in Chapter 2. The current measuring system is described in Chapter 4.1, and consists of $(r,s,t) - to - (\alpha,\beta)$ - transformations, vector identification of the (α,β) - components, and the symmetrical component transformation.

The modulation controller, as configured, has reference values equal to zero for **CRL** and **CIMG** respectively. Thus the PI controller is forced to adjust these parameters until the measured current real and imaginary components are both zero, resulting in zero input error. The filtering provided by the real-pole filter is not necessary to eliminate ripple (the averaging filter **AVGFIL25** is very effective in doing this), but allows for averaging the measured signal over several cycles. This is beneficial when the dc component is the control parameter.

The modulation controller is implemented in subroutine **PCONTR8**. The listing of this subroutine is included in Appendix 2.1.7. of Reference 7.

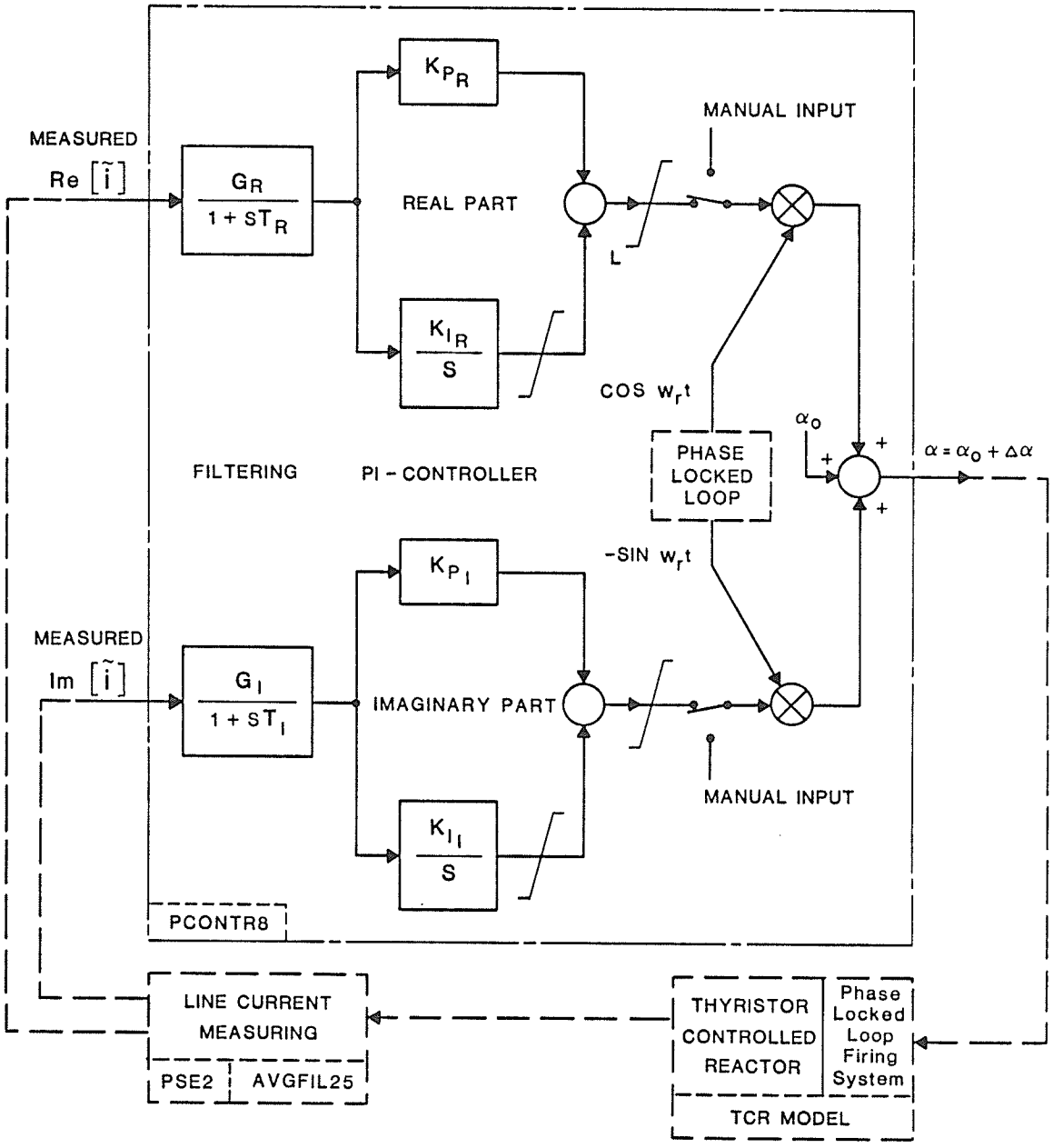

Figure 4.5. Proportional-Integral Controller For Firing Angle Modulation Of The TCR

4.3 EVALUATION OF FIRING ANGLE MODULATION CONTROL CONCEPT

The performance of the concept of sinusoidal modulation of the firing angle of a thyristor controlled reactor is evaluated using the digital model. The configuration that is studied is the one where the thyristor controlled reactor is operating with a second harmonic component superimposed on the fundamental frequency source. One objective is to eliminate the second harmonic component of the TCR line current by using the measured positive sequence second harmonic current as the control parameter. A second objective is to eliminate the dc component in the TCR line current by using the measured positive sequence dc current as the control parameter.

For both the dc and 120 Hz control parameters, the performance is evaluated for various phase angles of the second harmonic source voltage, and for various firing angles. The effect of firing angle limits on the modulation is also studied. Controller gains and time constants that work are selected. These parameters are not necessarily optimum. The stability of the closed-loop control system has not been studied theoretically.

It is useful to have a reference case in order to gauge the effects of the modulation on the harmonic content of the line and reactor currents of the thyristor controlled reactor. The reference case for this purpose is selected as the case with $\alpha_o = 45°$ and no modulation active. The TCR source voltage has a second harmonic component of 30% of the fundamental at a phase of -30°. Table 4.2 summarizes the harmonic content of the TCR positive sequence line and reactor currents obtained from an analysis of the model waveforms.

Note, the line and reactor currents are specified with respect to their respective bases. One per unit is defined to be equal to the magnitude of the 60 Hz component at $\alpha_o = 0°$. With no modulation, there is a 21.5% dc and a 42.6% second harmonic component, relative to the 60 Hz component at $\alpha = 45°$. Appendix 4.1. of

Table 4.2. TCR Current Components For No modulation $\alpha_o = 45°$. *Source* 2^{nd} *Harmonic*: 30 % @ $-30°$.				
****	Line Current		Reactor Current	
+ve Seq.	Mag-pu	Phase-deg.	Mag-pu	Phase-deg.
DC	.0450	-147.5	.0450	-117.5
60 Hz	.2041	-122.9	.2041	-92.9
120 Hz	.0889	-118.5	.0889	- 88.5

Reference 7 shows a more complete Fourier analysis of the TCR current waveforms, obtained with the program **FOURNUM**.

4.3.1 FIRING ANGLE MODULATION WITH POSITIVE SEQUENCE SECOND HARMONIC LINE CURRENT AS THE CONTROL PARAMETER

Table 4.3 shows the controller parameters that give good response. The various parameters can be identified from Figure 4.5.

Table 4.3. Control Variables For Positive Sequence 2^{nd} Harmonic As Control Parameter

Parameter	Real Part	Img. Part
G [--]	1.00	1.00
T [sec.]	0.016	0.016
K_P [$\frac{rad}{pu}$]	0.01	0.01
K_I [$\frac{rad}{pu-sec}$]	-100.0	-85.0
Limits [rad.]	± 1.0	± 1.0

The control variables were selected by evaluation of the digital model output for the reference case, $\alpha_o = 45°$ and a source voltage second harmonic of 30 % *at* $-30°$. Note that the proportional integral controllers have essentially an integral characteristic, with the proportional term being negligible.

Figure 4.6 shows the operation of the TCR for the reference case, and with modulation active. The simulation case is shown from start-up. The transient that is seen within the first 20 ms is due to initialization of the filter of the measuring system. At 20 ms the measured real part of the second harmonic component is -0.08 pu.

and the imaginary part is -0.19 pu.. The magnitude is $\sqrt{6}\,(0.084)pu.$ which is approximately the value for the *no modulation* case shown in Table 4.2. The controller then brings the second harmonic component to zero by 0.21 seconds. The PI - controller outputs **CRL** and **CIMG** are also shown in the figure. **CRL** = 0.0115 pu. and **CIMG** = 0.412 pu. , which gives the modulation peak $\hat{\Delta} = 23.6°$ and the modulation phase $\delta = 88.4°$. Modulation phase is measured relative to reference phasor which is the phasor associated with the sinusoid $\cos(\omega t)$.

The Fourier and symmetrical component analysis of the line and reactor currents is shown in Appendix 4.2.1. of Reference 7. Table 4.4 summarizes the significant positive sequence current components.

Table 4.4. Sequence Components Of TCR Currents

Control Parameter : +ve Sequence 2nd Harmonic

$\alpha_o = 45°$. *Source* 2^{nd} *Harmonic* : 30% @ $-30°$.

$\hat{\Delta} = 23.6°$. $\delta = 88.4°$.

****	Line Current		Reactor Current	
+ve Seq.	Mag-pu	Phase-deg.	Mag-pu	Phase-deg.
DC	.040	89.3	.040	119.3
60 Hz	.198	-121.3	.198	-91.3
120 Hz	.0025	-118.4	.0025	- 88.4

Table 4.4 shows that the second harmonic component has been reduced significantly, now being only 1.3 % of the fundamental and 2.9 % of its magnitude for the no modulation case(Table 4.2). The dc component has not been changed by the modulation, and the 60 Hz component has been reduced by 3 % . The

modulation has contributed to more unbalance (5 % at 60 Hz), but has not altered the other harmonic components significantly. The modulation would have a minor interaction with the normal fundamental frequency reactive power and voltage controls.

A peak modulation $\hat{\Delta} = 23.6°$ and phase $\delta = 88.4°$ gives

$$\Delta\alpha_{rs} = 0.66° \quad \Delta\alpha_{st} = -20.8° \quad \Delta\alpha_{tr} = 20.1° \tag{4.14}$$

Clearly, no firing angle limits are encountered with this level of modulation and $\alpha_o = 45°$. Figure 4.7 shows the TCR waveforms after the modulation controller has reached a steady-state. The actual firing angles can be measured from Figure 4.7(a), (b) and (c). The $\alpha = 0°$ reference should be taken from the peak of the phase-locked loop reference voltage **VREF**. Table 4.5 shows measured values of firing angles and compares these to expected values that should result from the modulation that is active. Note that the resolution in the plotted waveforms is limited to $\pm 2.16°$ due to the plot sampling period. Any other error is attributed to measuring inaccuracies.

Table 4.5. Firing Pulse Position And Sinusoidal Distribution

Control Parameter : +ve Sequence 2^{nd} Harmonic

α_o = 45°. *Source* 2^{nd} *Harmonic* : 30% @ −30°.

$\hat{\Delta}$ = 23.6°. δ = 88.4°.

Thyristor Alpha	Firing Angle		Interval Between Pulses	
	Expected (Deg.)	Measured (Deg.)	Expected (Deg.)	Measured (Deg.)
α_1	45.6	45.2	**	**
α_{2-1}	**	**	39.3	37.4
α_2	24.9	24.7	**	**
α_{3-2}	**	**	59.3	61.4
α_3	24.2	21.2	**	**
α_{4-3}	**	**	80.2	79.4
α_4	44.9	44.5	**	**
α_{5-4}	**	**	80.7	81.5
α_5	65.1	62.3	**	**
α_{6-5}	**	**	60.7	60.5
α_6	65.8	62.3	**	**
α_{1-6}	**	**	39.8	40.5

Table 4.5 also shows that the firing pulses are sinusoidally distributed. Expected values are determined using the values for $\Delta\alpha_{xy}$ from Equation 4.14 and the 60° intervals that normally occur with no modulation.

Figure 4.8 shows the line current waveforms of the TCR after the modulation has reached steady-state. Clearly the waveforms show a dc component, as can be verified from the Fourier analysis attached as Appendix 4.2.1. of Reference 7.

Changing the phase of the second harmonic component of the source voltage does not change the magnitude of the modulation required to eliminate the positive sequence 120 Hz component of line current. Only the phase of the modulation signal is changed since harmonics arising from the source are now at a different phase. An

example in Table 4.6 is shown where the source voltage has a second harmonic component of 30 % @ −210° .

Table 4.6. Sequence Components Of TCR Currents **Control Parameter : +ve Sequence 2^{nd} Harmonic** α_o = 45°. *Source* 2^{nd} *Harmonic*: 30 % @ −210°. $\hat{\Delta}$ = 23.6°. δ = −91.5°.		
****	Line Current	
+ve Seq.	Mag-pu	Phase-deg.
DC	.041	-92.3
60 Hz	.198	-121.1
120 Hz	.0018	-13.4

A 180° change in phase of the second harmonic source component is compensated by a corresponding 180° phase change of the modulation signal.

The performance of the modulation controls for different nominal firing angles α_o is evaluated next. It is observed that the positive sequence second harmonic component of the line current can be eliminated with firing angle modulation, even though firing angle limits restrict the sinusoidal modulation. For $\alpha_o = 0°$ the sinusoidal modulation is in fact one-sided.

Table 4.7 summarizes the data for some of the TCR line currents along with the relevant modulation data. For all cases in the table, the simulation was done with the source voltage second harmonic component of 30 % *at* −30° .

For the cases $\alpha_o = 45°$ and $\alpha_o = 30°$ no firing angle limits are encountered. The modulation magnitude increases proportionally, which is expected since the

Table 4.7. Effect Of Nominal

Firing Angle On Modulation

Control Parameter: 2nd Harmonic

Source 2nd Harmonic : 30 % @ - 30°.

***		TCR Line Currents			
Case		Modulation Off		Modulation On	
Data	Comp.	Mag-pu	Phase-Deg.	Mag-pu	Phase-Deg.
$\alpha_o = 45°$ $\hat{\Delta} = 23.6°$ $\delta = 88.4°$ $\Delta\alpha_{rs} = .66°$ $\Delta\alpha_{st} = -20.8°$ $\Delta\alpha_{tr} = 20.1°$	DC 60 Hz 120 Hz	.044 .204 .087	-147.7 -122.8 -118.4	.040 .198 .0025	89.3 -118.4 **
$\alpha_o = 30°$ $\hat{\Delta} = 33.0°$ $\delta = 74.0°$ $\Delta\alpha_{rs} = 9.25°$ $\Delta\alpha_{st} = -32.1°$ $\Delta\alpha_{tr} = 22.9°$	DC 60 Hz 120 Hz	.060 .408 .124	-132.7 -121.8 -135.5	.120 .430 .0024	85.0 -121.8 **
$\alpha_o = 15°$ $\hat{\Delta} = 55.2°$ $\delta = 70.3°$ $\Delta\alpha_{rs} = 18.6°$ $\Delta\alpha_{st} = -54.3°$ $\Delta\alpha_{tr} = 35.7°$	DC 60 Hz 120 Hz	.072 .690 .144	-114.4 -120.2 -145.3	.150 .530 .0027	88.4 -122.1 **
$\alpha_o = 0°$ $\hat{\Delta} = 81.0°$ $\delta = 66.7°$ $\Delta\alpha_{rs} = 32.0°$ $\Delta\alpha_{st} = -80.5°$ $\Delta\alpha_{tr} = 48.5°$	DC 60 Hz 120 Hz	.066 1.00 .150	- 91.0 -120.1 -149.2	.150 .533 .0038	89.3 -122.1 **

second harmonic component is larger, as can be seen from the **no modulation** case data.

For the $\alpha_o = 15°$ and $\alpha_o = 0°$ cases, firing angle limits severely restrict the sinusoidal modulation signal on one side. The second harmonic component is still virtually eliminated (less than 2.5 % of magnitude when no modulation is used), but this requires larger peak modulation magnitudes.

The elimination of the second harmonic component has an undesirable effect on the dc component for most cases. For all firing angles shown in Table 4.7, the absolute magnitude of the dc component at least doubles. This could cause transformer saturation and lead to larger second harmonic currents.

When the firing angle limits are not encountered, the effect of the modulation on the 60 Hz component is not significant. The modulation reduces the 60 Hz component by 3 % for the $\alpha_o = 45°$ case and 5 % for the $\alpha_o = 30°$ case. As firing angle limits are encountered, the 60 Hz component of the line current is severely reduced. At $\alpha_o = 0°$ the 60 Hz current component is 46 % of the current for the *no modulation* case. The modulation signal would obviously have a large interaction with the 60 Hz reactive power controls that determine the nominal firing angle α_o .

Figures 4.9 and 4.10 show the operation of the TCR with $\alpha = 0°$. Figure 4.9 shows that the controller successfully eliminates the 120 Hz line current component within 210 ms. Figure 4.10 shows the TCR waveforms after the modulation controller has reached steady-state. Table 4.8 shows the firing angle limits are clearly limiting the modulation. Note that the modulation magnitude and phase are given in Table 4.7 for the $\alpha_o = 0°$ case . Appendix 4.2.2 of Reference 7 shows the complete Fourier analysis for the case $\alpha_o = 0°$, with modulation such that the second harmonic line current is eliminated.

Table 4.8. Firing Pulse Position And Sinusoidal Distribution

Control Parameter : +ve Sequence 2^{nd} Harmonic

$\alpha_o = 0°$. *Source* 2^{nd} *Harmonic* : 30 % @ $-30°$.

$\hat{\Delta} = 81.°$. $\delta = 66.7°$.

Thyristor Alpha	Firing Angle		Interval Between Pulses	
	Expected (Deg.)	Measured (Deg.)	Expected (Deg.)	Measured (Deg.)
α_1	32.0	31.8	**	**
α_{2-1}	**	**	28.0	25.4
α_2	0.0	0.0	**	**
α_{3-2}	**	**	60.0	59.3
α_3	0.0	0.0	**	**
α_{4-3}	**	**	60.0	61.4
α_4	0.0	0.0	**	**
α_{5-4}	**	**	108.5	106.0
α_5	48.5	44.5	**	**
α_{6-5}	**	**	92.0	94.6
α_6	80.6	79.0	**	**
α_{1-6}	**	**	32.0	31.8

The digital model tests demonstrate that firing angle modulation using the 120 Hz positive sequence line current as a control parameter is effective in eliminating this component from the line current, even if firing angle limits are encountered. Elimination of the second harmonic can result in larger magnitudes of dc current, which is not desirable. To avoid significant interaction between the normal 60 Hz reactive power and voltage controls and the modulation controller it is desirable to incorporate,in the overall SVC control strategy, means for re-adjusting the nominal firing angle when modulation signals are restricted by firing angle limits.

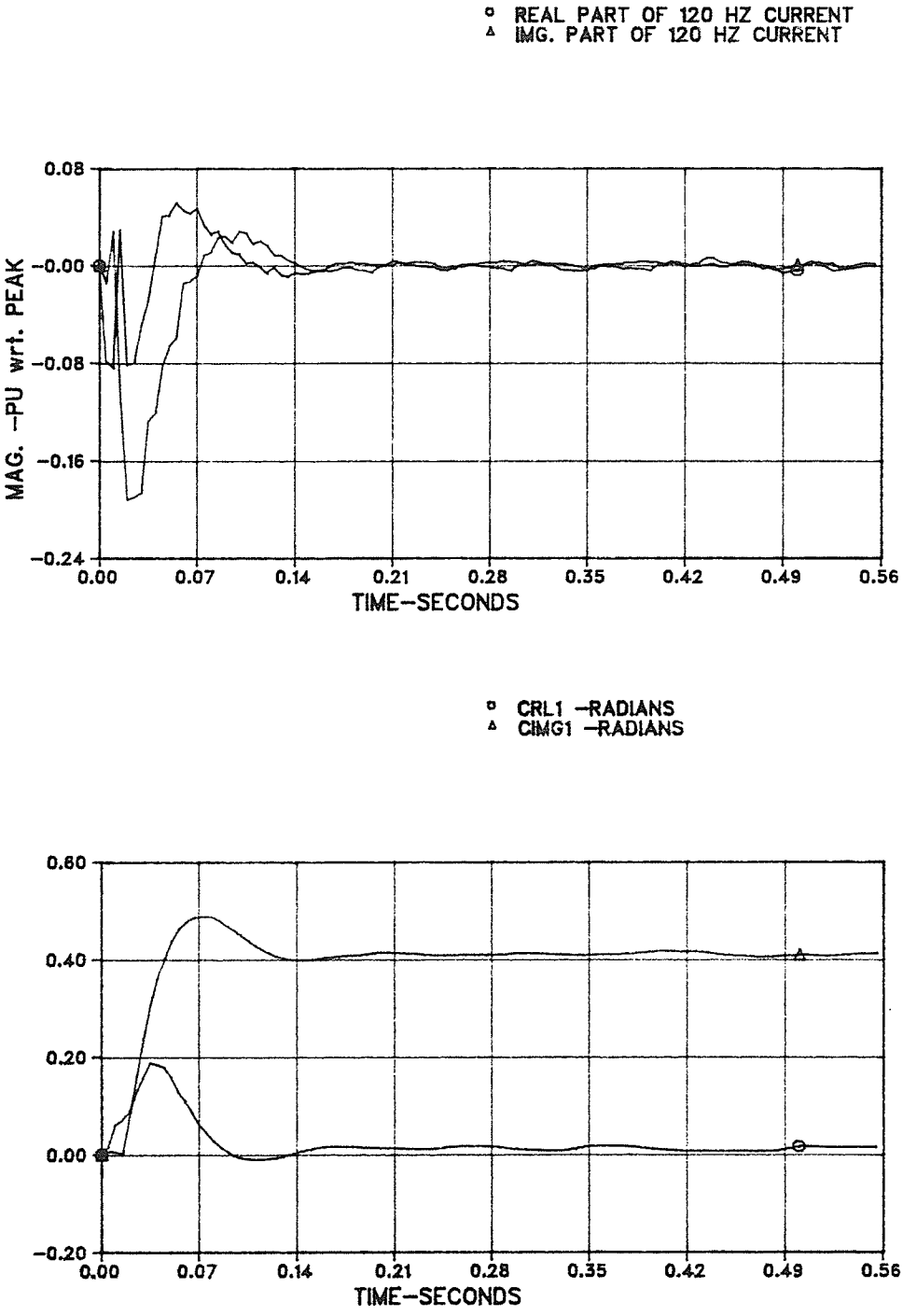

Figure 4.6. Control Of Postive Sequence 2^{nd} Harmonic Line Current With Firing Angle Modulation Source 2^{nd} Harmonic Voltage 30 % @ -30° $\alpha_o = 45°$ $\hat{\Delta} = 23.6°$ $\delta = 88.4°$

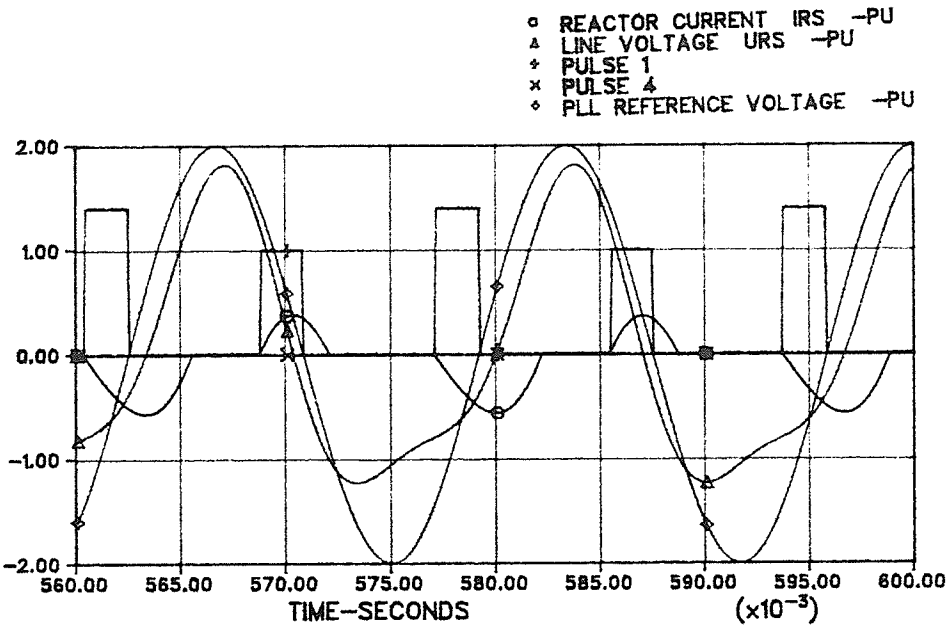

Figure 4.7.(a) TCR Waveforms With Second Harmonic As Control Parameter. $\alpha_o = 45°$
Source 2^{nd} Harmonic Voltage 30 % @ - 30°
$\hat{\Delta} = 23.6°$ $\delta = 88.4°$

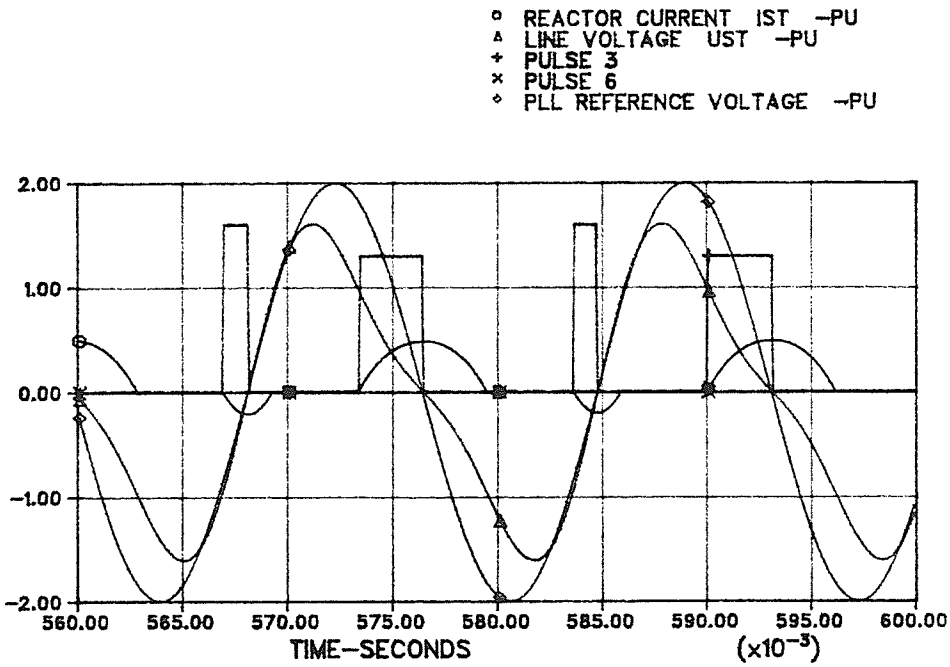

Figure 4.7.(b) TCR Waveforms With Second Harmonic As Control Parameter. $\alpha_o = 45°$
Source 2^{nd} Harmonic Voltage 30 % @ - 30°
$\hat{\Delta} = 23.6°$ $\delta = 88.4°$

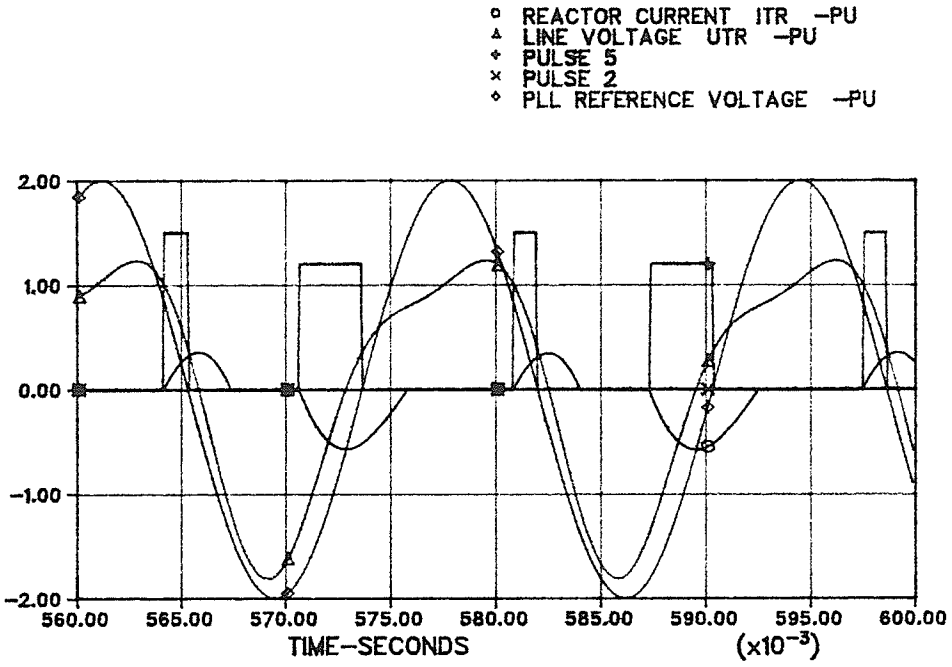

Figure 4.7.(c) TCR Waveforms With Second Harmonic As Control Parameter. $\alpha_o = 45°$
Source 2^{nd} Harmonic Voltage 30 % @ - 30°
$\hat{\Delta} = 23.6°$ $\delta = 88.4°$

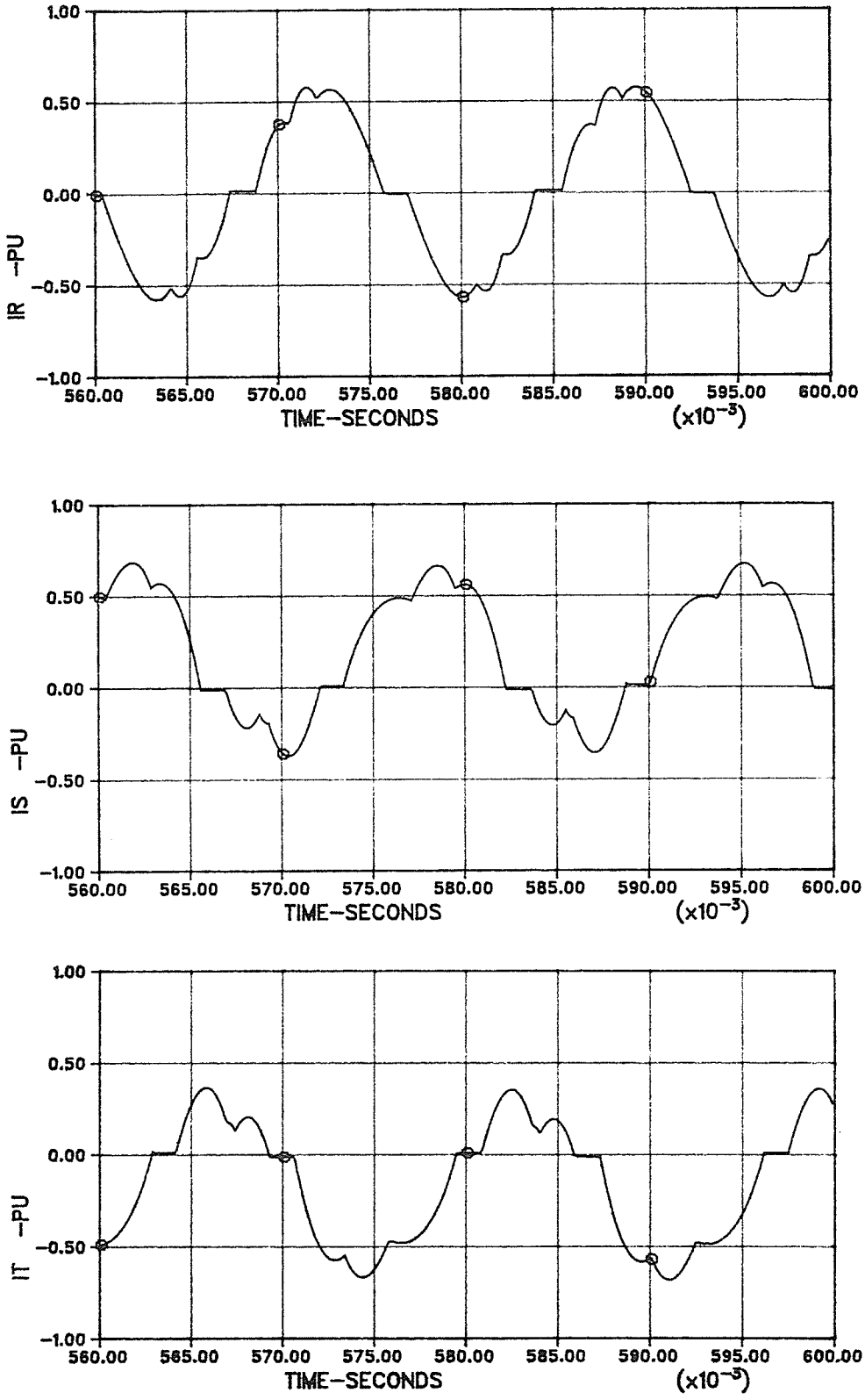

Figure 4.8. TCR Line Current Waveforms With Second Harmonic As Control Parameter. $\alpha_o = 45°$
Source 2^{nd} Harmonic Voltage 30 % @ - 30°
$\hat{\Delta} = 23.6°$ $\delta = 88.4°$

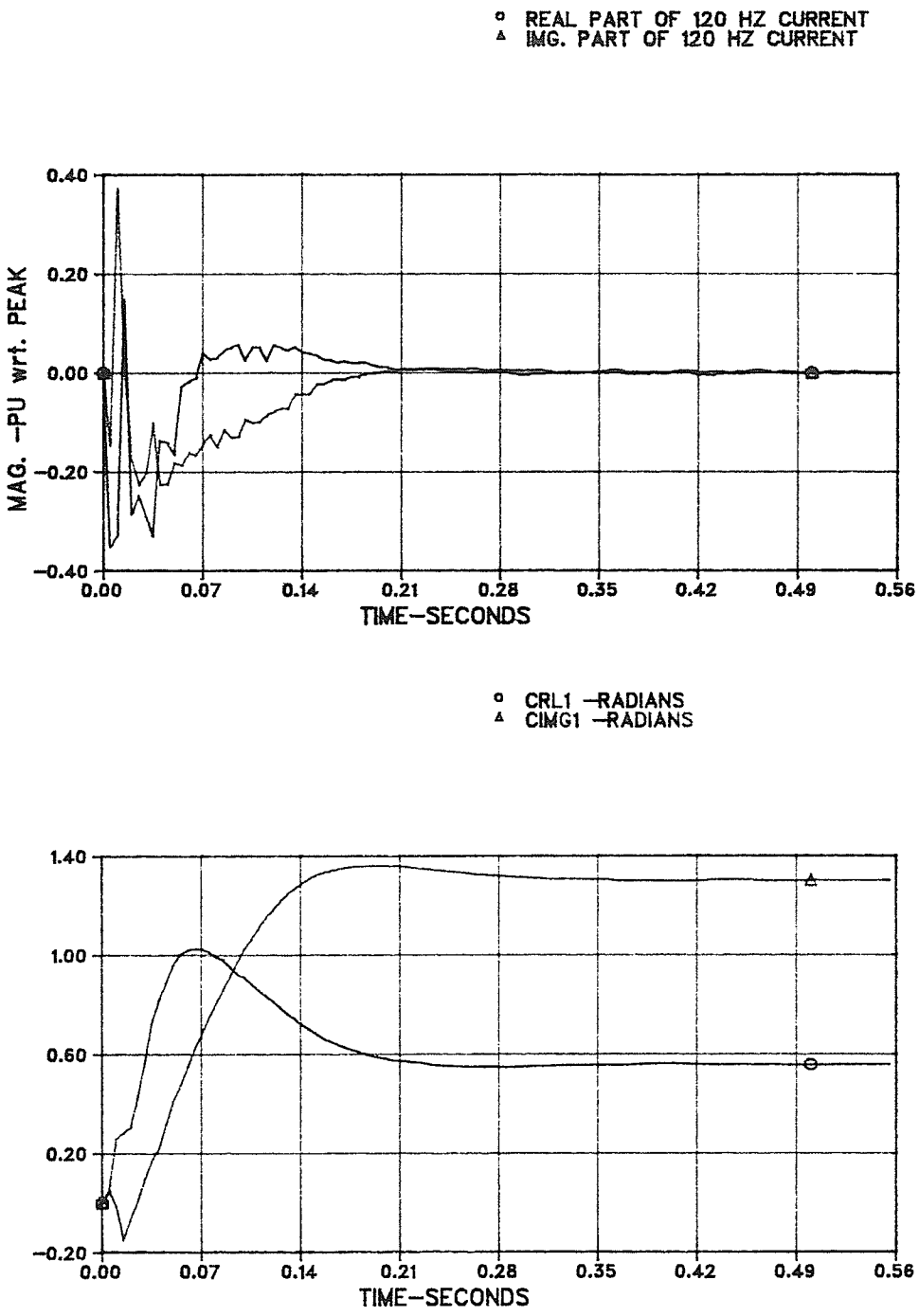

Figure 4.9. Control Of Postive Sequence 2^{nd} Harmonic Line Current With Firing Angle Modulation Source 2^{nd} Harmonic Voltage 30 % @ -30°
$\alpha_o = 0°$ $\hat{\Delta} = 81.0°$ $\delta = 66.7°$

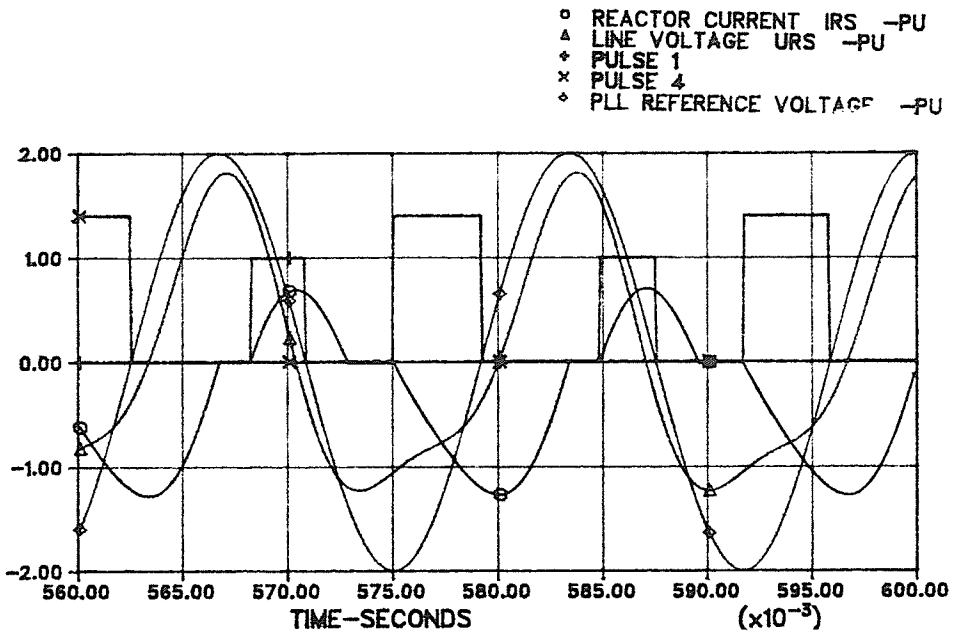

Figure 4.10.(a) TCR Waveforms With Second Harmonic As Control Parameter. $\alpha_o = 0°$
Source 2^{nd} Harmonic Voltage 30 % @ - 30°
$\hat{\Delta} = 81.0°$ $\delta = 66.7°$

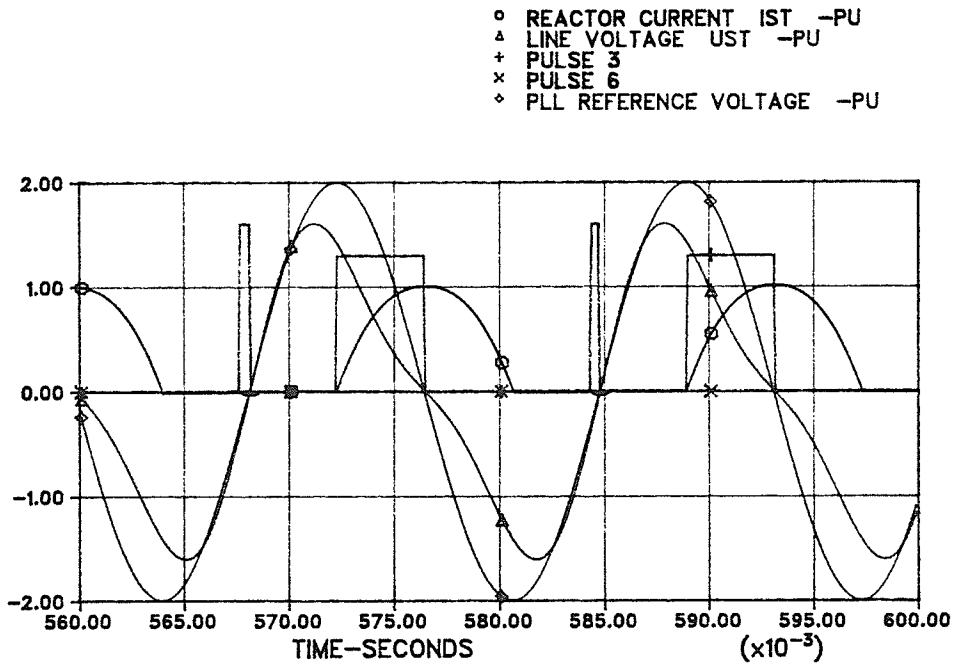

Figure 4.10.(b) TCR Waveforms With Second Harmonic As Control Parameter. $\alpha_o = 0°$
Source 2^{nd} Harmonic Voltage 30 % @ - 30°
$\hat{\Delta} = 81.0°$ $\delta = 66.7°$

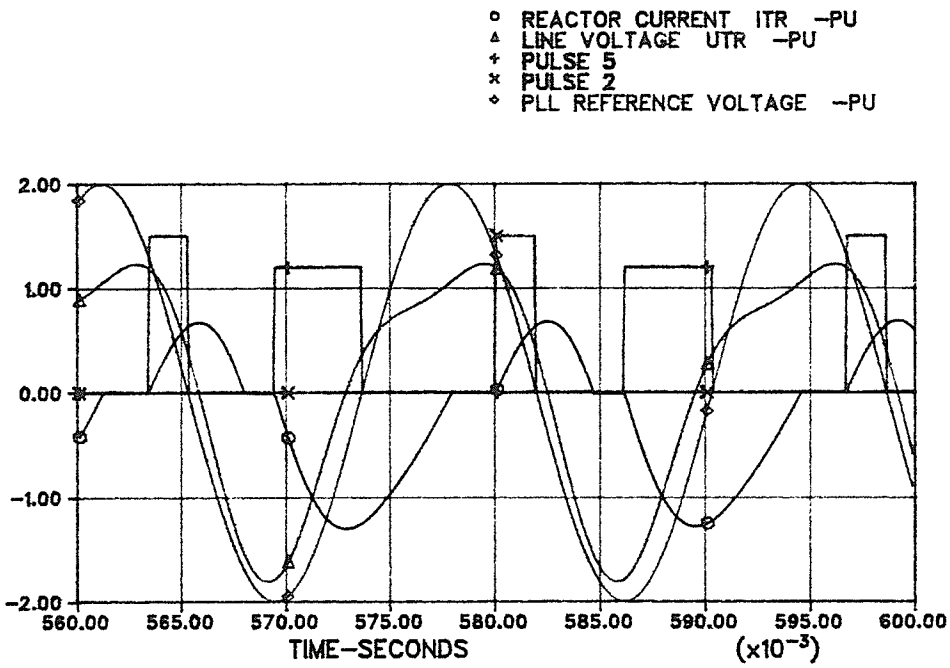

Figure 4.10.(c) TCR Waveforms With Second Harmonic As Control Parameter. $\alpha_o = 0°$
Source 2^{nd} Harmonic Voltage 30 % @ - 30°
$\hat{\Delta} = 81.0°$ $\delta = 66.7°$

4.3.2 FIRING ANGLE MODULATION WITH POSITIVE SEQUENCE DC LINE CURRENT AS THE CONTROL PARAMETER

Table 4.9 shows the controller parameters that give good response. The various parameters can be identified from Figure 4.5.

Table 4.9. Control Variables For Positive Sequence DC As Control Parameter

Parameter	Real Part	Img. Part
G [--]	1.00	1.00
T [sec.]	0.032	0.032
$K_P \left[\frac{rad}{pu} \right]$	0.01	0.01
$K_I \left[\frac{rad}{pu - sec} \right]$	20.0	-40.0
Limits [rad.]	± 1.0	± 1.0

The control variables were selected by evaluation of the digital model output for the reference case $\alpha_o = 45°$ and a source voltage second harmonic component of $30\ \%\ at\ -30°$. Again, the proportional integral controllers are essentially integral in nature, the proportional term being negligible. The smoothing from the real pole of 32 ms definitely improves the controller response, making the system less sensitive to asymmetrics resulting from larger time steps that could be used in the simulation (a time-step of 50 microseconds was usually used). Note smoothing of 16 ms used for the second harmonic as control parameter was not as important, but also

beneficial).

Figure 4.11 shows the response of the modulation controller for the reference case and with the dc modulation active. The first cycle of the simulation shows the start-up transient. At about 20 ms, the measured real part of the dc component is -0.058 pu. and the imaginary part is -0.088 pu.. The magnitude is $\sqrt{6}$ (0.043) pu., which is approximately the value for the **no modulation** case shown in Table 4.2. The controller is successful in reducing the dc component from this magnitude to zero within 280 milleseconds. The PI-controller outputs are also shown in the figure. **CRL** = -0.109 pu. and **CIMG** = 0.214 pu. which gives the modulation peak $\hat{\Delta} = 13.8°$ and phase $\delta = 117°$. Note that the modulation phase is measured with respect to the reference phasor $\cos(\omega t)$.

The Fourier and symmetrical component analysis of the TCR line and reactor currents is included in Appendix 4.3.1. of Reference 7. Table 4.10 summarizes some of the more significant positive sequence current components.

Table 4.10. Sequence Components Of TCR Currents

Control Parameter : +ve Sequence DC Component

$\alpha_o = 45°$. *Source* 2^{nd} *Harmonic* : 30% @ $-30°$.

$\hat{\Delta} = 13.8°$. $\delta = 117.0°$.

****	Line Current		Reactor Current	
+ve Seq.	Mag-pu	Phase-deg.	Mag-pu	Phase-deg.
DC	0.001	-129.5	0.001	-99.5
60 Hz	.1904	-121.3	.1904	-91.3
120 Hz	.048	-129.5	.048	- 121.3

Table 4.10 shows that the dc component has been eliminated. The second harmonic component has been reduced from 0.087 pu. to 0.048 pu. , now being 25.2 % of the fundamental. The 60 Hz component has been reduced by 6.6 % , which implies that the modulation controls will have some interaction with the normal fundamental frequency reactive power and voltage controls.

The peak modulation of $\hat{\Delta} = 13.8°$ and phase $\delta = 117°$ gives

$$\Delta\alpha_{rs} = -6.25° \quad \Delta\alpha_{st} = -7.5° \quad \Delta\alpha_{tr} = 13.8° \tag{4.15}$$

No firing angle limits are encountered with this level of modulation and $\alpha_o = 45°$. Figure 4.12 shows the TCR waveforms after the modulation controller has reached steady state. From Figure 4.12 (a), (b) and (c), the actual firing angles can be measured. The $\alpha = 0°$ reference is at the peak of the PLL reference voltage VREF. Table 4.11 shows the measured values of the firing angles and compares these to expected firing angles that should result from the modulation. Note that the plot sampling period gives a resolution of $\pm 2.16°$.

Table 4.11. Firing Pulse Position And Sinusoidal Distribution

Control Parameter : +ve Sequence DC Component

$\alpha_o = 45°$. *Source* 2^{nd} *Harmonic* : 30% @ $-30°$.

$\hat{\Delta} = 13.8°$. $\delta = 117.0°$.

Thyristor Alpha	Firing Angle		Interval Between Pulses	
	Expected (Deg.)	Measured (Deg.)	Expected (Deg.)	Measured (Deg.)
α_1	38.75	38.2	**	**
α_{2-1}	**	**	52.5	51.5
α_2	31.2	33.0	**	**
α_{3-2}	**	**	66.3	67.8
α_3	37.5	35.3	**	**
α_{4-3}	**	**	73.8	73.0
α_4	51.25	52.2	**	**
α_{5-4}	**	**	67.6	68.0
α_5	58.5	56.0	**	**
α_{6-5}	**	**	53.7	53.6
α_6	52.5	51.2	**	**
α_{1-6}	**	**	46.3	45.0

The table also shows that the firing pulses are sinusoidally distributed. Expected values are determined using the values for $\Delta\alpha_{xy}$ in Equation 4.15 and 60° firing intervals that normally occur with no modulation.

Figure 4.13 shows the line current waveforms for the TCR, when the modulation has reached steady state. These waveforms and the reactor current waveforms of Figure 4.10 show that there is a negligible dc component , which is verified by the Fourier analysis shown in Appendix 4.3.1. of Reference 7.

Changing the phase of the second harmonic component of the source voltage does not change the magnitude of the modulation required to eliminate the dc component. Only the phase of the modulation changes to compensate for the change in

the source voltage.

Table 4.12 shows the results of an analysis of TCR line currents for the case when the source voltage second harmonic component has a phase of -210°. A 180° phase change of the second harmonic component of source voltage is simply compensated by a corresponding 180° phase change in the modulation signal required to eliminate the dc component.

Table 4.12. Sequence Components Of TCR Currents

Control Parameter : +ve Sequence DC Component

$\alpha_o = 45°$. *Source* 2^{nd} *Harmonic* : 30 % @ $-210°$.

$\hat{\Delta} = 13.6°$. $\delta = -62.8°$.

****	Line Current	
+ve Seq.	Mag-pu	Phase-deg.
DC	.0008	**
60 Hz	.193	-121.2
120 Hz	.0488	26.2

The performance of the modulation controls for different nominal firing angles α_o , is evaluated next. It is observed that the positive sequence dc component of the line current can be eliminated with firing angle modulation, even though firing angle limits restrict the modulation. This was also the situation when the second harmonic was used as the control parameter.

Table 4.13 summarizes the data for some of the TCR line currents along with the relevant modulation data. For all cases shown in the table, the simulation was done with the source voltage second harmonic component at 30 % @ $-30°$.

Table 4.13. Effect Of Nominal

Firing Angle On Modulation

Control Parameter: +ve Sequence DC Component

Source 2nd Harmonic : 30 % @ - 30°.

***		TCR Line Currents			
Case		Modulation Off		Modulation On	
Data	Comp.	Mag-pu	Phase-Deg.	Mag-pu	Phase-Deg.
$\alpha_o = 45°$ $\hat{\Delta} = 13.8°$ $\delta = 117.0°$ $\Delta\alpha_{rs} = -6.25°$ $\Delta\alpha_{st} = -7.50°$ $\Delta\alpha_{tr} = 13.8°$	DC	.044	-147.7	.0008	**
	60 Hz	.204	-122.8	.193	-121.2
	120 Hz	.087	-118.4	.0488	26.2
$\alpha_o = 30°$ $\hat{\Delta} = 11.9°$ $\delta = 103.0°$ $\Delta\alpha_{rs} = -2.7°$ $\Delta\alpha_{st} = -8.7°$ $\Delta\alpha_{tr} = 11.4°$	DC	.060	-132.7	.0017	**
	60 Hz	.408	-121.1	.4074	-121.9
	120 Hz	.124	-133.5	.0865	-153.1
$\alpha_o = 0°$ $\hat{\Delta} = 17.7°$ $\delta = 65.6°$ $\Delta\alpha_{rs} = 7.30°$ $\Delta\alpha_{st} = -17.6°$ $\Delta\alpha_{tr} = 10.3°$	DC	.066	- 91.0	.002	86.5
	60 Hz	1.00	-120.1	.882	-122.3
	120 Hz	.150	-141.2	.135	-152.9

For case $\alpha_o = 45°$ and $\alpha_o = 30°$, no firing angle limits are encountered. The modulation peak $\hat{\Delta}$ does not increase much as α_o gets smaller. This is expected since the dc component for the **no modulation** case does not change significantly with firing angle.

For the $\alpha_o = 0°$ case, firing angle limits restrict the sinusoidal modulation to

be a one-sided signal. The dc component is still eliminated (less than 3 % of the no modulation case), but this requires a larger peak modulation.

The elimination of the dc component also reduces the absolute magnitude of the second harmonic component. For the $\alpha_o = 45°$ case the second harmonic current is 56 % and for the $\alpha = 0°$ case the second harmonic current is 90 % of the respective **no modulation** values respectively.

When firing angle limits are not encountered, the effect of the modulation on the 60 Hz component is not significant. With $\alpha_o = 45°$, the 60 Hz component is 94 % of the **no modulation** case. For $\alpha_o = 30°$, the 60 Hz component is virtually unchanged. When the modulation is restricted by firing angle limits, the 60 Hz component is more severely reduced. For $\alpha_o = 0°$, the 60 Hz component is reduced to 88 % of the **no modulation** value.

Figures 4.14 and 4.15 show the performance of the TCR with the dc component as the control parameter and when firing angle limits are encountered. Figure 4.14 shows that the controller succeeds in eliminating the dc component within 280 ms. Figure 4.15 (a), (b) and (c) show the waveforms after the controller reaches its steady state, having eliminated the dc component. Table 4.14 shows the firing angles that are measured from the figures . The firing angle limits are clearly acting. Note that the modulation magnitude and phase is shown in Table 4.13 for the $\alpha_o = 0°$ case.

Clearly, the reactor current waveforms appear symmetrical, having virtually no dc component. This is verified by the waveform analysis, included as Appendix 4.3.2. of Reference 7.

The digital model tests demonstrate that firing angle modulation using the positive sequence dc component of the line current as a control parameter is effective in eliminating this component from the line current, even if firing angle limits are encountered. Elimination of the dc component tends to reduce the 120 Hz

Table 4.14. Firing Pulse Position And Sinusoidal Distribution

Control Parameter : +ve Sequence DC Component

$\alpha_o = 0°$. *Source* 2^{nd} *Harmonic* : 30 % @ $-30°$.

$\hat{\Delta} = 17.7°$ $\quad \delta = 65.6°$

Thyristor Alpha	Firing Angle		Interval Between Pulses	
	Expected (Deg.)	Measured (Deg.)	Expected (Deg.)	Measured (Deg.)
α_1	7.3	6.3	**	**
α_{2-1}	**	**	52.7	52.2
α_2	0.0	0.0	**	**
α_{3-2}	**	**	60.0	59.3
α_3	0.0	0.0	**	**
α_{4-3}	**	**	60.0	60.7
α_4	0.0	0.0	**	**
α_{5-4}	**	**	70.3	72.0
α_5	10.3	9.9	**	**
α_{6-5}	**	**	67.3	66.3
α_6	17.6	17.6	**	**
α_{1-6}	**	**	52.7	50.8

component as well, but does not eliminate it. When firing angle limits are encountered, the 60 Hz component is reduced more significantly by the modulation.

Some cases were tried where a weighted average of the modulation signals from the dc component controller and the second harmonic component controller was used as the control parameter in an attempt to eliminate both currents simultaneously. Such attempts were not successful, a result which was expected. With a balanced fundamental frequency source the only source of even harmonics is firing assymetries. Then one could expect to eliminate all even harmonics by some modulation which eliminates the asymmetries. In the case where the TCR source has a second harmonic component, this component causes non-equidistant voltage zero

crossing which results in even harmonic currents. In addition, the source itself contributes an additional second harmonic current component.

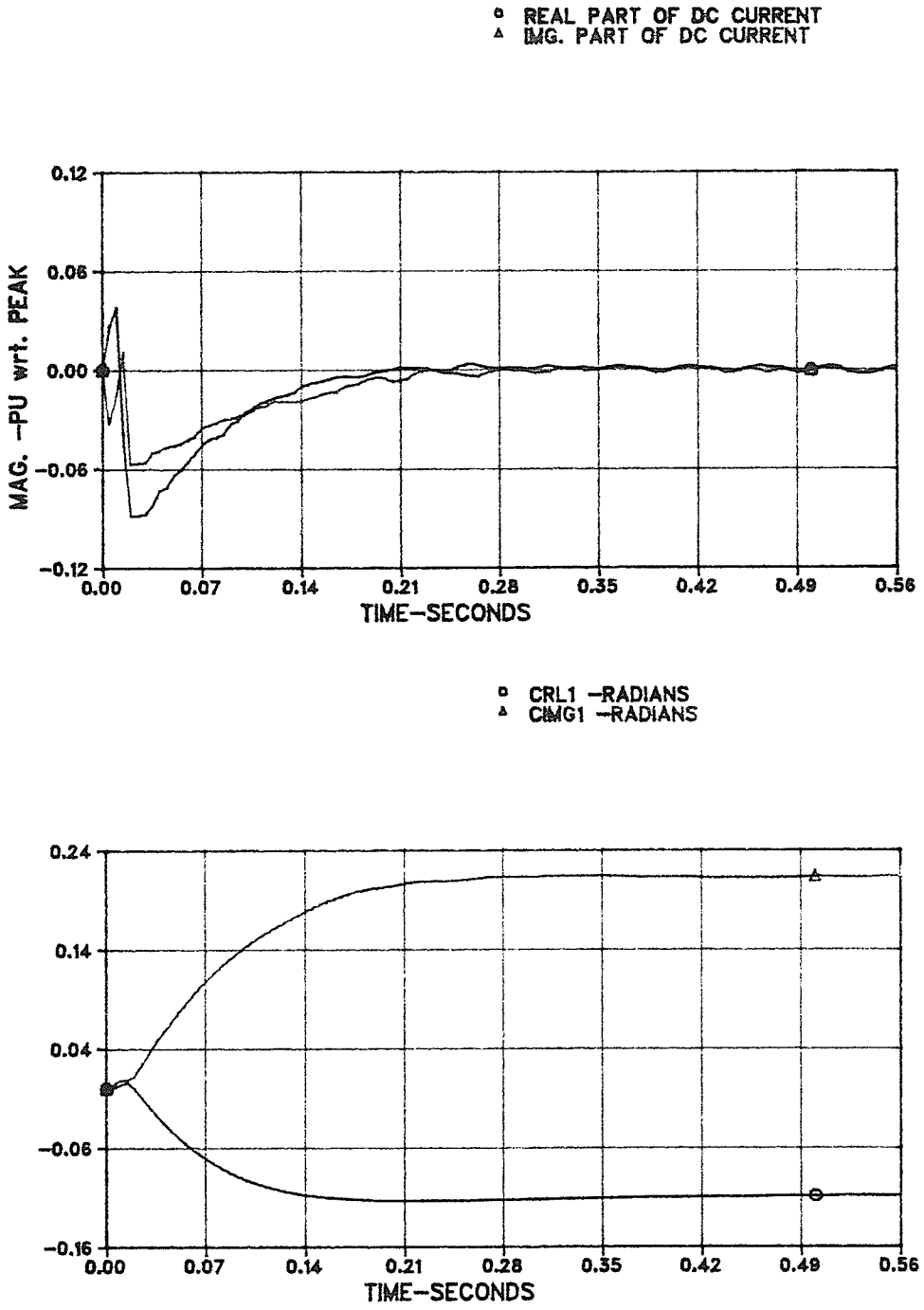

Figure 4.11. Control Of Postive Sequence DC
Line Current With Firing Angle Modulation
Source 2^{nd} Harmonic Voltage 30 % @ -30°
α_o = 45° $\hat{\Delta}$ = 13.8° δ = 117.0°

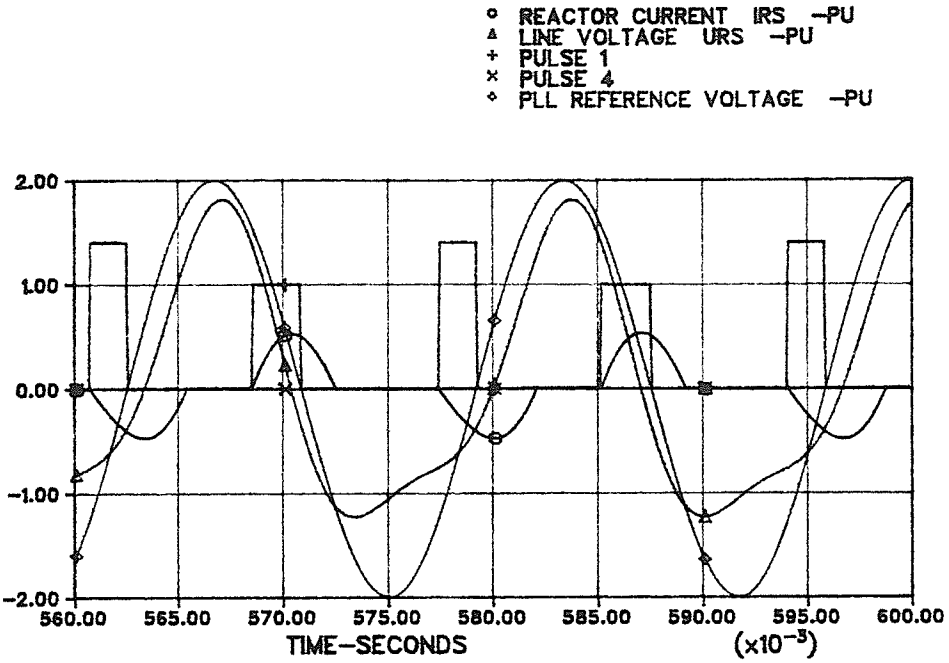

Figure 4.12.(a) TCR Waveforms With DC As
Control Parameter. $\alpha_o = 45°$
Source 2^{nd} Harmonic Voltage 30 % @ - 30°
$\hat{\Delta} = 13.8°$ $\delta = 117.0°$

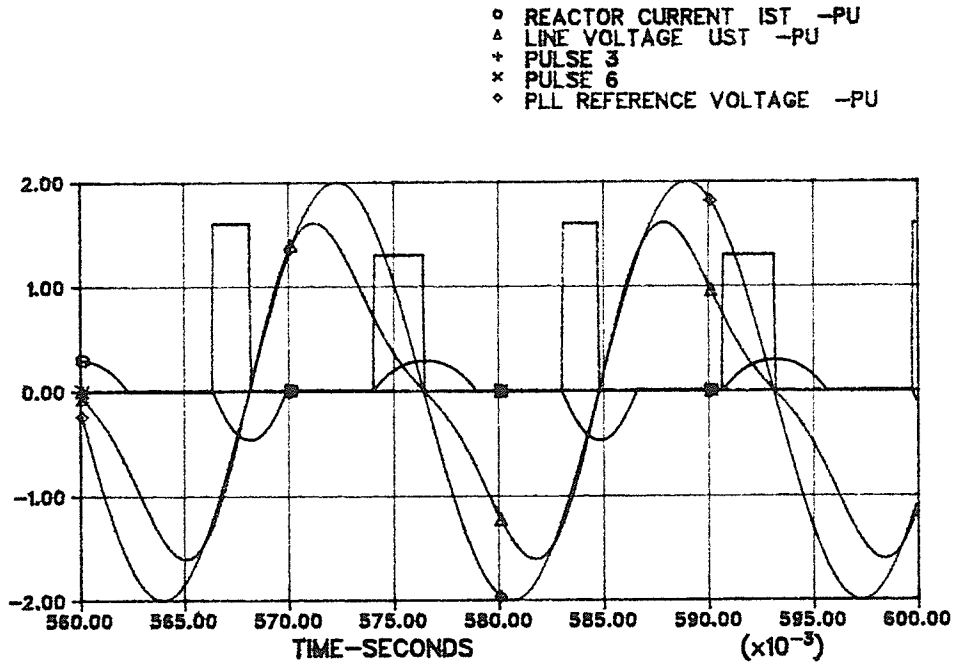

Figure 4.12.(b) TCR Waveforms With DC As
Control Parameter. $\alpha_o = 45°$
Source 2^{nd} Harmonic Voltage 30 % @ - 30°
$\hat{\Delta} = 13.8°$ $\delta = 117.0°$

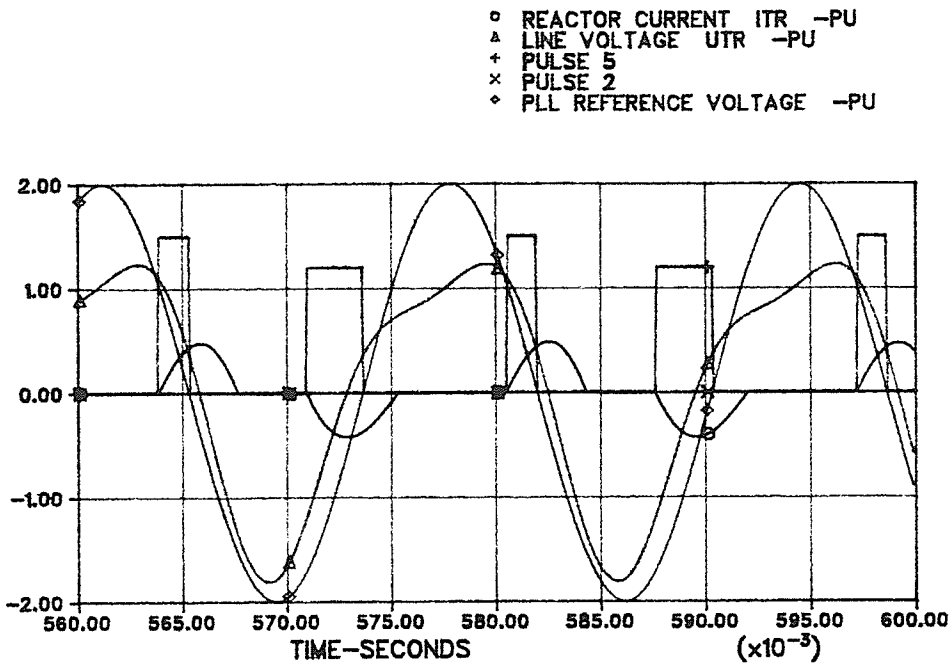

Figure 4.12.(c) TCR Waveforms With DC As
Control Parameter. $\alpha_o = 45°$
Source 2^{nd} Harmonic Voltage 30 % @ - 30°
$\hat{\Delta} = 13.8°$ $\delta = 117.0°$

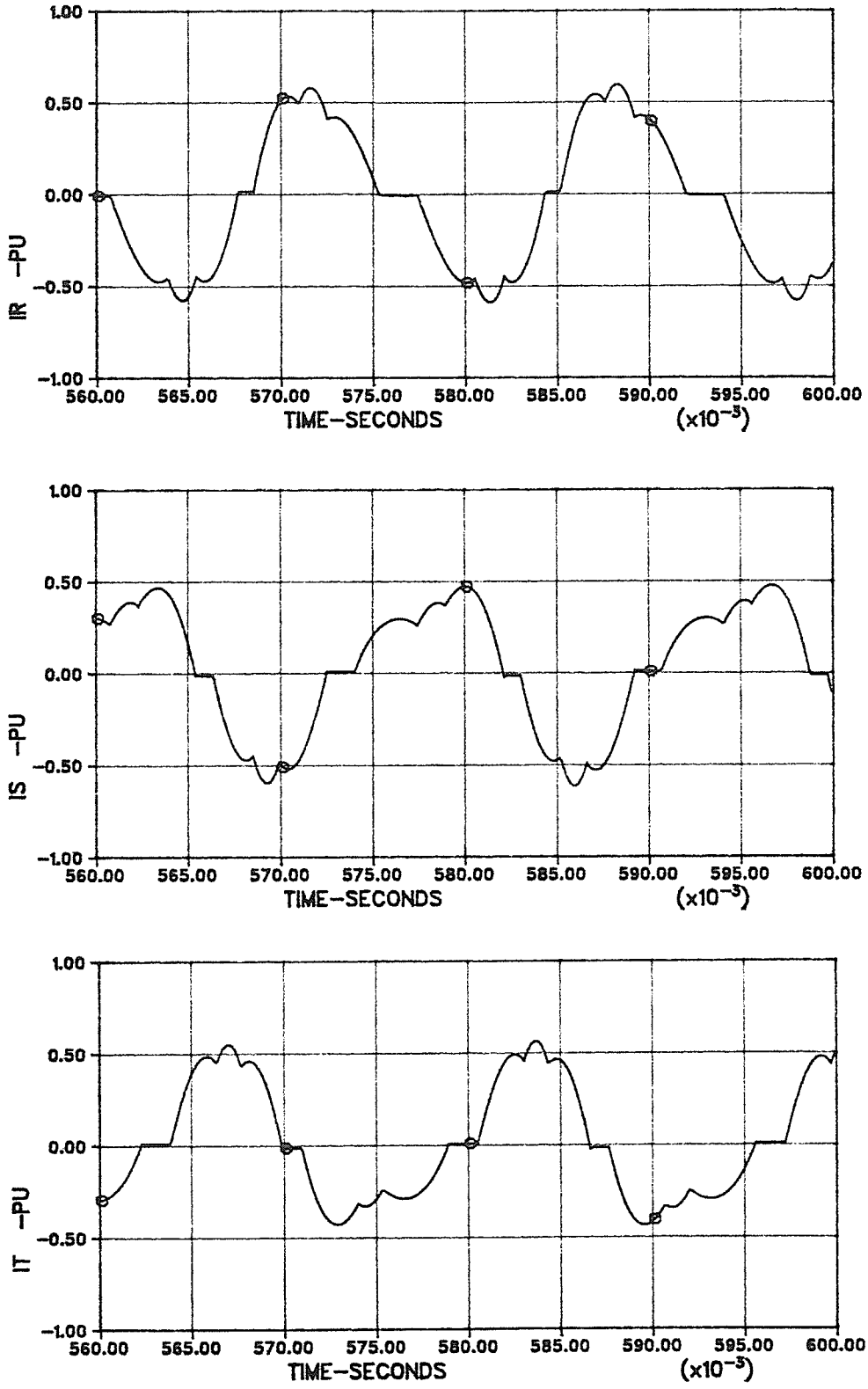

Figure 4.13. TCR Line Current Waveforms With DC
As Control Parameter. $\alpha_o = 45°$
Source 2^{nd} Harmonic Voltage 30 % @ - 30°
$\hat{\Delta} = 13.8°$ $\delta = 117.0°$

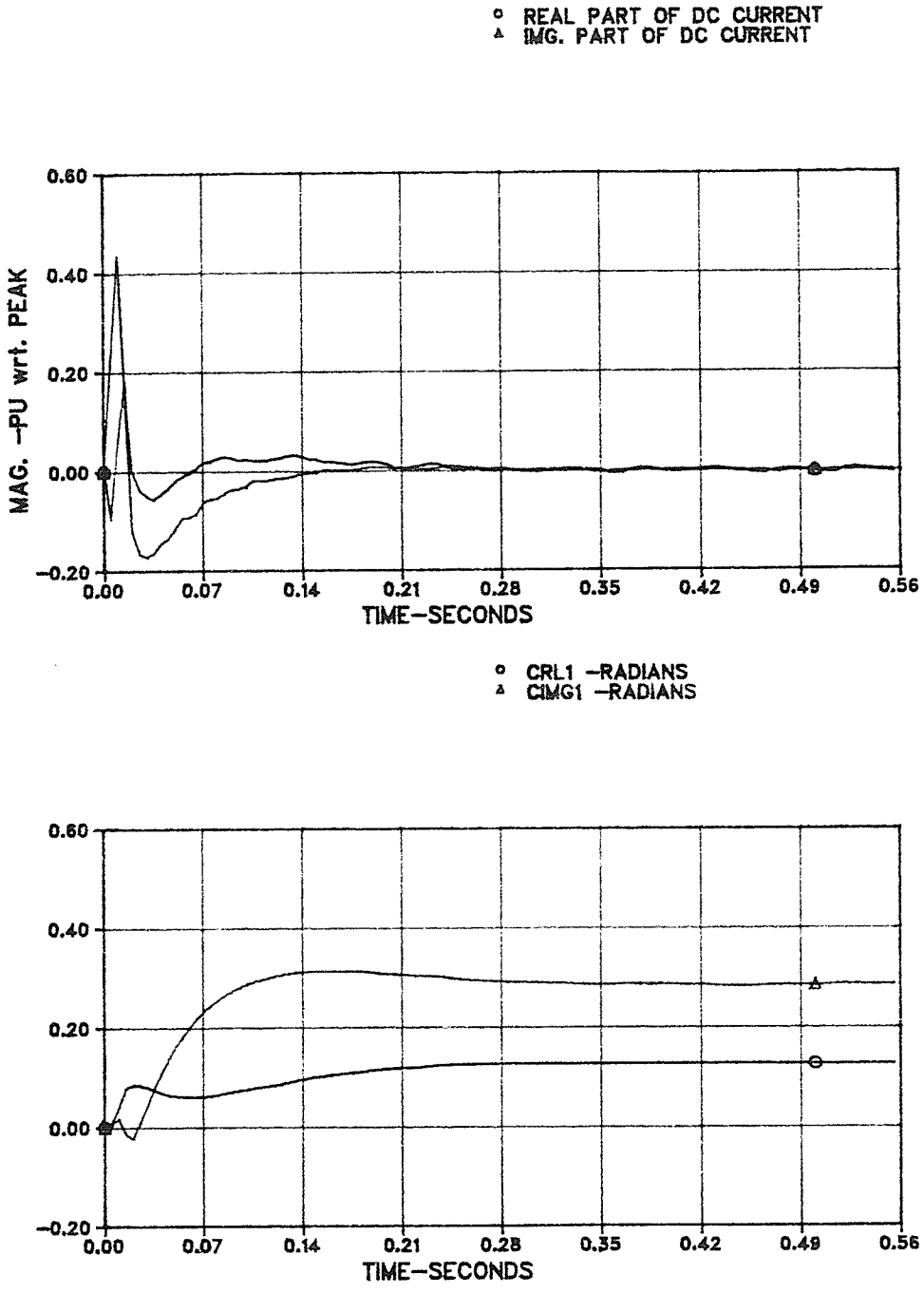

Figure 4.14. Control Of Postive Sequence DC Line Current With Firing Angle Modulation Source 2^{nd} Harmonic Voltage 30 % @ -30° $\alpha_o = 0°$ $\hat{\Delta} = 17.7°$ $\delta = 65.6°$

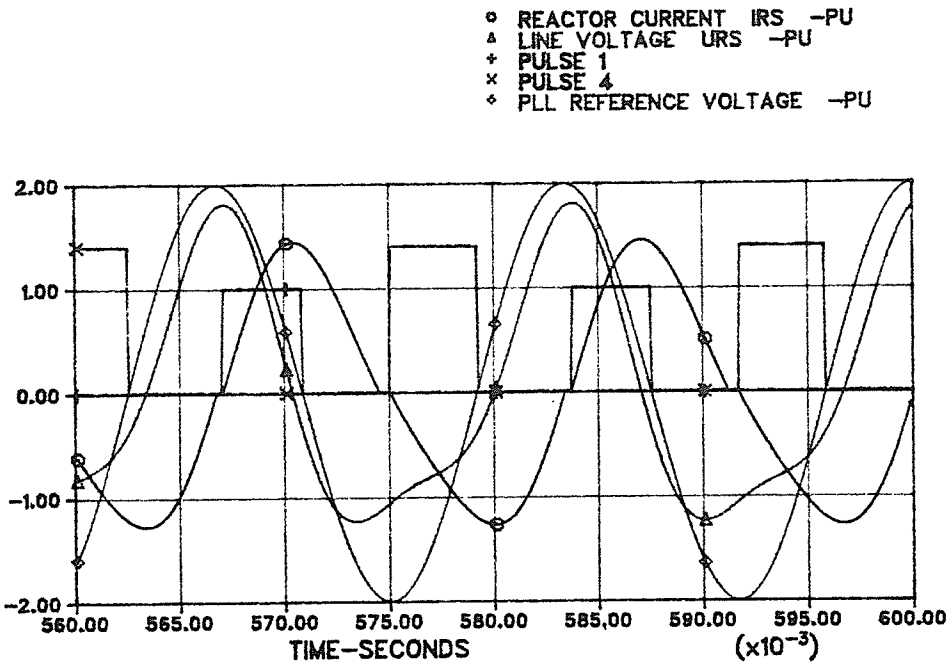

Figure 4.15.(a) TCR Waveforms With DC As Control Parameter. $\alpha_o = 0°$
Source 2^{nd} Harmonic Voltage 30 % @ - 30°
$\hat{\Delta} = 17.7°$ $\delta = 65.6°$

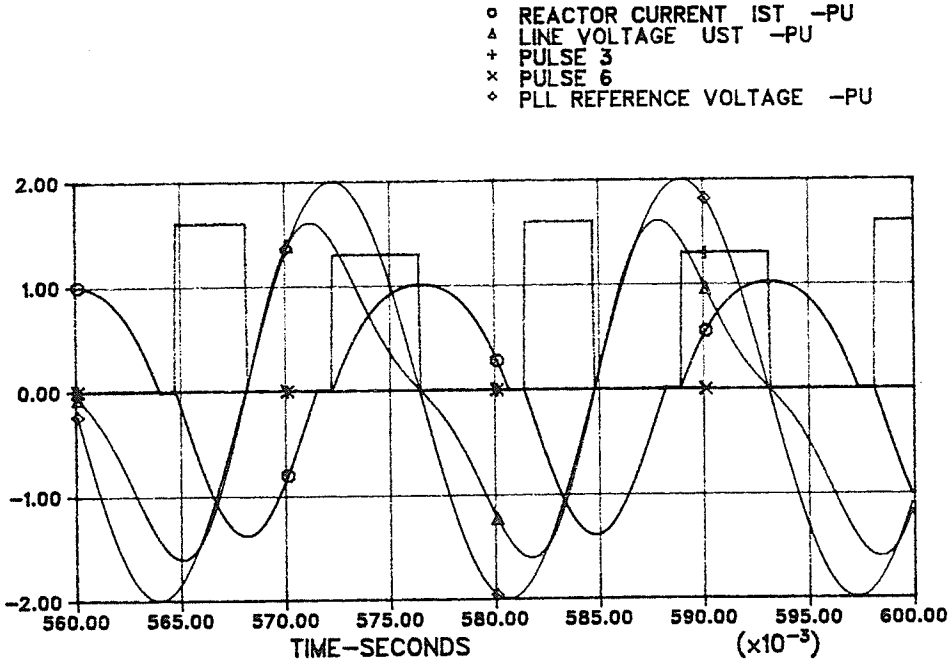

Figure 4.15.(b) TCR Waveforms With DC As Control Parameter. $\alpha_o = 0°$
Source 2^{nd} Harmonic Voltage 30 % @ - 30°
$\hat{\Delta} = 17.7°$ $\delta = 65.6°$

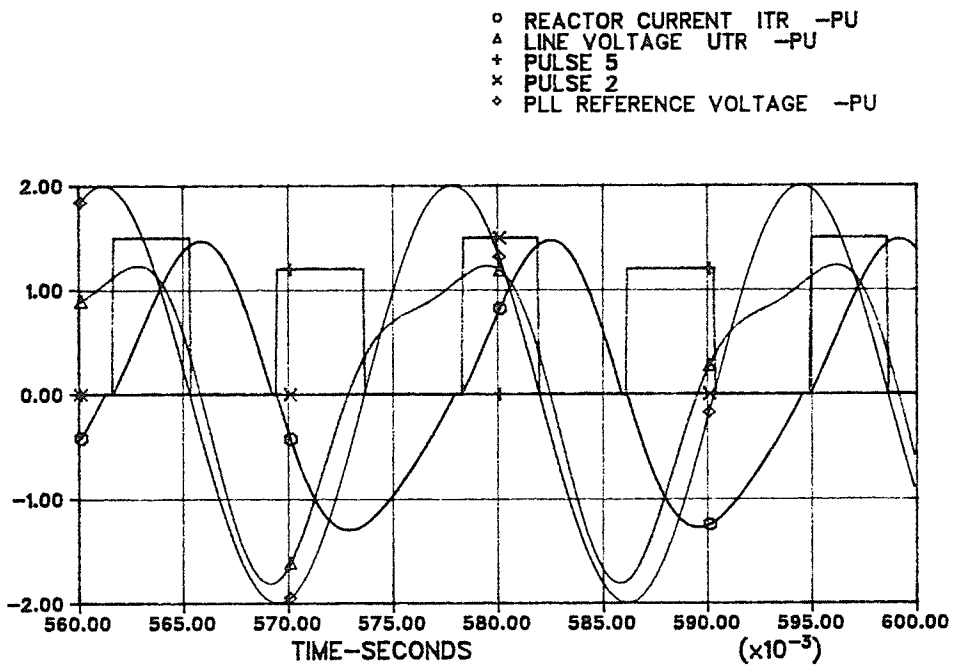

Figure 4.15.(c) TCR Waveforms With DC As Control Parameter. $\alpha_o = 0°$
Source 2^{nd} Harmonic Voltage 30 % @ - 30°
$\hat{\Delta} = 17.7°$ $\delta = 65.6°$

CHAPTER 5

CONCLUSIONS AND RECOMENDATIONS

5.1 CONCLUSIONS

The concept of using firing modulation on a thyristor controlled reactor to control or more correctly manipulate the harmonic content of its currents was developed and demonstrated using a simple model of the TCR static var compensator.

Based on the studies with the simple model, the main conclusions are as follows:

(a) Sinusoidal modulation of the TCR firing angle provides the capabilty to control the magnitude and phase of a specified harmonic component of the TCR line current. Thus the modulation concept has merit for improving system performance in practical situations such as at Châteaguay by injecting currents into the ac system at the appropriate magnitude and phase to damp resonances at the lower harmonic frequencies.

(b) It is technically feasible to use sinusoidal firing angle modulation to eliminate a problem harmonic component of the line current of the TCR.

Digital simulation of the TCR system verified this for the dc component and for the second harmonic component of the line current. It is possible to eliminate the desired harmonic current even when severe firing angle limits are encountered, including when the limits result in a modulation signal that is one-sided.

(c) For the circuit studied , it was not possible to control or eliminate the dc component and the 120 Hz component simultaneously by using a weighted average of the two respective modulation signals. This is not very surprising. The presence of the second harmonic voltage component in the source causes non-symmetrical voltage zero crossings. This asymmetry results in non-characteristic

even harmonic currents, the dc and second harmonic for example. However, for the second harmonic current another factor contributing to the total 120 Hz current is the source itself. One point to note is that eliminating the dc current component tends to reduce the second harmonic current component in most cases.

(d) An analysis of TCR currents when sinusoidal firing modulation is used shows that positive sequence harmonic components of the TCR line currents are suitable measured signals to use as control parameters.

The algorithm described in Chapter 4.1 that uses a coordinate transformation, phase-locked loop signals for vector identification and the symmetrical component transformation to provide an instantaneous measurement of the positive sequence harmonic current components works very well. The measuring delay is at most a cycle (at 60 Hz). The algorithm output of the magnitude and phase of the dc, 60 Hz and the 120 Hz currents is virtually the same as that computed with the numerical Fourier analysis program FOURNUM. This measuring concept would be suitable for measuring other sequence voltages or currents. If these quantities are influenced by the TCR currents,then these quantities would also be suitable inputs for the modulation controller.

(e) When firing angle limits restrict the magnitude of the modulation signal, the 60 Hz component of the TCR line current is significantly reduced. This reduction represents an interaction between the modulation controller and the 60 Hz voltage and reactive power controls. Such an interaction is undesirable. When it is beneficial to use modulation of the TCR, control strategies that set limits on α_o to allow for anticipated peak modulation angles should be adopted to minimize such undesirable interactions.

5.2 RECOMMENDATIONS

The following points are suggestions for additional work in order to demonstrate further the practical feasibility of the modulation concept:

(a) Clearly firing modulation influences the magnitude and phase of the TCR line currents. Firing angle modulation of the TCR should be applied for controlling a resonant system operating condition. The circuit shown in Figure 2.2, with the circuit parameters adjusted such that there is a parallel resonance between the system and the SVC capacitors, should be studied to check that the modulation can damp the resonance. The impedance between the TCR and the system should be varied to evaluate the performance of the TCR when operating in a weak and strong system. The circuit defined above is representative of the Châteauguay station when the ac system is in a resonant situation.

(b) When firing angle limits do not limit the modulation, there is only a small interaction between the modulation controller and the normal 60 Hz voltage and reactive controls (reference Figure 3.7). When limits restrict the modulation, the interaction is more severe. A study should be done to develop an overall control strategy that allows all controllers to operate satisfactorily and without compromising the overall SVC performance criteria. In many applications, the TCR is operated at large firing angles to minimize steady-state losses in the reactors. Strategies to keep the operating firing angle in a range that accomodates modulation would likely increase losses, and perhaps influence the overvoltage profile at the station if more capacitors are normally switched on to maintain mid-range firing angles. These are some factors to be considered.

(c) The studies suggested above and the studies done for this thesis consider that the SVC is connected directly to the high voltage bus. A series of studies should be done which consider the performance of the TCR with firing modulation when the SVC is connected to the ac system with a step-up transformer.

(d) A theoretical analysis of the stability of the closed modulation control system, including the non-linearity of the TCR , should be done in view of the interesting modulation controller configuration that is used.

REFERENCES

1. J. E. Miller
   Reactive Power Control In Electrical Systems
   General Electrical Company
   Wiley Interscience

2. L. Gyugyi, R. A. Otto, T. H. Putman
   Principles And Applicatiions Of Static Thyristor
   Controlled Shunt Compensators
   IEEE Transactions PAS, Vol. PAS-97 Sept./Oct. 1978

3. B. Markgraf, F. Labrenz, H. Tyll
   Harmonic Characteristics Of Static Var Compensators
   CEA Conference, June 1985

4. W. Meusel, H. Waldmann
   Coordinate Transformations Of Multi-term Regulation Systems
   For Compensation And Symmetrization Of Three Phase Supplies
   Siemens Review, Oct. 1976

5. E. Wanner, W. Herbst
   Static Power Factor Compensators For Use With Arc Furnaces
   Brown Boveri Review, Rev. 64 1977

6. E. Wirth, B. Roesle, K. Sadek, M. Häusler, M. Franze
   Static Var Compensators For HV Power Systems
   Brown Boveri Pub. No. CH-N 22.001.0E

7. G. B. Mazur
   Control Of Power System Harmonics With Firing Angle
   Modulation Of A Thyristor Controlled Reactor
   Technical Report TR86-1
   Department Of Electrical Engineering
   University of Manitoba,Winnipeg,Canada

APPENDICES

APPENDIX 1.1

PER UNIT SYSTEM

Per unit representation of power system quantities such as voltage, current, power and impedance is a convenient and advantageous method of carrying out power system calculations. Per unit quantities are normalized with respect to a chosen base value, rated apparent and rated system voltage. Quantites calculated in per unit can be related to a specific system by the appropriate choice of the base values.

For this study, the thyristor reactor system has a three phase rating of 332.4 MVA and a line-to-line voltage rating of 120 KV at the high voltage bus. Thus $S_B = 332.4$ MVA is taken as the base MVA, and $U_B = 120$ KV is taken as the base voltage. The reactor base current is $I_{br} = 923.4$ amperes and the line cuurent base is $I_{bl} = 1599.0$ amperes. The base impedance for the TCR reactor circuit is $Z_{base} = 129.96$ ohms. The base impedance relative to the line current base is 43.32 ohms.

The above quantites are used to derive the per unit quantities used in the analytical analysis equations and the digital modelling equations of the TCR.